

Option Pricing Formulae using Fourier Transform: Theory and Application

Martin Schmelzle*

April 2010

Abstract

Fourier transform techniques are playing an increasingly important role in Mathematical Finance. For arbitrary stochastic price processes for which the characteristic functions are tractable either analytically or numerically, prices for a wide range of derivatives contracts are readily available by means of Fourier inversion methods. In this paper we first review the convenient mathematical properties of Fourier transforms and characteristic functions, survey the most popular pricing algorithms and finally compare numerical quadratures for the evaluation of density functions and option prices. At the end, we discuss practical implementation details and possible refinements with respect to computational efficiency.

Keywords: option pricing, characteristic functions, Fourier inversion methods, Lévy processes, stochastic volatility, density approximation, numerical quadratures.

* Contact information:

✉ martin.schmelzle@pfadintegral.com

1 Introduction

The first important contribution to quantitative modeling of derivatives securities dates back to [Black and Scholes \(1973\)](#) who deduce a precise formula for the value of a European option on an underlying whose price on maturity follows a log-normal diffusion process. Despite the success of the Black–Scholes model on pricing and hedging derivatives, [Merton \(1976\)](#) noted early that options quoted on the markets differ systematically from their predicted values, which led up to questioning the distributional assumptions based on geometric Brownian motion.

By adding jumps to the archetypal price process with Gaussian innovations [Merton \(1976\)](#) is able to partly explain the observed deviations from the benchmark model which are characterized by fat tails and excess kurtosis in the returns distribution [for an overview of ‘stylized facts’ on asset returns see [Cont \(2001\)](#), statistical properties of implied volatilities are summarized in [Cont & al. \(2002\)](#)]. In the sequel also other authors develop more realistic models based on jump processes [e.g. [Eberlein and Keller \(1995\)](#), [Madan & al. \(1998\)](#) and [Kou \(2002\)](#)]. They derive option values from an analytical form of the conditional density function, for the value of the underlying on maturity given the initial state. Many of these original results are quite complicated requiring special functions or infinite summations.

As an alternative to model the option payoff directly by an analytical stochastic process, it has been recognized that by mapping the characteristic function of the density function to the payoff in Fourier space, option values can be usually computed much easier for these sophisticated processes. The characteristic function developed as a tool for the solution of problems in Probability Theory is the Fourier transform of the density function and the main idea using the transform methods is then to take an integral of the payoff function over the probability distribution obtained by inverting the corresponding Fourier transform. There is growing interest in applying these methods using characteristic functions and Fourier transforms which stems from the need to apply more complex pricing models than the Gaussian, which are more conveniently characterized through a characteristic function primarily rather than a probability distribution.

Transform methods turn out to be a very effective tool for the solution of many technical problems, since calculations in Image space are often much easier than in the spatial domain. The solution to the problem in Image space is then described through an Image function. Examples for these Image functions are calculations in Laplace or Fourier Space which are widely used in financial applications. To finally obtain the solution in original Space domain the Image function has to be inverted via inversion methods.

The Fourier transform is a widely used and a well understood mathematical tool from Physics and Engineering disciplines applicable to numerous tasks, for example signal processing [[Allen and Mills \(2004\)](#)], or as a method for solving partial differential equations [[Duffy \(2004\)](#)]. It is interesting to note that already [Merton](#)

(1973) noticed the possibility of using Fourier transforms to solve the Black–Scholes partial differential equation.

Inside the field of Finance the Fourier inversion method was first proposed in the Stein and Stein (1991) stochastic volatility model that uses the transform method in order to find the distribution of the underlying. Settling on the characteristic function approach, Heston (1993) obtains an analytical pricing formula for the valuation of European options with time varying volatility of the underlying. By using a variant of Lévy's *Inversion Theorem* for the probability functions the options prices result as the differences from the numerical evaluation of two Fourier integrals.

Since then Fourier inversion methods became a very active field of research in finance theory. Bakshi and Madan (2000) provide an economic foundation for characteristic functions, generalize the approach of Heston (1993) and Stein and Stein (1991) in many significant ways, and develop valuation formulae for a wide variety of contingent claims. Duffie & al. (2000) offer a comprehensive survey that the Fourier methods are applicable to a wide range of stochastic processes, the class of exponential affine jump diffusions.

A numerically very efficient methodology is introduced in Carr and Madan (1999) who pioneer the use of fast Fourier transform algorithms by mapping the Fourier transform directly to call option prices via the characteristic function of an arbitrary price process. Lee (2004) generalizes their approach to other payoff functions and unifies it with other known Fourier pricing elements. In Carr and Wu (2004) the authors extend the Carr and Madan (1999) methodology for general claims and apply these to *time changed* Lévy processes, the class of *generalized affine* models [Filipović (2001)] and *Quadratic activity rate* models [Leippold and Wu (2002)].

Given the characteristic function for some price dynamics and a Fourier transformed payoff function determining the contract type, Lewis (2001) develops a highly modular pricing framework. In the Carr and Madan (1999) approach the whole option price is Fourier transformed including the particular payoff function, whereas Lewis (2001) entirely separates the underlying stochastic process from the derivative payoff by the aid of the *Plancherel–Parseval Theorem* and obtains a variety of valuation formulae by the application of Residual Calculus.

More techniques have been developed to compute option values as an integral in Fourier space, using Fourier transform methods. Throughout the paper we will mention some of them and give more details. Density calculations and option pricing are then, as we will see, a matter of numerical integration for the Fourier inversion, usually employing direct integration methods or the Discrete Fourier Transform, where the Fast Fourier Transform is an efficient way to compute it in practice. Methodological aspects concerning numerical implementation should be considered sensibly since the semi-infinite domain Fourier integrals might exhibit oscillations in the integrand, which is complicating numerical analysis.

Computational performance also becomes a critical factor when calibrating the models to observed market prices which can afterwards be used to value exotic products or devise hedging strategies. The complexity of these new models require sophisticated numerical algorithms which ensure fast and reliable option pricing, calculations of hedge parameters, volatility surface calculations and density approximations.

The structure of the paper is organized as described in the following. In the next section, we briefly outline the general valuation framework for European option pricing. We start by considering the standard martingale pricing approach and then point to the inherent connections to Arrow–Debreu securities and state price densities. In Section 3, we give an overview of the most fundamental ideas and mathematical tools needed for characteristic function methods, we also present the most relevant properties of Fourier Transforms and their inversion. Section 4 provides an exhibition of the most popular Fourier pricing algorithms. We begin with the Black–Scholes style valuation formula and proceed with the more flexible single integral solutions. With a focus on an intuitive understanding, we emphasize on a concise presentation of the main results of the various methodologies without too much technical details. Thereafter, we accentuate some of the similarities between these approaches and point out recent developments which are based on these procedures or which apply them to other fields in mathematical finance. In Section 5, we finally show how to apply Fourier inversion methods to density approximations and option pricing. To do so we first present and discuss some qualitative features of popular numerical quadratures and fast Fourier transform methods. Then, we give detailed numerical examples, show convergence properties of the Fourier integrands, compare accuracy and run times. At the end, in Section 6, we review various mathematical and numerical methods regarding implementational issues and computational performance. A thorough quantitative and numerical analysis is a important factor and relevant for the stability of the Fourier transform methods, the choice of adequate truncation levels for the numerical evaluation and integration sample spacing of the Fourier integrands. Section 7 concludes.

2 Valuation Problem for European Options

Asset prices are modeled by stochastic processes whose evolutions are governed by an underlying probability measure. In the well established theory of arbitrage pricing, there exists a *risk neutral* probability measure under which asset prices are arbitrage free. Moreover, in terms of probability, the absence of arbitrage is essentially equivalent to the existence of a risk neutral *equivalent martingale measure* for the stochastic process making the underlying process become a martingale.

Consequently, as Ross (1976) and Cox and Ross (1976) have shown, the price of a European option can be reduced to taking their discounted expected values of a

future payoff with respect to a risk neutral measure \mathbb{Q} . This is known as martingale pricing or pricing by expectation

$$V(S_t, K, T) = e^{-r(T-t)} \mathbb{E}^{\mathbb{Q}}[w(S_T) | \mathfrak{F}_t]. \quad (2.1)$$

For a European call option with strike K , risk-free rate r and time to maturity T , the value of the arbitrage free option with payoff $w(S_T) = \max\{S - K, 0\} = (S_T - K)^+$ is then given by

$$\begin{aligned} C(S_t, K, T) &= e^{-r(T-t)} \mathbb{E}^{\mathbb{Q}}[(S_T - K)^+ | \mathfrak{F}_t], \\ &= e^{-r(T-t)} \int_0^\infty (S_T - K)^+ q(S_T | \mathfrak{F}_t) dS_T, \\ &= e^{-r(T-t)} \int_K^\infty (S_T - K) q(S_T | \mathfrak{F}_t) dS_T. \end{aligned} \quad (2.2)$$

The expectation is calculated on the basis of the risk neutral density function $q(S_T | \mathfrak{F}_t)$. It is the conditional transition probability density of the underlying S at time T conditional upon the information flow \mathfrak{F}_t (filtration) of the asset price available up to time t [Harrison and Pliska (1981)]. From Harrison and Kreps (1979) we know that under technical conditions the existence of an equivalent martingale measure and the absence of arbitrage are essentially equivalent properties. This equivalent martingale measure makes the discounted price process $\tilde{S}_T = e^{-rT} S_T$ a martingale and satisfies the martingale property $\tilde{S}_0 = \mathbb{E}^{\mathbb{Q}}[\tilde{S}_T]$.

Under the risk neutral pricing measure, all assets have the same expected rate of return which is the risk free rate. In other words, under no-arbitrage conditions the risk preferences of investors do not enter into valuation decisions, thus, we can assume risk neutrality and price any security in a preference free world. For recent treatments and more details on the approach to arbitrage pricing see e.g. Delbaen and Schachermayer (2006) and the references therein.

Commonly, the risk neutral probability measure is used for arbitrage pricing. A market place free from arbitrage opportunities is usually characterized by a unique set of state contingent claims. Arrow–Debreu prices, or similarly Arrow–Debreu securities, are the most elementary contingent claims. An Arrow–Debreu security pays off one unit of the numéraire at time T , if, and only if, a specific state occurs. For this reason Arrow–Debreu prices are also known as state prices. The continuous state equivalent of Arrow–Debreu securities constitutes a state price density.

Any possible payoff can be replicated with a linear combination of state prices whereas this particular replication portfolio implies a unique arbitrage free price. These elementary relations are illustrated in Figure 1.

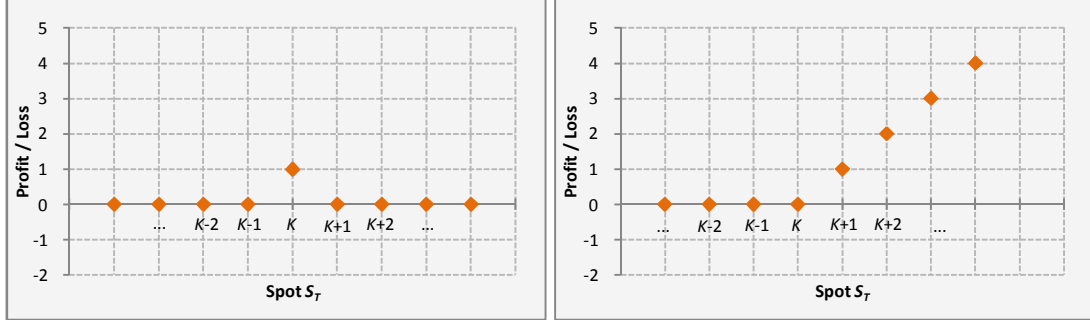


Figure 1: Arrow-Debreu securities. Left: Payoff diagram of a state price. Right: Payoff diagram for a European call option.

This observation suggests that risk neutral probabilities can be expressed in terms of state prices and *vice versa*. Following [Breedon and Litzenberger \(1978\)](#), the state price density is related to the risk neutral density by $e^{-rT}q(S_T)$ and can be derived by twice differentiating either a call or put option with respect to its strike price

$$q(S_T) = e^{rT} \left. \frac{\partial^2 V}{\partial K^2} \right|_{K=S_T}. \quad (2.3)$$

This result shows that it is possible to construct an Arrow-Debreu security which pays off one unit at time T exactly if $K = S_T$. Suppose w is the final payoff to a derivative security maturing at T

$$w(S_T) = \int_{-\infty}^{\infty} w(K) \delta(S_T - K) dK. \quad (2.4)$$

Following [Carr \(2003\)](#) this is a spectral decomposition of the payoff w into the payoffs or delta claims $\delta(S_T - K)$ respectively from an infinite collection of Arrow-Debreu securities

$$\frac{\partial^2}{\partial K^2} (S_T - K)^+ = \delta(S_T - K). \quad (2.5)$$

The risk neutral probability function and the state price density are completely interchangeable concepts, only distinguished by a discount factor.

Under the martingale pricing approach, an option value can be represented as a convolution of a payoff function with a discounted probability density function or equivalently the state price density of the state variables. It is well known that if the density of the underlying is known in closed form, option prices can be obtained by a single integration of their payoff against this density function.

For example if we assume Brownian motion for the price dynamic, the density function is known in closed form. The stock price on maturity then reveal a random variable having a log-normal distribution. Under \mathbb{Q} its density is given by

$$q(S_T) = \frac{1}{S_T \sigma \sqrt{2\pi T}} e^{-\frac{\left\{ \ln S_T - \left(\ln S_0 + \left(r - \frac{1}{2}\sigma^2 \right) T \right) \right\}^2}{2\sigma^2 T}}, \quad (2.6)$$

i.e. the density of a Normal Distribution with mean $\ln S_0 + \left(r - \frac{1}{2}\sigma^2\right)T$ and variance $\sigma^2 T$. By a single integration the value for the Black–Scholes call of today is obtained

$$C(S_0, K, T) = e^{-rT} \int_K^\infty (S_T - K) \frac{1}{S_T \sigma \sqrt{2\pi T}} e^{-\frac{\{\ln S_T - (\ln S_0 + (r - \frac{1}{2}\sigma^2)T)\}^2}{2\sigma^2 T}} dS_T. \quad (2.7)$$

Unfortunately, more sophisticated price dynamics like affine jump diffusions and Lévy processes often do not possess density functions in closed form or have quite complicated analytical expressions involving special functions and infinite summations. However, for many of the more advanced asset price models characteristic functions are available in closed form. By analogy, if the characteristic function of the underlying is tractable, option prices can also be obtained by a single integration.

3 Fourier Transform, Inversion Theorem and Characteristic Functions

The power and versatility of *Fourier Analysis* and the *Calculus of Characteristic Functions* have been used in many recent publications relating to probability distributions. Generally this is gaining strong momentum in the field of financial modeling, too. The successful application of these techniques require a considerable degree of mathematical sophistication. The purpose of this section is to give an overview of this theory, and to show how to apply characteristic functions and Fourier transforms in mathematical finance.

3.1 Characteristic Functions

If not in all statistical analyses, at least in most of them, the calculation of the distribution function of random variables is required. A very interesting fact is that even if the random variable of interest does not have an analytical expression, the characteristic function of this random variable always exists. There is a one to one relationship between the probability density and a characteristic function. If the characteristic function is known in closed form, is tractable numerically, or given by empirical data, then we can compute the distribution function by using the Inversion theorem.

The characteristic function $\phi_X(u) = \mathbb{E}[e^{iuX}]$ of a real valued random variable X is defined for arbitrary real numbers u as the expectation of the complex valued transformation e^{iuX} , where $i = \sqrt{-1}$ is the imaginary unit. If $f_X(x)$ is the probability function (PDF) of the random variable then the integral

$$\phi_X(u) = \mathbb{E}[e^{iuX}] = \int_{-\infty}^{\infty} e^{iuX} f_X(x) dx, \quad (3.1)$$

defines the expected value and is by definition the Fourier transform of the density function $f_X(x)$ denoted by $\mathcal{F}[f_X(x)]$. At a given u , $\phi_X(u)$ is a single random variable and for $-\infty < u < \infty$ we have a stochastic process. An intuitive understanding of characteristic functions is offered by Epps (1993) who give clear geometric interpretations of the characteristic functions to elucidate their properties and use in statistical applications. From *Euler's Identity* the random variable X can be represented by sine and cosine function as

$$e^{iuX} = \cos(uX) + i \sin(uX). \quad (3.2)$$

From this operation we can see that exponential e^{iuX} for a given u represents a point on the unit circle in the complex plane. The unit circle is a circle with unit radius. It can be considered as a contour in the complex plane defined by $|z| = 1$, where $|z|$ is the complex modulus which can be interpreted as a distance measure.

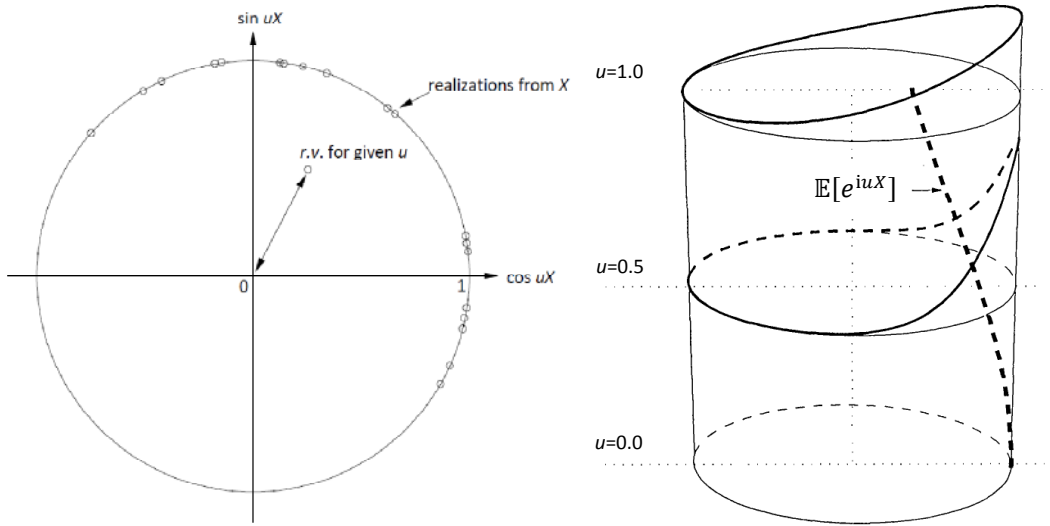


Figure 2: Geometrical interpretations of characteristic functions. Left: Operation of a characteristic function. Right: Wrapped around distribution of uX , $X \sim \Phi(0, 1)$ at $u = 0, 0.5, 1$ and characteristic function of $\Phi(0, 1)$ on $[0, 1]$. Source: Epps (1993), p 34.

Since $\phi_X(u) = \mathbb{E}[e^{iuX}]$, the characteristic function evaluated at any u can be interpreted as the center of mass of the distribution of uX wrapped around the unit circle in the complex plane. If the domain of $\phi_X(u)$ is given by the whole real line, we have the geometrical representation of the characteristic function as a curve confined to an infinitely long circular ‘cylinder’ or ‘tube’ which is illustrated in Figure 2. Further we can see that the norm of the characteristic function $|\phi_X(u)|$ is always within the unit circle. At $u = 0$ we have the value one since in this case uX is degenerated.

Comparing the wrapped around distribution of uX and $-uX$ for $u \neq 0$, it becomes apparent that one is the mirror image of the other about the real axis. The

real parts of their centers are equal and the imaginary parts are equal, too, but of opposite sign, hence $\overline{\phi_X(u)} = \phi_X(-u)$ is the complex conjugate of $\phi_X(u)$. Due to this symmetry around $u = 0$, it is sufficient to concentrate on $u > 0$ to fully describe the distribution function.

If a characteristic function is absolutely integrable over the real line $(-\infty, +\infty)$ then X has an absolutely continuous probability distribution. This is said to be integrable in the Lebesgue sense and belongs to $L^1(\mathbb{R})$.

Below follows a summary of elementary properties of characteristic functions

1. $\phi_X(u)$ always exists since $|e^{iuX}|$ is a continuous and bounded function for all finite real u and x ; further $|\int_{-\infty}^{\infty} f(x) dx| \leq \int_{-\infty}^{\infty} |f(x)| dx$ so that the defining integral converges absolutely
2. $\phi_X(0) = 1$ for any distribution
3. $|\phi_X(u)| \leq 1$
4. $\overline{\phi_X(u)} = \phi_X(-u)$
5. If $Y = a + bX$, then $\phi_Y(u) = e^{iua} \phi_X(bu)$
6. If X_1 and X_2 are stochastically independent, then the characteristic function $\phi_Y(u)$ of the new random variable $Y = X_1 + X_2$ is the product of the characteristic function of each random variable $\phi_{X_1}(u)\phi_{X_2}(u)$, which are allowed to be drawn from different distributions

Another important property of characteristic functions is the possibility to derive the moments and cumulants of a distribution function. By k th differentiation of the characteristic function at the origin of u , the k th moment $\mathbb{E}[X^k]$ of the distribution (if they exist) is obtained

$$\mathbb{E}[X^k] = \frac{1}{i^k} \frac{d^k \phi_X(u)}{du^k} \Big|_{u=0}. \quad (3.3)$$

In the same way that the characteristic function generates the moments, cumulants $c_k(X)$ are computed by taking the logarithm of $\phi_X(u)$ which is then called the cumulant characteristic function $\ln \phi_X(u)$

$$c_k(X) = \frac{1}{i^k} \frac{d^k \ln \phi_X(u)}{du^k} \Big|_{u=0}. \quad (3.4)$$

Thus, important qualitative statistical properties such as variance, skewness and kurtosis have analogons in Image space and are readily available if the characteristic function is known

$$\mathbb{E}[X] = c_1(X), \quad (3.5)$$

$$\mathbb{Var}(X) = c_2(X), \quad (3.6)$$

$$s(X) = \frac{c_3(X)}{c_2(X)^{3/2}}, \quad (3.7)$$

$$k(X) = \frac{c_4(X)}{c_2(X)^2}. \quad (3.8)$$

These fundamental properties make characteristic functions a viable tool in Probability Theory and to applications in stochastic inference.

3.2 The Inversion Theorem

An essential property of characteristic functions is their one to one relationship with distribution functions. Every random variable possesses a unique characteristic function and the characteristic function indeed *characterizes* the distribution uniquely [Waller (1995)]. The Inversion Theorem is the *Fundamental Theorem of the Theory of Characteristic Functions* since it links the characteristic function back to its probability distribution via an inverse Fourier transform.

Based on the fundamental results from Lévy (1925) who gave a general inversion formula, Gurland (1948) and Gil-Pelaez (1951) develop useful representations of the Inversion Theorem. In the following we will follow the form given by Gil-Pelaez (1951) [see Waller & al. (1995) for a review on inversion methods].

The inversion algorithms are based on the following particular form of the Gil-Pelaez inversion integral for cumulative distribution function (CDF) $\int_{-\infty}^x f_X(x) dx$

$$F_X(x) = \mathbb{P}(X \leq x) = \frac{1}{2} - \frac{1}{2\pi} \int_{-\infty}^{\infty} \frac{e^{-iux} \phi_X(u)}{iu} du. \quad (3.9)$$

We see that the recovered distribution function is expressed as an integral in terms of the characteristic function. Taking the derivate of $F_X(x)$ yields the probability density function $f_X(x)$

$$f_X(x) = \mathcal{F}^{-1}[\phi_X(u)] = \frac{1}{2\pi} \int_{-\infty}^{\infty} e^{-iux} \phi_X(u) du. \quad (3.10)$$

The comparison of (3.1) with (3.10) exhibits the reciprocal relationship which exists between $f_X(x)$ and $\phi_X(u)$.

The Fourier transform of a real valued function can be written as a two dimensional vector in the complex plane. These complex values are expressed as $z = a + ib$, where $\Re[z] = a$ is the real part and $\Im[z] = b$ is the imaginary part of the complex number z with a and b being real numbers. The complex conjugate is given by $\bar{z} = a - ib$, the modulus is $|z| = \sqrt{a^2 + b^2}$ and the real part is $\Re[z] = (z + \bar{z})/2$ and imaginary part $\Im[z] = (z - \bar{z})/2i$. Further we have

$$\Re[\phi_X(u)] = \frac{\phi_X(u) + \phi_X(-u)}{2}, \quad (3.11)$$

$$\Im[\phi_X(u)] = \frac{\phi_X(u) - \phi_X(-u)}{2i}, \quad (3.12)$$

which implies that the function $\phi_X(u)$ is even in its real part and odd in its imaginary part for all u . An even function is said to be symmetric with respect to $u = 0$. Therefore, the integral of the positive and the negative halves of an even function are the same.

This special symmetry property allows us to further simplify the Fourier integrals. Using these results the expression for $f_X(x)$ reduces to

$$\begin{aligned} f_X(x) &= \frac{1}{2\pi} \Re \left[\int_{-\infty}^0 e^{-iux} \phi_X(u) du \right] + \frac{1}{2\pi} \Re \left[\int_0^{\infty} e^{-iux} \phi_X(u) du \right], \\ &= \frac{1}{2\pi} \Re \left[\int_0^{\infty} \overline{e^{-iux} \phi_X(u)} du \right] + \frac{1}{2\pi} \Re \left[\int_0^{\infty} e^{-iux} \phi_X(u) du \right], \\ &= \frac{1}{2\pi} \Re \left[2 \int_0^{\infty} e^{-iux} \phi_X(u) du \right], \\ &= \frac{1}{\pi} \int_0^{\infty} \Re[e^{-iux} \phi_X(u)] du. \end{aligned} \quad (3.13)$$

Similar calculations for the CDF yield

$$\begin{aligned} F_X(x) &= \frac{1}{2} + \frac{1}{2\pi} \int_0^{\infty} \frac{e^{iux} \phi_X(-u) - e^{-iux} \phi_X(u)}{iu} du, \\ &= \frac{1}{2} + \frac{1}{2\pi} \int_0^{\infty} \frac{\overline{-e^{-iux} \phi_X(u)} - e^{-iux} \phi_X(u)}{iu} du, \end{aligned} \quad (3.14)$$

$$= \frac{1}{2} - \frac{1}{\pi} \int_0^{\infty} \Re \left[\frac{e^{-iux} \phi_X(u)}{iu} \right] du, \quad (3.15)$$

$$= \frac{1}{2} - \frac{1}{\pi} \int_0^{\infty} \Im \left[\frac{e^{-iux} \phi_X(u)}{u} \right] du. \quad (3.16)$$

For the probability $\mathbb{P}(X > x) = \int_x^{\infty} f_X(x) dx$ we can use the simple relation $F_X^c(x) = \mathbb{P}(X > x) = 1 - F_X(x)$ to obtain the complementary CDF (cCDF)

$$F_X^c(x) = \frac{1}{2} + \frac{1}{\pi} \int_0^{\infty} \Re \left[\frac{e^{-iux} \phi_X(u)}{iu} \right] du, \quad (3.17)$$

$$= \frac{1}{2} + \frac{1}{\pi} \int_0^{\infty} \Im \left[\frac{e^{-iux} \phi_X(u)}{u} \right] du. \quad (3.18)$$

In certain cases it will be convenient to employ Euler's identity and express the complex exponential as two separate cosine and sine functions. For (3.1) we have the equivalent representation

$$\phi_X(u) = \int_{-\infty}^{\infty} \cos(ux) f_X(x) dx + i \int_{-\infty}^{\infty} \sin(ux) f_X(x) dx. \quad (3.19)$$

Using this transformation the density function in (3.10) results in a real valued integral of a real variable [see Abate and Whitt (1992)]

$$f_X(x) = \frac{1}{\pi} \int_0^{\infty} (\cos(ux) \Re[\phi_X(u)] + \sin(ux) \Im[\phi_X(u)]) du. \quad (3.20)$$

And finally, for the CDF we get

$$F_X(x) = \frac{1}{2} - \frac{1}{\pi} \int_0^{\infty} (\cos(ux) \Im[\phi_X(u)] - \sin(ux) \Re[\phi_X(u)]) \frac{du}{u}. \quad (3.21)$$

3.3 Elementary Properties of the Fourier Transform

Next, we mention some more relevant properties of Fourier transforms. We denote the Fourier transform from $f(x)$ as $\hat{f}(u) = \mathcal{F}[f](u)$ or just $\mathcal{F}[f]$.

Linearity For arbitrary a, b the transform is a linear operator

$$\mathcal{F}[af(x) + bg(x)](u) = a\hat{f}(u) + b\hat{g}(u). \quad (3.22)$$

Translation The Fourier transform turns a multiplication by a variable x_0 into translation

$$\mathcal{F}[f(x - x_0)](u) = e^{iux_0} \hat{f}(u). \quad (3.23)$$

Differentiation If $n > 0$ is an integer, $f^{(n)}$ is piecewise continuously differentiable, and each derivative is absolutely integrable on the entire real line, then

$$\mathcal{F}[f^{(n)}](u) = (-iu)^n \hat{f}(u). \quad (3.24)$$

Thus, a differentiation converts to multiplication in Fourier space.

Convolution Theorem One of the most fundamental and important properties of Fourier transforms is convolution (Faltung). In Fourier space a convolution is mapped into multiplication. Define the convolution by

$$(f * g)(x) = \int_{-\infty}^{\infty} f(x - y)g(y)dy, \quad (3.25)$$

where $*$ denotes the convolution operator. Then we have

$$\mathcal{F}[f * g](u) = \hat{f}(u)\hat{g}(u), \quad (3.26)$$

and

$$\mathcal{F}[fg](u) = \hat{f}(u) * \hat{g}(u). \quad (3.27)$$

Thus, the Fourier transform of the convolution of two functions equals the product of the Fourier transforms of each of the functions.

Absolutely and Square Integrable Functions Many concepts in the field of Fourier Transform Theory draw heavily on the notion of absolute integrability. A function is absolutely integrable (or simply integrable) if the integral of its absolute value over \mathbb{R} is finite

$$\int_{-\infty}^{\infty} |f(x)| dx < \infty. \quad (3.28)$$

This is a very important relation since for a Fourier transform and its inverse to exist, then the condition in equation (3.28) must hold. The space of absolutely integrable functions is called L^1 or $L^1(\mathbb{R})$. Functions that are integrable on an interval (a, b) are said to be on $L^1(a, b)$.

If $f(x)$ is absolutely integrable, which is true for $f(x) \in L^1(\mathbb{R})$, then the Fourier transform exists. Given $\mathcal{F}[f](u)$ is absolutely integrable, the inverse Fourier transform $\mathcal{F}^{-1}[\mathcal{F}[f]](u)$ exists. However, it is important to note that the Fourier transform of an $L^1(\mathbb{R})$ function is not necessarily integrable even though it often is. This is why we cannot simply assume to take its inverse transform.

Fourier transforms are extendable to square integrable functions as well. A function is square integrable if

$$\int_{-\infty}^{\infty} |f(x)|^2 dx < \infty. \quad (3.29)$$

The space of square integrable functions is denoted by L^2 or $L^2(\mathbb{R})$. The space L^2 delineates an inner product space. Functions $L^1(a, b)$ that are integrable on an interval (a, b) also satisfy

$$\int_a^b |f(x)|^2 dx < \infty. \quad (3.30)$$

The last inequality is of great importance since it implies that a function well defined on an interval (a, b) is defined on the inner product space as well, i.e. a vector space equipped with an inner product relation $\langle \cdot, \cdot \rangle$. The notion of inner products is introduced in the next part about the Plancherel–Parseval Theorem.

The Plancherel Theorem and Parseval's Theorem Another very important property is that under certain conditions inner or scalar products are preserved under Fourier transforms. In the context of Probability Theory, these results are especially significant for the reconstruction of a distribution from its characteristic function.

The scalar product or inner product of two functions $f(x)$ and $g(x)$ on L^2 is defined as

$$\langle f, g \rangle = \int_{-\infty}^{\infty} f(x) \overline{g(x)} dx. \quad (3.31)$$

And equally for the Fourier transforms $\mathcal{F}[f]$ and $\mathcal{F}[g]$

$$\langle \mathcal{F}[f], \mathcal{F}[g] \rangle = \int_{-\infty}^{\infty} \mathcal{F}[f] \overline{\mathcal{F}[g]} dx. \quad (3.32)$$

Since $f(x) = \frac{1}{2\pi} \int_{-\infty}^{\infty} e^{-iux} \mathcal{F}[f] du$, then we have

$$\begin{aligned} \int_{-\infty}^{\infty} f(x) \overline{g(x)} dx &= \int_{-\infty}^{\infty} \frac{1}{2\pi} \int_{-\infty}^{\infty} e^{-iux} \mathcal{F}[f] g(u) du dx, \\ &= \frac{1}{2\pi} \int_{-\infty}^{\infty} \mathcal{F}[f] \int_{-\infty}^{\infty} e^{-iux} g(u) dx du, \\ &= \frac{1}{2\pi} \int_{-\infty}^{\infty} \mathcal{F}[f] \overline{\mathcal{F}[g]} du. \end{aligned} \quad (3.33)$$

There are subtle aspects involved in the interchange of integration carried out in the preceding equations. By applying *Fubini's Theorem*, which states in principle that if a function of two variables is absolutely integrable over a region, then its iterated integrals and its double integral over the region are all equal. Hence, we may freely interchange the order of integration.

If $f = g$ then the integral of the squared modulus of f is equal to the integral of the squared modulus of its Fourier transform $\mathcal{F}[f]$

$$\int_{-\infty}^{\infty} |f|^2 dx = \int_{-\infty}^{\infty} |\mathcal{F}[f]|^2 du. \quad (3.34)$$

Via a Fourier inversion the scalar or inner product can be transformed from Fourier domain to spatial domain and *vice versa*. This identity is sometimes also referred to as the Parseval's Identity, who discovered a discrete version in the context of Fourier series. The inner product on $L^2(\mathbb{R})$, restricted to those functions that are also absolutely integrable, furnishes a inner product operation $\langle \cdot, \cdot \rangle$ for $L^1 \cap L^2$, where the inner product induces a norm $\|x\| = \sqrt{\langle x, x \rangle}$ on this space. One of the main consequences of the Plancherel Theorem or Parseval's Identity for later purposes is that Fourier transforms preserve the norms of functions.

There seems to be no unique naming convention about the theorem, i.e. in different fields the theorem might be referred to as the Plancherel Identity or the Parseval's Identity. This is why we will refer to it as the Plancherel–Parseval theorem within this paper.

Generalized Fourier Transform Up to this point we have defined the characteristic function in terms of real valued transform variables u . In certain cases it is convenient or even necessary to integrate a characteristic function along a line parallel to the real axis. For this case we can extend the domain of the transform variable u to the complex plane $u \rightarrow z \in \mathbb{C}$, where the characteristic function is well behaved [Lukacs (1970), Theorem 7.1.1]. The set of values for $z = z_r + iz_i$, for which the expectation in Eq. (3.1) is well defined, is within some *strip of regularity* \mathcal{S}_X with $\alpha < \Im[z] < \beta$ parallel to the real z -axis. In these z -plane strips the extended characteristic functions $\phi_T(z)$ are typically regular functions, also known as *analytic characteristic functions*. Following Lukacs (1970), an analytic characteristic function is a characteristic function which coincides with a regular analytic function in some neighborhood of the origin in the complex z -plane. Under this extended definition $\phi_T(z)$ is called the *generalized Fourier transform* [see also Titchmarsh (1975)]. Since the transform variable is now extended to the complex plane the transform is also sometimes referred to as the *complex Fourier transform*. The inverse of this generalized Fourier transform is given by

$$f(x) = \frac{1}{2\pi} \int_{iz_i - \infty}^{iz_i + \infty} e^{-izx} \phi(z) dz. \quad (3.35)$$

It is interesting to note that the generalized Fourier transform contains the Laplace transform if $\Im[z] > 0$ and the cumulant generating function if $\Im[z] < 0$ as special cases, provided that they are well defined.

Generally, the properties for the ordinary Fourier transform also apply with little or no modification to the generalized Fourier transform. For example, we mention the important fact that the Plancherel–Parseval identity also work for complex numbers z by an integration along a straight line parallel to the real axis

$$\int_{-\infty}^{\infty} f \bar{g} dx = \frac{1}{2\pi} \int_{-\infty}^{\infty} \mathcal{F}[f](z_r + iz_i) \overline{\mathcal{F}[g](z_r + iz_i)} dz_r, \quad (3.36)$$

if the functions $f(x)$ and $g(x)$ are well behaved at z_i . This will be an important property for later purposes.

Further informations on the topic and a comprehensive reference for the theory of characteristic functions can be found in Lukacs (1970). More detailed discussions in the context of Fourier transforms can be found in Rudin (1987) and Titchmarsh (1975). Broad treatments of Fourier Theory including other scientific fields are e.g. Allen and Mills (2004) and Duffy (2004).

4 Pricing Formulae using Characteristic Functions

With the knowledge of the characteristic function of the stochastic process determining the price dynamic of the state variables option prices are available by

Fourier inversion methods. In general there are two approaches in literature considering inverse Fourier transform. The first approach obtains option prices with respect to the Fourier inversion of cumulative distribution functions with an appearance like the classical Black–Scholes formula. This route was pioneered by the famous work of [Heston \(1993\)](#) and was refined and extended in many ways. Most noticeable is the work by [Bakshi and Madan \(2000\)](#) who give a clear economical interpretation of characteristic functions with respect to market completeness and Arrow–Debreu securities in a state space framework. [Ross \(1976\)](#) showed that options are completing or spanning markets by expanding the asset space. [Bakshi and Madan \(2000\)](#) demonstrate that markets can be equivalently spanned by characteristic functions.

It is convenient to specify the characteristic function ϕ_T as the expected value of the complex exponential of the logarithmic price $x = \ln S_T$

$$\phi_T(u) = \mathbb{E}[e^{iux}] = \int_{-\infty}^{\infty} e^{iux} q_T(x) dx, \quad (4.1)$$

where q_T is the risk neutral density of x relative to the martingale measure \mathbb{Q} . By Euler identity we can express $\phi_T(u)$ as $\mathbb{E}^{\mathbb{Q}}[\cos(ux) + i \sin(ux)]$. As we have seen the payoff of a European option can be replicated by a portfolio of Arrow–Debreu securities and similarly the payoff on characteristic functions can be composed of trigonometric sine and cosine functions. Therefore the characteristic function can be viewed as an Arrow–Debreu security in Fourier space

$$\delta(e^x - K) = \frac{1}{2\pi} \int_{-\infty}^{\infty} e^{-iu(e^x - K)} du. \quad (4.2)$$

The characteristic function of the state price density is defined as follows

$$\begin{aligned} \phi_T(u) &= \mathbb{E}[e^{-rT} e^{iux}], \\ &= \int_{-\infty}^{\infty} e^{iux} e^{-rT} q_T(x) dx, \end{aligned} \quad (4.3)$$

which corresponds to a hypothetical claim that pays e^{iux} at T .

The second approach considers the pricing of options analogue to the Fourier inversion of the probability density function. [Carr and Madan \(1999\)](#) show how this analogy can be used by analytically relating the Fourier transform of an option to its characteristic function. Along the same idea [Lewis \(2001\)](#) develops an option pricing framework where the payoff structure is modeled explicitly and takes the Fourier transform with respect to the state variable, whereas [Carr and Madan \(1999\)](#) apply the transform to the strike value. In these cases the argument of the characteristic function is evaluated in a particular domain of the complex plane depending on the specific option payoff to ensure the existence of the Fourier transform.

Both Fourier inversion methodologies are applicable to a wide range of European payoff structures. In the following we will focus on European options to illustrate the

various transform methods prevailing in the option pricing literature. Starting from the quasi Black–Scholes formula first introduced in [Heston \(1993\)](#), we discuss the similar developments by [Attari \(2004\)](#) and [Bates \(2006\)](#) and move on to the more flexible [Carr and Madan \(1999\)](#), [Lewis \(2001\)](#) and [Lipton \(2002\)](#) option price characterizations.

4.1 The Black–Scholes Style Formula

Beginning with [Heston \(1993\)](#), many authors use the Fourier inversion methods to solve advanced valuation problems. Generalizing previous work [Bakshi and Madan \(2000\)](#) demonstrate the power and versatility of using characteristic functions for the pricing of contingent claims. They illustrate the use of Fourier transformed state price densities or Arrow–Debreu securities respectively, and how generic payoffs can be spanned by positions in characteristic functions. In fact [Bakshi and Madan \(2000\)](#) reduce the valuation problem to the estimation of Arrow–Debreu securities under appropriately modified equivalent probability measures.

The price of a European call with spot S and strike K is

$$\begin{aligned} C(S_0, K, T) &= e^{-rT} \mathbb{E}^{\mathbb{Q}}[(S_T - K)^+], \\ &= e^{-rT} \int_0^\infty (S_T - K)^+ q(S_T) dS_T. \end{aligned} \quad (4.4)$$

Decomposing the expression yields a portfolio of Arrow–Debreu securities

$$\begin{aligned} C(S_0, K, T) &= e^{-rT} \int_K^\infty S_T q(S_T) dS_T - e^{-rT} K \int_K^\infty q(S_T) dS_T, \\ &= e^{-rT} \int_k^\infty e^x q(x) dx - e^{-rT} K \int_k^\infty q(x) dx, \\ &= S \Pi_1 - e^{-rT} K \Pi_2, \end{aligned} \quad (4.5)$$

where $k = \ln K$. The quantities Π_1 and Π_2 are both conditional probabilities of finishing in-the-money at maturity. Π_1 is computed with the stock as numéraire asset whereas Π_2 is computed with a zero coupon bond as underlying numéraire asset. For Π_2 we use $\int_k^\infty q(x) dx$ which is the probability $\mathbb{P}(x \geq k)$. The characteristic function for Π_2 is $\phi_2(u) = \phi_T(u) = \int_{-\infty}^\infty e^{iux} q_T(x) dx$, hence

$$\Pi_2 = \int_k^\infty \left(\frac{1}{2\pi} \int_{-\infty}^\infty e^{-iux} \phi_T(u) du \right) dx. \quad (4.6)$$

Changing the order of integration yields to

$$\Pi_2 = \frac{1}{2\pi} \int_{-\infty}^\infty \phi_T(u) \left(\int_k^\infty e^{-iux} dx \right) du, \quad (4.7)$$

which simplifies to

$$\Pi_2 = \frac{1}{2} + \frac{1}{\pi} \int_0^\infty \Re \left[\frac{e^{-iuk} \phi_T(u)}{iu} \right] du. \quad (4.8)$$

The situation for $\Pi_1 = e^{-rT} \int_0^\infty e^x q(x) dx$ is a bit more subtle, since in this case the stock serves as numéraire. Introducing a change of measure from \mathbb{Q} to $\tilde{\mathbb{Q}}$ by a Radon-Nikodym derivative [compare [Geman & al. \(1995\)](#)] we get

$$\frac{d\tilde{\mathbb{Q}}}{d\mathbb{Q}} = \frac{e^{x_T}}{\mathbb{E}[e^{x_T}]}. \quad (4.9)$$

With this new measure $\tilde{\mathbb{Q}}$ the Fourier transform of Π_1 is defined as

$$\mathbb{E}^{\tilde{\mathbb{Q}}}[e^{iux}] = \frac{\mathbb{E}[e^{x_T} e^{iux}]}{\mathbb{E}[e^{x_T}]} = \frac{\phi_T(u - i)}{\phi_T(-i)}. \quad (4.10)$$

Because of the no arbitrage condition $\mathbb{E}^{\mathbb{Q}}[S_T] = S_0 e^{rT}$ we get $\phi_T(-i)$ as its characteristic function and for $\mathbb{E}[e^{x_T} e^{iux}]$ we get $\phi_T(u - i)$. Further note that $e^x q(x)$ is nonnegative for all x and the integral over $(0, \infty)$ equals one. Hence, we can treat $\mathbb{E}^{\tilde{\mathbb{Q}}}[e^{iux}]$ as a probability function and invert it accordingly

$$\Pi_1 = \frac{1}{2} + \frac{1}{\pi} \int_0^\infty \Re \left[\frac{e^{-iuk} \phi_T(u - i)}{iu \phi_T(-i)} \right] du. \quad (4.11)$$

The specific form of the formulae depend on the chosen definition of the characteristic function, i.e. whether it is defined for $\ln \frac{S_T}{S_0} - rT$ or $\ln S_T$ [see Section 5.2]. By using the second definition and depending on the definition of k , the above expression can be rewritten in a slightly different form. For example, by changing k to a ‘dimensionless’ moneyness $k = \ln \frac{S_0}{K} + rT$ we obtain [as described in [Lewis \(2001\)](#)]

$$\Pi_1 = \frac{1}{2} + \frac{1}{\pi} \int_0^\infty \Re \left[\frac{e^{iuk} \phi_T(u - i)}{iu} \right] du, \quad (4.12)$$

$$\Pi_2 = \frac{1}{2} + \frac{1}{\pi} \int_0^\infty \Re \left[\frac{e^{iuk} \phi_T(u)}{iu} \right] du. \quad (4.13)$$

The two integrals Π_1 and Π_2 can be combined into one integral. By rearranging the involved equations the Black-Scholes style formula for a call option reduces to

$$\begin{aligned} C(S_0, K, T) &= \frac{1}{2} (S_t - e^{-rT} K) \\ &+ \frac{1}{\pi} \int_0^\infty S_0 \Re \left[\frac{e^{iuk} \phi_T(u - i)}{iu} \right] - e^{-rT} K \Re \left[\frac{e^{iuk} \phi_T(u)}{iu} \right] du. \end{aligned} \quad (4.14)$$

While most authors use the real part of the complex valued integrand, it is also possible to use equation (3.18) instead of (3.17) [see, e.g. [Duffie & al. \(2000\)](#) and [Bates \(1996\)](#)]. This leads to

$$\Pi_j = \frac{1}{2} + \frac{1}{\pi} \int_0^\infty \Im \left[\frac{e^{-iuk} \phi_j(u)}{u} \right] du. \quad (4.15)$$

Applying Euler identity to the probabilities Π_1 and Π_2 it yields to

$$\Pi_j = \frac{1}{2} + \frac{1}{\pi} \int_0^\infty \frac{\Im[\phi_j(u)] \cos(uk) - \Re[\phi_j(u)] \sin(uk)}{u} du. \quad (4.16)$$

4.2 Attari's Approach

Attari (2004) proposes a modification to the Black–Scholes Style solution. His inversion formula exploits the inherent relationship between the two probabilities Π_1 and Π_2 of a European option. Merging the two integrals Π_1 and Π_2 into one expression the calculation requires only one integral. Pointing out that $q(x) = \frac{1}{2\pi} \int_{-\infty}^\infty e^{-iux} \phi_T(u) du$ and $\Pi_1 = \int_k^\infty e^x q(x) dx$, substituting the expression for $q(x)$ in Π_1 and defining $k = \ln \frac{Ke^{-rT}}{S_0}$ yields

$$\Pi_1 = \int_k^\infty e^x \left(\frac{1}{2\pi} \int_{-\infty}^\infty e^{-iux} \phi_T(u) du \right) dx. \quad (4.17)$$

Changing the order of integration by Fubini's theorem gives

$$\Pi_1 = \frac{1}{2\pi} \int_{-\infty}^\infty \phi_T(u) \left(\int_k^\infty e^x e^{-iux} dx \right) du. \quad (4.18)$$

Using the fact that $\Pi_1|_{k=-\infty} = 1$, since a zero strike option equals S , we have

$$\begin{aligned} \Pi_1 &= \frac{1}{2} + \frac{1}{4\pi} \int_{-\infty}^\infty \phi_T(u) \left(\int_k^\infty e^x e^{-iux} dx \right) du, \\ &\quad - \frac{1}{4\pi} \int_{-\infty}^\infty \phi_T(u) \left(\int_{-\infty}^k e^x e^{-iux} dx \right) du. \end{aligned} \quad (4.19)$$

Integrating the expression yields

$$\begin{aligned} \Pi_1 &= \frac{1}{2} + \frac{1}{2\pi} \int_{-\infty}^\infty \phi_T(u) \frac{e^{-i(u+i)k}}{i(u+i)} du \\ &\quad - \frac{1}{4\pi} \lim_{R \rightarrow \infty} \int_{-\infty}^\infty \phi_T(u) \left(\frac{e^{i(u+i)R} + e^{-i(u+i)R}}{i(u+i)} \right) du. \end{aligned} \quad (4.20)$$

Expanding the last term and taking $u \rightarrow -u$ in the resulting second term gives

$$\frac{1}{4\pi} \lim_{R \rightarrow \infty} \int_{-\infty}^\infty \phi_T(u) \left(\frac{e^{i(u+i)R}}{i(u+i)} \right) du - \frac{1}{4\pi} \lim_{R \rightarrow \infty} \int_{-\infty}^\infty \phi_T(-u) \left(\frac{e^{i(u-i)R}}{i(u-i)} \right) du. \quad (4.21)$$

In the first integrand we have a pole at $u = -i$ while for the integrand we have a pole at $u = i$. By using Residue Theorem the second integral for Π_1 and $2\pi i$ times the residues at its poles we get $2\pi i(\text{Res}(-i) + \text{Res}(i)) = 2\pi i\left(-\frac{i\phi_T(-i)}{4\pi}\right) = \frac{\phi_T(-i)}{2}$

$$\Pi_1 = \frac{1}{2} + \frac{1}{2\pi} \int_{-\infty}^{\infty} \phi_T(u) \frac{e^{-i(u+i)k}}{i(u+i)} du + \frac{\phi_T(-i)}{2}. \quad (4.22)$$

The term $\phi_T(-i)$ equals 1 (since $\Pi_1|_{k=-\infty} = 1$), hence we have

$$\Pi_1 = 1 + \frac{e^k}{2\pi} \int_{-\infty}^{\infty} \frac{e^{-iuk} \phi_T(u)}{i(u+i)} du. \quad (4.23)$$

Bringing it together with the expression of the call value this results in

$$\begin{aligned} C(S_0, K, T) = S_0 & \left(1 + \frac{e^k}{2\pi} \int_{-\infty}^{\infty} \frac{e^{-iuk} \phi_T(u)}{i(u+i)} du \right) \\ & - e^{-rT} K \left(\frac{1}{2} + \frac{1}{2\pi} \int_{-\infty}^{\infty} \frac{e^{-iuk} \phi_T(u)}{iu} du \right). \end{aligned} \quad (4.24)$$

Rearranging terms, applying Euler identity, and symmetry for real valued functions finally turns to

$$\begin{aligned} C(S_0, T, K) = S_0 & - \frac{1}{2} e^{-rT} K \\ & - e^{-rT} K \frac{1}{\pi} \int_0^{\infty} \frac{\left(\Re[\phi(u)] + \frac{\Im[\phi(u)]}{u} \right) \cos(uk) + \left(\Im[\phi(u)] - \frac{\Re[\phi(u)]}{u} \right) \sin(uk)}{1 + u^2} du. \end{aligned} \quad (4.25)$$

This formulation offers a pricing formula involving a single one dimensional integration. We note that in comparison to the Black-Scholes like solution the integrand now has a quadratic term in the denominator which ensures a faster convergence of the integrand.

4.3 Bates' Approach

A similar approach to that of Attari (2004) is outlined in Bates (2006). Here, the value of a European call option is evaluated by using the discounted CDF $\frac{\partial C}{\partial K} = -e^{-rT} \int_K^{\infty} q(S_T) dS_T$ [see Breeden and Litzenberger (1978)], substituting the inversion formula for an arbitrary stochastic process governing $q(S_T)$, and finally integrating with respect to K results in

$$C(S_0, T, K) = S_0 - e^{-rT} K \left(\frac{1}{2} + \frac{1}{2\pi} \int_{-\infty}^{\infty} \frac{e^{-iu \ln \frac{K}{S_0}} \phi_T(u)}{iu(1-iu)} du \right). \quad (4.26)$$

S_0 is an integration constant determined by the value of a zero strike call. Using the fact that option prices are real valued yields to

$$C(S_0, T, K) = S_0 - e^{-rT} K \left(\frac{1}{2} + \frac{1}{\pi} \int_0^\infty \Re \left[\frac{e^{-iu \ln \frac{K}{S_0}} \phi_T(u)}{iu(1 - iu)} \right] du \right). \quad (4.27)$$

Compared to the Black–Scholes style solution an advantage against is that this formulation requires only one integration and has an integrand which will converge faster due to the quadratic term in the denominator.

4.4 Carr and Madan Approach

Carr and Madan (1999) develop a different method designed to use the fast Fourier transform (FFT) to value options. Unfortunately, the FFT cannot be applied directly to evaluate the integrals we mentioned above, since the integrands are singular at the evaluation point $u = 0$. Therefore, instead of solving for the risk neutral exercise probabilities of finishing in-the-money they introduce a new technique with the key idea to calculate the Fourier transform of a *modified* call option price with respect to the logarithmic strike price k . With this specification and a FFT routine a whole range of option prices can be obtained within a single Fourier inversion.

Again, beginning from the risk neutral valuation formula and a change of variables $x = \ln S_T$ and $k = \ln K$ we get for a European call option

$$\begin{aligned} C_T(k) &= e^{-rT} \mathbb{E}^{\mathbb{Q}}[(S_T - K)^+], \\ &= e^{-rT} \int_k^\infty (e^x - e^k) q(x) dx. \end{aligned} \quad (4.28)$$

Unfortunately, expressing the call in terms of the log strike in (4.28), $C(k)$ tends to S_0 as k goes to $-\infty$

$$\begin{aligned} C_T(k) &= e^{-rT} \int_{-\infty}^\infty (e^x - e^{-\infty}) q(x) dx, \\ &= e^{-rT} \int_{-\infty}^\infty e^x q(x) dx, \\ &= e^{-rT} \mathbb{E}^{\mathbb{Q}}[e^x]. \end{aligned} \quad (4.29)$$

From martingale property $\mathbb{E}^{\mathbb{Q}}[S_T] = S_0 e^{rT}$ we see that $\lim_{k \rightarrow -\infty} C(k) = S_0$ is not converging to zero. Hence, $C(k)$ is not L^1 and a Fourier transform does not exist [see integrability condition (3.28)]. However, by introducing an exponential damping factor $e^{\alpha k}$ with $\alpha > 0$ it is possible to make $C(k)$ an integrable function

$$c_T(k) = e^{\alpha k} C_T(k), \quad (4.30)$$

where the modified call price $c_T(k)$ is an integrable function, since

$$\int_{-\infty}^{\infty} |e^{\alpha k} C_T(k)| dk < \infty, \quad (4.31)$$

for a suitable α . The effect of an exponential damping factor on the integrability of call price functions is shown in Figure 3.

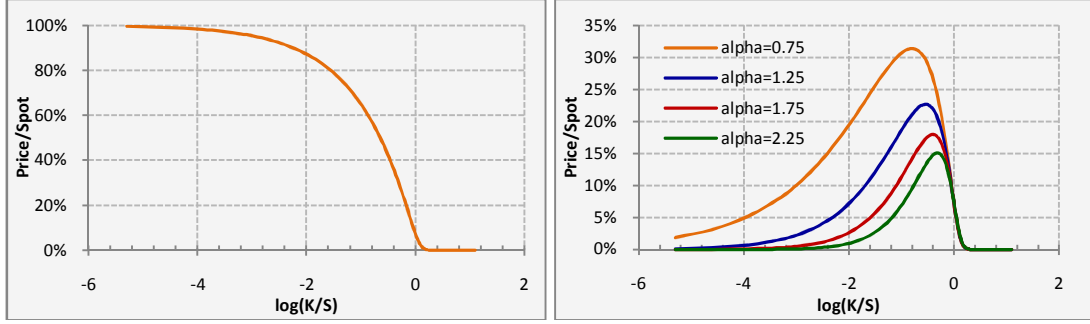


Figure 3: Effect of damping on the square integrability of call price functions. Left: Without damping the call price tends to S_0 as k approaches minus infinity. Right: Damping the call price function with different values for the damping factor α . Heston model parameters: $S = K = 100$, $T = 1$, $r = 0.05$, $\kappa = 2$, $\theta = 0.01$, $\rho = -0.5$, $\sigma_v = 0.25$ and $v_0 = 0.02$.

The Fourier transform of $c(k)$ is then given by

$$\begin{aligned} \psi(u) &= \int_{-\infty}^{\infty} e^{iuk} c(k) dk, \\ &= \int_{-\infty}^{\infty} e^{iuk} \int_{-\infty}^{\infty} e^{\alpha k} e^{-rT} (e^x - e^k)^+ q(x) dx dk, \\ &= \int_{-\infty}^{\infty} e^{iuk} \int_k^{\infty} e^{\alpha k} e^{-rT} (e^x - e^k) q(x) dx dk, \\ &= \int_{-\infty}^{\infty} e^{-rT} q(x) \left(\int_{-\infty}^x (e^x - e^k) e^{iuk} e^{\alpha k} dk \right) dx. \end{aligned} \quad (4.32)$$

For the inner integral, representing the call payoff, we get

$$\begin{aligned} \int_{-\infty}^x (e^x - e^k) e^{iuk} e^{\alpha k} dk &= e^x \int_{-\infty}^x e^{(\alpha+iu)k} dk - \int_{-\infty}^x e^{(\alpha+iu+1)k} dk, \\ &= \frac{e^x}{\alpha + iu} [e^{(\alpha+iu)k}]_{-\infty}^x - \frac{1}{\alpha + iu + 1} [e^{(\alpha+iu+1)k}]_{-\infty}^x. \end{aligned} \quad (4.33)$$

Taking the limit for $\lim_{k \rightarrow -\infty} e^{(\alpha+iu)k} = 0$ with $\alpha > 0$ we get

$$\left(\frac{e^{(\alpha+1+iu)x}}{\alpha + iu} - \frac{e^{(\alpha+1+iu)x}}{\alpha + 1 + iu} \right). \quad (4.34)$$

Hence leading to

$$\begin{aligned}\psi(u) &= \int_{-\infty}^{\infty} e^{-rT} q(x) \left(\frac{e^{(\alpha+1+iu)x}}{\alpha+iu} - \frac{e^{(\alpha+1+iu)x}}{\alpha+1+iu} \right) dx, \\ &= e^{-rT} \int_{-\infty}^{\infty} q(x) \frac{e^{(\alpha+1+iu)x}}{(\alpha+iu)(\alpha+1+iu)} dx.\end{aligned}\quad (4.35)$$

Taking the Fourier transform for $\int_{-\infty}^{\infty} q(x) e^{(\alpha+1+iu)x} = \int_{-\infty}^{\infty} q(x) e^{i(u-(\alpha+1))x}$ we get the characteristic function for the risk neutral price process $\phi_T(u - (\alpha+1)i)$.

Finally we have

$$\psi(u) = \frac{e^{-rT} \phi_T(u - (\alpha+1)i)}{\alpha^2 + \alpha - u^2 + i(2\alpha+1)u}, \quad (4.36)$$

where $\psi(u)$ is expressed in terms of the characteristic function ϕ_T .

In a last step, given $\psi(u)$, an inverse Fourier transform multiplied by the reciprocal of the exponential factor yields to the undamped call prices

$$\begin{aligned}C_T(k) &= \frac{e^{-\alpha k}}{2\pi} \int_{-\infty}^{\infty} e^{-iuk} \psi(u) du, \\ &= \frac{e^{-\alpha k}}{\pi} \int_0^{\infty} \Re[e^{-iuk} \psi(u)] du.\end{aligned}\quad (4.37)$$

This method is viable when α is chosen in a way that the damped option price is well behaved. Damping the option price with $e^{\alpha k}$ makes it integrable for the negative axis $k < 0$. On the other hand for $k > 0$ the option prices increase by the exponential $e^{\alpha k}$ which influences the integrability for the positive axis. A sufficient condition of $c_T(k)$ to be integrable for both sides (square integrability) is given by $\psi(0)$ being finite [compare Section 3.3 on the Fourier transform to square integrable functions via the Plancherel–Parseval identity]. With $u = 0$

$$\psi(0) = \frac{e^{-rT} \phi_T(-(\alpha+1)i)}{\alpha^2 + \alpha}. \quad (4.38)$$

Thus we need $\phi_T(-(\alpha+1)i) < \infty$ which is equivalent to

$$\phi_T(-(\alpha+1)i) = \mathbb{E}^{\mathbb{Q}}[S_T^{1+\alpha}] < \infty \quad (4.39)$$

Therefore, $c_T(k)$ is well behaved when the moments of order $1 + \alpha$ of the underlying exist and are finite. If not all moments of S_T exist, this will impose an upper bound on α .

The corresponding put values can be obtained by defining

$$p_T(k) = e^{-\alpha k} P_T(k), \quad (4.40)$$

with Fourier transform

$$\psi_p(u) = \frac{e^{-rT} \phi_T(u - (-\alpha+1)i)}{\alpha^2 - \alpha - u^2 + i(-2\alpha+1)u}. \quad (4.41)$$

And finally the put prices can be written as

$$P_T(k) = \frac{e^{\alpha k}}{\pi} \int_0^\infty \Re[e^{-iuk} \psi_p(u)] du. \quad (4.42)$$

For the put formula to be well defined, it suffices to choose an appropriate $\alpha > 0$ in a way that $\mathbb{E}^\mathbb{Q}[S_T^{-\alpha}] < \infty$ [see Lee (2004)].

The Carr and Madan (1999) formulation is different to the previous described ones in a sense that not only the risk neutral density function but the whole option price is Fourier transformed. This is possible through the introduction of an additional degree of freedom which makes the integral in (4.37) in fact a generalized Fourier transform, since

$$\begin{aligned} \frac{1}{2\pi} \int_{iz_i - \infty}^{iz_i + \infty} e^{-izk} \psi(z) dz_r &= \frac{1}{\pi} \int_{0+iz_i}^{\infty+iz_i} \Re[e^{-izk} \psi(z)] dz_r, \\ &= \frac{e^{z_i k}}{\pi} \int_0^\infty \Re[e^{-iz_r k} \psi(z_r + iz_i)] dz_r. \end{aligned} \quad (4.43)$$

Therefore, the modification technique removes the non-smooth-behavior of the pole at the origin by shifting the pole to a less numerically sensitive position on the imaginary axis. The interpretation of the integration of a damped function as a contour integral in the complex plane is first considered by Lewis (2001) and is discussed in detail in Lee (2004).

Carr and Madan (1999) notice that for very short maturities, the call value approaches its non analytic intrinsic value causing the integrand in the Fourier inversion to be highly oscillatory and therefore difficult to integrate numerically. To mitigate this numerical inconvenience, the authors propose an alternative approach which they call the Time Value method. The reasoning is quite similar to the previous approach. But in this case the call price is obtained via the Fourier transform of a modified time value, where the modification involves a hyperbolic sine function instead of an exponential function.

Let $z_T(k)$ denote the time value of an out-of-the-money option, i.e. for $k < x$ we have the put price for $z_T(k)$ and for $k > x$ we have the call price. Scaling $S_0 = 1$ for simplicity, $z_T(k)$ is defined by

$$z_T(k) = e^{-rT} \int_{-\infty}^\infty [(e^x - e^k) \mathbb{I}_{x < k, k < 0} + (e^x - e^k) \mathbb{I}_{x > k, k > 0}] q(x) dx, \quad (4.44)$$

where \mathbb{I} denotes the indicator function. Furthermore let $\xi_T(u)$ be the Fourier transform of $z_T(k)$

$$\xi_T(u) = \int_{-\infty}^\infty e^{iuk} z_T(k) dk. \quad (4.45)$$

The prices of out-of-the-money options can be obtained by an inverse Fourier transform

$$z_T(k) = \frac{1}{2\pi} \int_{-\infty}^{\infty} e^{-iuk} \xi_T(u) du. \quad (4.46)$$

By substituting (4.44) into (4.45) and writing in terms of characteristic functions¹ the expression for $\xi_T(u)$ follows as

$$\xi_T(u) = e^{-rT} \left(\frac{1}{iu + 1} - \frac{\phi_T(-i)}{iu} - \frac{\phi_T(u - i)}{iu(iu + 1)} \right). \quad (4.47)$$

There are no issues regarding the integrability of this function as k tends to ∞ or $-\infty$, but the time value at $k = 0$ can get rather steep as $T \rightarrow 0$ which is making the Fourier transform wide and oscillatory. This effect can be alleviated by considering a damping function $\sinh(\alpha k)$

$$\begin{aligned} \gamma_T(u) &= \int_{-\infty}^{\infty} e^{iuk} \sinh(\alpha k) z_T(k) dk, \\ &= \int_{-\infty}^{\infty} e^{iuk} \frac{e^{\alpha k} - e^{-\alpha k}}{2} z_T(k) dk, \\ &= \frac{\xi_T(u - i\alpha) - \xi_T(u + i\alpha)}{2}. \end{aligned} \quad (4.48)$$

Hence, the time value of an option follows a Fourier inversion

$$\begin{aligned} z_T(k) &= \frac{1}{\sinh(\alpha k)} \frac{1}{2\pi} \int_{-\infty}^{\infty} e^{-iuk} \gamma_T(u) du, \\ &= \frac{1}{\sinh(\alpha k)} \frac{1}{\pi} \int_0^{\infty} e^{-iuk} \gamma_T(u) du. \end{aligned} \quad (4.49)$$

Another refinement to the sharp peak at $k = 0$ is due to the simple observation that $k < x$ for puts and $k > x$ for calls unnecessarily creates a small discontinuity in $z_T(0)$. By using $\ln F$ with $F = Se^{rT}$ instead, $z_T(k)$ is ensured to be continuous [see McCulloch (2003)]. The Time Value modification is also designed for the use of the FFT and claims more regular results for short maturities.

4.5 Lewis' Approach

The Fourier pricing setup introduced in Lewis (2001) generalizes previous work on Fourier transform methods². Key to his contribution is the idea to express the option value as convolution of generalized Fourier transforms and then apply the

¹ The formulation slightly differs from the one in Carr and Madan (1999), there seems to be no uniformity for the normalization of $\phi_T(-i)$. If the martingale property requires $\phi_T(-i) = e^{rT}$ the expressions are all equal.

² The pricing method was first developed in Lewis (2000) as 'The Fundamental Transform', however, due to the detailed discussion and thorough derivations in Lewis (2001), the pricing framework is commonly referred to as the Lewis (2001) methodology.

Plancherel–Parseval identity instead of integrating over a discounted transition density times a payoff function. The transform representations of option prices may be interpreted as contour integrals in the complex plane. By shifting the contours and applying Residual Calculus it is possible to generate alternative pricing formulae.

For each derivative there exists a known payoff function $w(S_T)$ at maturity. The payoff for a call option is $w(x) = (e^x - K)^+$ with $x = \ln S_T$. Instead of transforming the whole option price including the payoff function as described in Carr and Madan (1999), Lewis (2001) emphasizes the fact that payoff functions also have representations in Fourier space $\hat{w}(z) = \int_{-\infty}^{\infty} e^{izx} w(x) dx$. Unfortunately, $(e^x - K)^+$ is an unbounded function and does not belong to L^1 . Thus, the defining integral is not finite as $\hat{w}(z) = \mathcal{F}[w(x)] \rightarrow \infty$ and the Fourier transform does not exist. This issue can be circumvented by considering an exponential damping factor, just like in the Carr and Madan (1999) approach. For a modified payoff we have a regular Fourier transform, since $(e^x - K)^+ e^{-z_i x} \rightarrow 0$ as $x \rightarrow \infty$ for some appropriate z_i . This corresponds to a Fourier transform along a line in the complex plane where the path of integration is parallel to the real axis. A direct calculation for the call option payoff yields to

$$\begin{aligned}
 \hat{w}(z) &= \int_{-\infty}^{\infty} e^{izx} (e^x - K)^+ dx, \\
 &= \int_{\ln K}^{\infty} e^{izx} (e^x - K) dx, \\
 &= \left(\frac{e^{(iz+1)x}}{iz+1} - K \frac{e^{izx}}{iz} \right) \Big|_{\ln K}^{x=\infty}, \\
 &= 0 - \left(\frac{K^{iz+1}}{iz+1} - K \frac{K^{iz}}{iz} \right), \\
 &= -\frac{K^{iz+1}}{z^2 - iz}, \tag{4.50}
 \end{aligned}$$

with z being a complex valued number. The upper limit $x = \infty$ only exist under the condition $\Im[z] > 1$ which implies that the Fourier transform is well behaved only within a certain strip of regularity \mathcal{S}_w in the complex domain (K^{iz+1} has a branch point at $z = i$). It is interesting to note that the transformed payoff for the put has the same functional form, but it is defined in a different strip in the complex plane with $z_i < 0$.

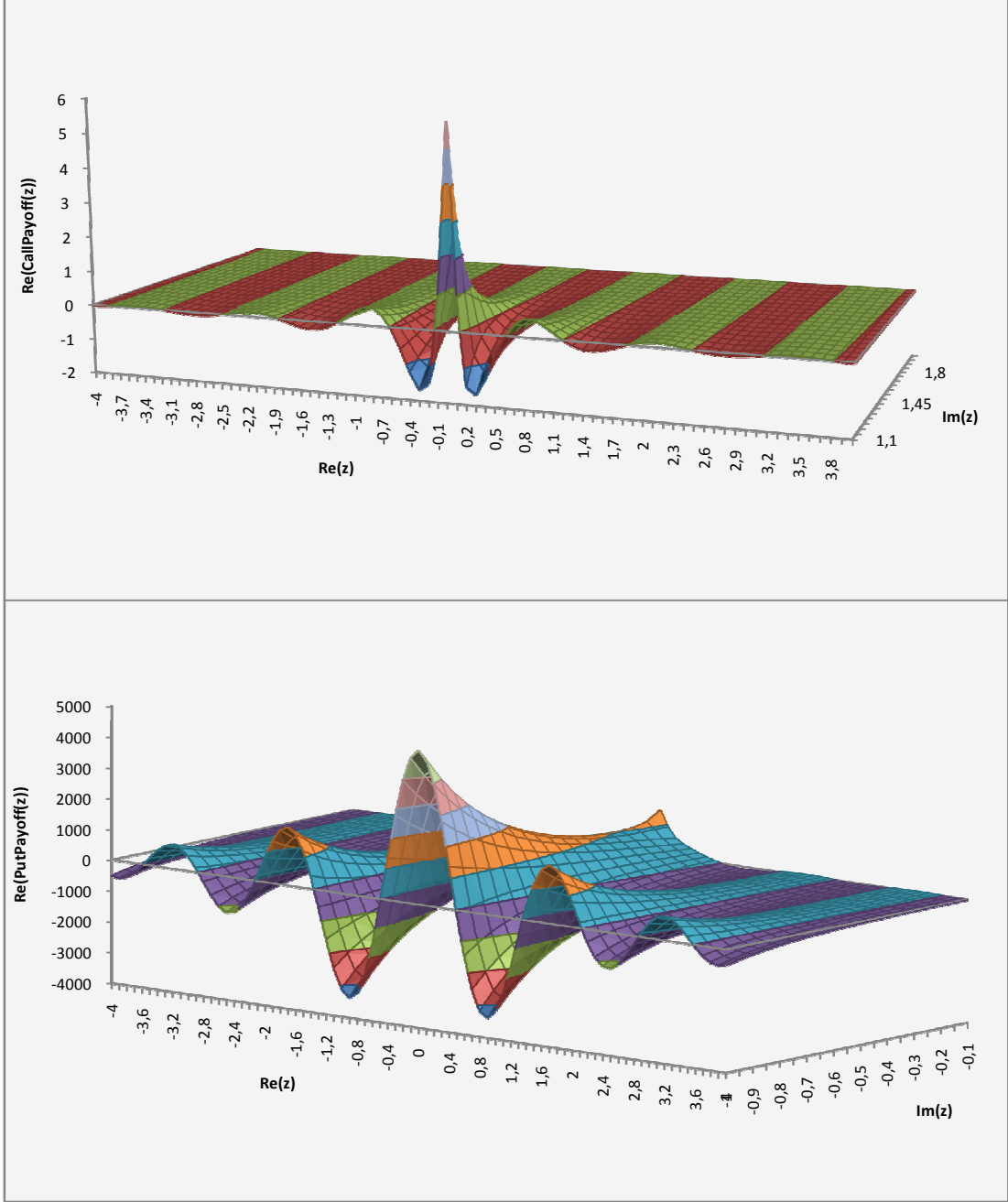


Figure 4: Strip of regularity for transformed call and put payoff functions. Upper figure: Strip for call options with $\Im[z] > 1$. Lower figure: Strip for put options with $\Im[z] < 0$.

In general, the strip of regularity is restricted to $\alpha < \Im[z] < \beta$ for typical derivatives payoffs with $(\alpha, \beta) \in \mathbb{R}$ [see Table 1]. Given the generalized payoff transform the corresponding inverse transform is then

$$w(x) = \frac{1}{2\pi} \int_{i z_i - \infty}^{i z_i + \infty} e^{-izx} \hat{w}(z) dz. \quad (4.51)$$

Table 1: Generalized Fourier Transforms for a variety of financial claims. The expression $\delta(x - x_o)$ denotes the Dirac delta function and \mathbb{I} is the indicator function.

Financial Claim	Payoff Function $w(x)$	Payoff Transform $\hat{w}(z) = \mathcal{F}[w(x)]$	Strip of Regularity \mathcal{S}_w
Call	$(e^x - K)^+$	$-\frac{K^{iz+1}}{z^2 - iz}$	$\Im[z] > 1$
Put	$(K - e^x)^+$	$-\frac{K^{iz+1}}{z^2 - iz}$	$\Im[z] < 0$
Covered Call; Cash-Secured Put	$\min\{e^x, K\}$	$\frac{K^{iz+1}}{z^2 - iz}$	$0 < \Im[z] < 1$
Cash-or-Nothing Call	$\mathbb{I}_{e^x \geq K}$	$-\frac{K^{iz}}{iz}$	$\Im[z] > 0$
Cash-or-Nothing Put	$\mathbb{I}_{e^x \leq K}$	$\frac{K^{iz}}{iz}$	$\Im[z] < 0$
Asset-or-Nothing Call	$e^x \mathbb{I}_{e^x \geq K}$	$-\frac{K^{iz+1}}{iz + 1}$	$\Im[z] > 1$
Asset-or-Nothing Put	$e^x \mathbb{I}_{e^x \leq K}$	$\frac{K^{iz+1}}{iz + 1}$	$\Im[z] < 0$
Delta function; Arrow-Debreu	$\delta(x - \ln K)$	K^{iz}	entire z -plane
Money market	1	$2\pi\delta(z)$	$\Im[z] = 0$

Assuming that we have a well defined characteristic function $\phi_T(z)$ with $z \in \mathcal{S}_X$ for an arbitrary price dynamic and a transformed payoff $\hat{w}(z)$ with $z \in \mathcal{S}_w$, we can proceed by applying martingale pricing to obtain the option value

$$\begin{aligned}
V(S_0, K, T) &= e^{-rT} \mathbb{E}^{\mathbb{Q}}[w(x)], \\
&= \frac{e^{-rT}}{2\pi} \mathbb{E}^{\mathbb{Q}} \left[\int_{iz_i - \infty}^{iz_i + \infty} e^{-izx} \hat{w}(z) dz \right], \\
&= \frac{e^{-rT}}{2\pi} \int_{iz_i - \infty}^{iz_i + \infty} \mathbb{E}^{\mathbb{Q}}[e^{-izx}] \hat{w}(z) dz, \\
&= \frac{e^{-rT}}{2\pi} \int_{iz_i - \infty}^{iz_i + \infty} \phi_T(-z) \hat{w}(z) dz.
\end{aligned} \tag{4.52}$$

Above we have stated that the extended characteristic function $\phi_T(z)$ with $z \in \mathbb{C}$ is well defined in \mathcal{S}_X . Due to the reflection symmetry property for a real valued function $\overline{\phi_T(z)} = \phi_T(-\bar{z})$, $\phi_T(-z)$ is well behaved in the conjugate strip of regularity $\overline{\mathcal{S}_X}$ as well, where the real z -axis is the line of symmetry. For the whole integral being well

behaved we need a $z \in \mathcal{S}_V$ in a way that there is a intersection between $\overline{\mathcal{S}_X}$ and \mathcal{S}_W ($\mathcal{S}_V = \overline{\mathcal{S}_X} \cap \mathcal{S}_W$). If the inversion contour is taken along this strip \mathcal{S}_V then the integral converges absolutely and we may change the order of integration by Fubini's Theorem. The change of integration is required to take the expectation inside the integral.

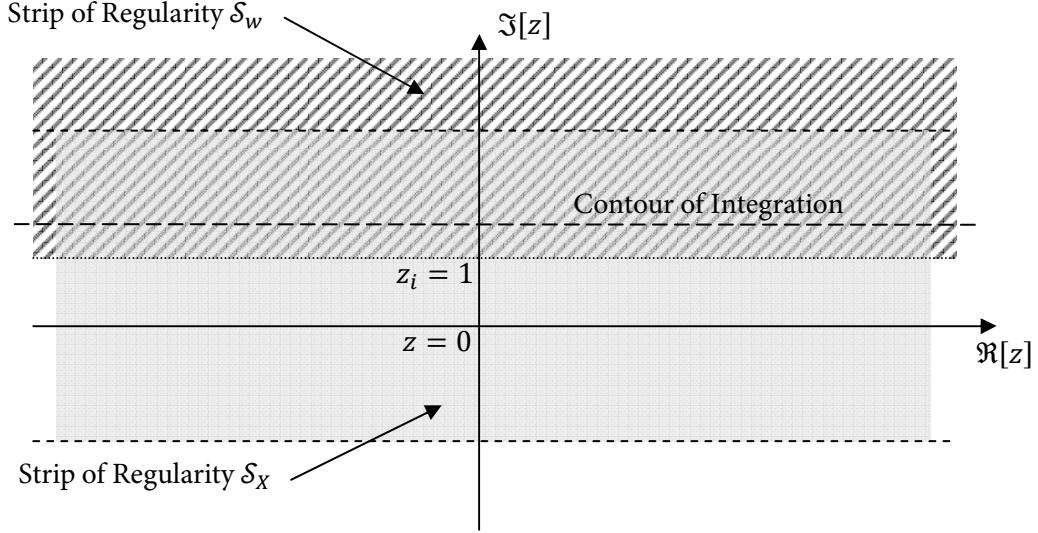


Figure 5: Contour of integration for the European call option. The contour of integration is shifted from the real axis to $z \in \mathcal{S}_V$ in order to make both the option payoff (here the call) and the price process well behaved.

The valuation formula is obtained by considering the integration of a state price density times the payoff function as a convolution representation in Fourier space by a direct application of the Plancherel–Parseval identity

$$e^{-rT} \int_{-\infty}^{\infty} w(x)q(x) dx = \frac{e^{-rT}}{2\pi} \int_{iz_i - \infty}^{iz_i + \infty} \phi_T(-z) \hat{w}(z) dz, \quad (4.53)$$

where $\phi_T(-z)$ is the conjugate Fourier transform of the risk neutral density of the log spot.

Applying the payoff transform of a call option (4.50) the call price is given by

$$C(S_0, K, T) = -\frac{K e^{-rT}}{2\pi} \int_{iz_i - \infty}^{iz_i + \infty} e^{-izk} \phi_T(-z) \frac{dz}{z^2 - iz}, \quad (4.54)$$

with $k = \ln \frac{S_0}{K} + rT$ in the phase factor e^{-izk} and $z_i \in \mathcal{S}_V$. With the definition of k , the forward stock price is equal to the strike price for the option at-the-money. Incidentally the same formula works for the put option value by imposing $z_i < 0$.

The integrand in (4.54) is regular in the strip $\overline{\mathcal{S}_X}$, except in the case where the denominator $z^2 - iz$ is zero. This will happen at two poles, at $z = 0$ and $z = i$. The residue for the pole at $z = i$ is

$$\begin{aligned}\text{Res}(i) &= \lim_{z \rightarrow i} \left[(z - i) \left(-\frac{K e^{-rT}}{2\pi} e^{-izk} \frac{\phi_T(-z)}{z^2 - iz} \right) \right], \\ &= \frac{S \phi_T(-i) i}{2\pi} = \frac{iS}{2\pi}.\end{aligned}\quad (4.55)$$

By moving the integration contour to $z_i \in (0,1)$ and according to the Residue Theorem the call option value must equal the integral along $\Im[z] = z_i$ minus $2\pi i$ times the residue at $z = i$ which is S . This is leading to a slightly different formula

$$C(S_0, K, T) = S_0 - \frac{K e^{-rT}}{2\pi} \int_{iz_i - \infty}^{iz_i + \infty} e^{-izk} \phi_T(-z) \frac{dz}{z^2 - iz}. \quad (4.56)$$

A convenient choice is to shift the contour by $z_i = \frac{1}{2}$, because then the path of integration is symmetrically located between the two poles. The change of variables $z = u + \frac{i}{2}$ and employing the symmetry property for real valued functions gives

$$\begin{aligned}C(S_0, K, T) &= S_0 - \frac{\sqrt{SK} e^{-rT/2}}{\pi} \int_0^\infty \Re \left[e^{-iuk} \phi_T \left(-u - \frac{i}{2} \right) \right] \frac{du}{u^2 + \frac{1}{4}}, \\ &= S_0 - \frac{\sqrt{SK} e^{-rT/2}}{\pi} \int_0^\infty \Re \left[e^{iuk} \phi_T \left(u - \frac{i}{2} \right) \right] \frac{du}{u^2 + \frac{1}{4}}.\end{aligned}\quad (4.57)$$

For this particular case the change of sign in the characteristic function does not change the value of the integral as long as the sign in the corresponding phase factor is changed as well. The first representation can be found in [Itkin \(2005\)](#) while in [Lewis \(2001\)](#) the lower expression is deduced.

For the put option a similar contour as in (4.54) can be used, however, the strip is then defined by $\Im[z] < 0$. By shifting the contour crossing both poles at $z = 0$ and $z = i$ we additionally pick up the residue for $z = 0$ and find that

$$\begin{aligned}\text{Res}(i) &= \lim_{z \rightarrow 0} \left[z \left(-\frac{K e^{-rT}}{2\pi} e^{-izk} \frac{\phi_T(-z)}{z^2 - iz} \right) \right], \\ &= -\frac{e^{-rT} K \phi_T(0) i}{2\pi} = -\frac{iK e^{-rT}}{2\pi}.\end{aligned}\quad (4.58)$$

By Residue Theorem we then find an alternative formulation for the put option

$$P(S_0, K, T) = K e^{-rT} - \frac{K e^{-rT}}{2\pi} \int_{iz_i - \infty}^{iz_i + \infty} e^{-izk} \phi_T(-z) \frac{dz}{z^2 - iz}. \quad (4.59)$$

Putting together the resulting formulae for calls and puts we obtain

$$C = S - e^{-rT} K + P, \quad (4.60)$$

and receive the put call parity relation.

By moving the contours to exactly $\Im[z] = 1$ and $\Im[z] = 0$ the integrals become principal value integrals and by Residue Calculus one half of the residues are picked up. Calculating the resulting two integrals at the two involved poles recover the Black-Scholes like solution [see [Lewis \(2000\)](#), [Lewis \(2001\)](#) and [Sepp \(2003\)](#) for details].

4.6 Lipton's approach

A similar approach to [Lewis \(2001\)](#) is described by [Lipton \(2002\)](#) in the context of FX option pricing. Lipton presents his approach tailored towards some selected models. First we state a general formulation

$$\begin{aligned} C(S_0, K, T) &= S_0 - \frac{Ke^{-rT}}{2\pi} \int_{-\infty}^{\infty} e^{(iu+\frac{1}{2})k} \phi_T\left(u - \frac{i}{2}\right) \frac{du}{u^2 + \frac{1}{4}}, \\ &= S_0 - \frac{Ke^{-rT}}{\pi} \int_0^{\infty} \Re \left[e^{(iu+\frac{1}{2})k} \phi_T\left(u - \frac{i}{2}\right) \right] \frac{du}{u^2 + \frac{1}{4}}. \end{aligned} \quad (4.61)$$

The derivation of the [Lipton \(2002\)](#) approach is similar to the reasoning of [Lewis \(2001\)](#) by considering a Plancherel–Parseval style relation [see [Lipton \(2001\)](#)].

As an example, we derive the formulation for Black–Scholes model given in [Lipton \(2002\)](#). Recalling the characteristic function for the Gaussian model (5.10) we have $\phi_{BS} = \exp \left[iz\omega T - \frac{1}{2} z^2 \sigma^2 T \right]$ with $\omega = -\frac{1}{2} \sigma^2$. Substituting $z = u + \frac{i}{2}$ into ϕ_{BS} gives $\exp \left[-\frac{\sigma^2}{2} T \left(u^2 + \frac{1}{4} \right) \right]$ and finally leads to

$$\begin{aligned} C_{BS}(S_0, K, T) &= S_0 - \frac{Ke^{-rT}}{2\pi} \int_{-\infty}^{\infty} \frac{e^{(iu+\frac{1}{2})k - (u^2+\frac{1}{4})\frac{\sigma^2}{2}T}}{u^2 + \frac{1}{4}} du, \\ &= S_0 - \frac{Ke^{-rT}}{\pi} \int_0^{\infty} \Re \left[e^{(iu+\frac{1}{2})k - (u^2+\frac{1}{4})\frac{\sigma^2}{2}T} \right] \frac{du}{u^2 + \frac{1}{4}}. \end{aligned} \quad (4.62)$$

We note that the Lipton formulation looks somewhat different to the Lewis approach, and they are in fact equivalent. The connection lies in between the term $\sqrt{SK}e^{-\frac{rT}{2}}$ in Lewis' formula and the phase factor $e^{(iu+\frac{1}{2})k}$ in Lipton's formula. Expanding the last term yields to $e^{iuk}e^{\frac{1}{2}k}$, then bringing $e^{\frac{1}{2}k}$ outside the integrand and using the definition of k , and we get the results of Lewis' representation.

4.7 Concluding Remarks and Recent Developments

In this section we revisited numerous Fourier inversion methods for the pricing of European options. There are a number of similarities and parallelisms between those prevailing concepts. The method developed at first in [Heston \(1993\)](#) offers the same

intuitive interpretation of the valuation problem as the classical Black–Scholes formula and it was remarked the method of choice for Fourier pricing applications until more efficient methods came up. The two methodologies from Attari (2004) and Bates (2006) exploit the tight relation of the risk neutral exercise probabilities offering a single integral solution with advantageous convergence properties. An algorithm similar to Attari (2004) and Bates (2006) is developed in Wu (2008) by treating an option value analogous to a cumulative density function.

In Lewis (2001), the direct relationship of the log spot characteristic function in Image space is used from a more general point of view by representing the valuation formulae as contour integrals in the complex plane. The impact of an additional damping parameter is hereby characterized as the effect on the option prices depending on the choice of a particular path of integration in the complex plane. In this sense, the Carr and Madan (1999) methodology appears as a special case of Lewis option pricing formulae. Another aspect is that the entire separation of Fourier transforms for the underlying price dynamics and the payoff function allows for a modular pricing framework which is facilitating particular valuation problems for more advanced payoff structures.

A great effort is made by Lee (2004) in unifying and generalizing the previous work of Duffie & al. (2000), Bakshi and Madan (2000), Carr and Madan (1999) and Lewis (2001). In Duffie & al. (2000) four different payoff classes are considered and are extended to the Carr and Madan (1999) framework. From Bakshi and Madan (2000) the concept of a *discounted* characteristic function is adapted to allow for stochastic interest rates. By recognizing the Carr and Madan (1999) formulation as a contour integral [see Lewis (2001)] complementary valuation formulae are provided by shifting the contour integrals in the complex plane and applying Residue Theory. Moreover Lee (2004) provides error bounds for the discretized Fourier inversion and discusses error minimization strategies.

Other authors have derived similar formulae for the valuation problem of European options. For example, the approach chosen by Raible (2000) is nearly identical to the Lewis (2001) methods by using a convolution representation for the expectation of the payoff at maturity. The only difference is considering a two sided (or bilateral) Laplace transform of a modified payoff function instead of a generalized Fourier transform. His discussion also includes other European payoffs like power and self-quanto options. The inversion integrals are then evaluated by means of the FFT algorithm. Besides, methods for simple vanilla products using similar assumptions like Raible (2000) or Lewis (2001), Borovkov and Novikov (2002) develop an approach for the valuation of barrier type options based on the integration of moment generating functions for general Lévy processes.

One purpose of this section is to give a detailed overview of the underlying theory to value options with Fourier inversion methods. These methods are refined in many ways for more elaborate valuation problems, or serve as building blocks to

other areas in the field of mathematical finance. In the following we concisely present more methods and techniques which are tightly related to the discussed approaches.

As mentioned previously, the Fourier transform based approach works for a lot of European payoff structures. Agliardi (2009) provides a comprehensive characterization for Compound Options, Multi-period Power Binaries, Power Digitals, and Supershare Options including relevant strips of regularity for arbitrary Lévy processes. While the mathematical foundations in Section 3 suffice for the payoff functions considered in this paper, more elaborate payoffs or multidimensional applications need a much more detailed consideration. A systematic analysis is offered by Eberlein & al. (2009) of the conditions required for the existence of Fourier transform formulae in a general framework, i.e. when options have arbitrary payoff functions and possibly depend on the path of the stochastic process.

Dempster and Hong (2000) introduce an integration methodology based on double fast Fourier transforms for spread option pricing that is efficient for geometric Brownian motion and more sophisticated price processes. A recent contribution for the use of Fourier transform methods for spread options comes from Hurd and Zhou (2009) by expressing the spread option payoff in terms of the gamma function and applying the FFT technology from Carr and Madan (1999).

The introduced Fourier techniques have been extended in many different ways, including the pricing of path dependent derivatives. For instance Cardi (2005) develops a valuation formula to discrete Barrier options based on the Lewis (2001) methodology. Use of FFT methods to price discrete Asian options is considered in Benhamou (2000).

A versatile numerical method to the valuation problem of early exercise options and certain path dependent options by means of a quadrature method (QUAD) is introduced in Andricopoulos & al. (2003). By recognizing that the payoff of an option can be segmented, the integration of the payoff is only carried out over continuous segments of the payoff and evaluated with numerical quadratures. However, the method requires analytical transition densities like the Gaussian. To relax this requirement O'Sullivan (2005) introduces the QUAD-FFT method, by considering the one to one connection from density functions with their characteristic functions makes the QUAD method applicable for a wide range of stochastic processes. Exotic features can be incorporated by applying the option pricing formula recursively. The Convolution method (CONV) developed in Lord & al. (2007) follows a similar idea by considering option values as a convolution of a payoff function with a probability distribution and taking the QUAD and QUAD-FFT methods into Fourier domain.

In an empirical study about Lévy option pricing models by Ji and Zapatero (2008) the authors extend the quadratic approximation method from Barone-Adesi and Whaley (1987) which approximates the early exercise premium of American options under Black-Scholes assumptions to exponential Lévy models. American options are then the sum of the European Fourier prices and the approximated early exercise premium.

It must not be the case that the characteristic functions are known in closed form, for instance the [Heston \(1993\)](#) characteristic function is an analytic solution to a system of ordinary differential equations (ODE). In fact, these ODE's can be solved numerically, too, which is often the only choice for similar advanced price dynamics [see e.g. [Dobránszky \(2009\)](#)]. Fourier pricing is even applicable in non parametric models by replacing the unknown characteristic function with its empirical version, e.g. [Binkowski \(2007\)](#) infers the empirical characteristic functions from quoted option prices and compares the results to some parametric cases.

[Kruse and Nögel \(2005\)](#) extend the Fourier valuation method to European forward starting options assuming the stochastic volatility framework initially introduced in [Heston \(1993\)](#) by a change of measure technique. [Nunes and Alcaria \(2009\)](#) amend the two dimensional [Kruse and Nögel \(2005\)](#) approach to a single integral solution based on the [Attari \(2004\)](#) formulation.

Fourier inversion methods are applicable for the efficient calculations of derivatives in other frameworks as well. By noting that the call and put like payoffs also occur frequently in insurance industry [Dufresne & al. \(2009\)](#) consider the Plancherel–Parseval identity to calculate stop-loss or excess-of-loss premiums. In addition to the exponential damping ensuring the integrability of the payoffs, they additionally examine polynomial damping factors and illustrate their findings with Compound Poisson, (Generalized) Pareto and α -stable distributions.

Another important area is the valuation of interest rate derivatives. [Attari \(2004\)](#) is also considering his modification to interest rate products. [Andreasen \(2006\)](#) develops a full yield curve model with stochastic volatility following the work of [Andersen and Andreasen \(2002\)](#) and using results from [Heston \(1993\)](#), [Lewis \(2000\)](#) and [Lipton \(2002\)](#). The resulting model resembles a *shifted* Heston model which allows the use of the introduced Fourier inversion techniques and gives good fit to observed cap and swaption prices.

In [Bouziane \(2008\)](#) a general pricing framework is established for the pricing of interest rate derivatives based on the methodology introduced in [Lewis \(2001\)](#). In this flexible framework a wide range of interest rate derivatives are priced with either conditional or unconditional exercise rights. He further develops an efficient method to price derivatives for a whole range of strike prices similar to the FFT methodology from [Carr and Madan \(1999\)](#) named the IFFT algorithm.

Fourier based methods also gain increasingly popularity in the field of defaultable assets. For example, [Grundke \(2007\)](#) presents an integrated market and credit portfolio model and extends the CreditMetrics model by correlated interest rate and credit spread risk. [Sepp \(2006\)](#) generalizes the CreditGrades model for stochastic volatility and jump diffusion specifications, estimates default probabilities using equity options, and applies these models for the modeling of credit default swap and equity default swap spreads. Stochastic volatility frameworks for credit and interest rate derivatives using numerical quadratures can be found in [Tahani \(2004\)](#) and [Tahani and Li \(2007\)](#).

In Gatheral (2006) an overview of applications to volatility derivatives is given. Further, he shows how to infer at-the-money Black–Scholes implied volatilities or the at-the-money Volatility Skew directly from characteristic functions without the need of first calculating the price and then using a root finding algorithm in conjunction with a Black–Scholes pricing engine. The exposition in this section resembles only a small subset of possible applications, but gives an idea of the versatility of Fourier methods in financial modeling.

5 Applications of Inverse Fourier Methods to Distribution Functions and Option Pricing

In this section we will illustrate some of the most widely used concepts of numerical evaluation of inverse Fourier integrals. Two methods will be compared. On one hand the direct integration methods, on the other hand the fast Fourier transform algorithms are considered. Each of these procedures has their own advantageous properties compared to the other routines. In any case, the application of the procedures requires considering numerical and technical issues with precautions.

5.1 Numerical Evaluation of Inverse Fourier Integrals

To obtain probability densities or option prices, the inversion of the Fourier integrals can be evaluated by means of standard numerical integration schemes. Numerical integration of functions is a broad subject and rich in terms of possible techniques. In this section we will briefly review some of the most frequently used numerical quadrature schemes to evaluate the semi-infinite domain of oscillatory functions encountered in Fourier analysis.

Direct Integration Methods

It is well known that an integral can be represented as the area under the curve of a function in between a specified interval. A powerful procedure is to approximate the searched interval by simple geometrical objects like rectangles. More sophisticated rules are the *Newton–Côtes* formulae where the interval is approximated by some interpolating polynomials usually in Lagrange form which in turn are easily computable. The *Trapezoidal* and *Simpson’s* rules are probably the most popular and commonly used Newton–Côtes integration schemes available. While having a clear geometrical and intuitively obvious interpretation, there are alternatives which offer higher computational efficiency, namely the family of Gaussian quadratures. A Gaussian quadrature tries to give an accurate estimate for an integral by optimally choosing abscissas where to evaluate a particular function. Following the *Fundamental Theorem of Gaussian Quadrature* the optimal abscissas are exactly the roots of orthogonal polynomials for the same interval and weighting function. In the sequel we implement and compare a number of widely used algorithms.

Gauss–Legendre quadrature formula This is perhaps the best known Gaussian quadrature formula usually specified for an integration domain over $[-1,1]$. A N -point quadrature is then given by

$$\int_{-1}^1 f(x)dx \approx \sum_{i=0}^{N-1} w_i f(x_i). \quad (5.1)$$

The resulting orthogonal polynomials are the Legendre polynomials for the weighting function $w(x) = 1$. Thus the nodes are the N zeroes of the Legendre polynomial of degree N .

The integration interval may be changed to arbitrary interval $[a, b]$ by following change of variables

$$\int_a^b f(x)dx \approx \frac{b-a}{2} \sum_{i=0}^{N-1} w_i f\left(\frac{b+a}{2} + \frac{b-a}{2} x_i\right). \quad (5.2)$$

Proceeding this way the quadrature is applied to the transformed integrand with modified integration limits.

Depending on the actual problem it may be an appropriate procedure to apply the Gauss–Legendre formula not on the whole interval but decompose the integration region into subintervals and sum up the particular approximations

$$Q(x) = \int_0^\infty f(x)dx = \lim_{N \rightarrow \infty} \sum_{j=0}^{N-1} \int_{jh}^{(j+1)h} f(x)dx. \quad (5.3)$$

The fixed step size h denotes the discretisation length and N is the truncation point. As $N \rightarrow \infty$ and $h \rightarrow 0$ the numerical quadrature will approach the theoretical value.

Gauss–Laguerre quadrature formula The Gauss–Laguerre quadrature evaluates an exponentially weighted integral from zero to infinity as

$$\begin{aligned} \int_0^\infty f(x)dx &= \int_0^\infty e^{-x} [e^x f(x)]dx = \int_0^\infty w_i e^x f(x)dx, \\ &\approx \sum_{i=0}^{N-1} w_i e^{x_i} f(x_i) = \sum_{i=0}^{N-1} w_i f(x_i). \end{aligned} \quad (5.4)$$

The resulting orthogonal polynomials are the Lagrange polynomials with weighting function $w(x) = e^{-x}$. This quadrature is particular interesting since all of our applications have semi-infinite domains of integration ranges.

Adaptive Simpson quadrature The idea of using adaptive algorithms for the numerical calculation of integrals is dating back to at least [McKeeman \(1962\)](#). Since then many new and sophisticated algorithms have been developed, among these

[Gander and Gautschi \(2000\)](#) propose an efficient and reliable implementation of the adaptive Simpson rule.

The adaptive control strategy divides the area of integration in subintervals, evaluates the integral at each region and uses an error estimate of the integral to check if a specified error tolerance is met. At regions where the function is well approximated by a quadratic function, only a few function evaluations are needed, in other areas the adaptive strategy evaluates the subintervals in a recursive manner.

Adaptive Gauss–Lobatto quadrature The second quadrature implemented in the paper from [Gander and Gautschi \(2000\)](#) builds upon a Gauss–Lobatto quadrature modified by a Kronrod extension to add an effective error control procedure. The Lobatto formula has preassigned abscissas at the end points of the interval. The remaining nodes and all weights are then determined in a way to obtain the highest exactness possible. The Kronrod extension is used to provide an estimate of the approximation error. If the error exceeds a specified tolerance, regions where the function is not so well behaved will be divided over again and again.

Adaptive Gauss–Kronrod quadrature The Gauss–Kronrod quadrature is an extension of the Gauss–Legendre algorithm. For well behaved regions the error estimates will be small and the numerical approximations will be accepted. For integration areas where the function is not smooth, the algorithm subdivides the interval until the desired accuracy will be reached.

For detailed discussion on numerical quadratures we refer to the extensive literature available on this subject. Key reference on numerical integration is [Davis and Rabinowitz \(1984\)](#). Detailed descriptions in a financial context can be found in [Fusai and Roncoroni \(2008\)](#) and [Judd \(1998\)](#).

Fast Fourier Transform and Fractional Fourier Transform

The Fast Fourier Transform (FFT) is a highly efficient implementation of the discrete Fourier transform (DFT) which maps a vector $\mathbf{h} = (h_j)_{j=0}^{N-1}$ onto some vector $D_k(\mathbf{h})$

$$D_k(\mathbf{h}) = \sum_{j=0}^{N-1} e^{-i\frac{2\pi}{N}jk} h_j, k = 0, \dots, N-1 \quad (5.5)$$

By choosing N as a power of two, the complexity of the algorithm reduces from an order of N^2 for the direct numerical integration methods to that of $N \log_2 N$ operations to compute N values. The Fourier transform of the vector \mathbf{h} will be denoted with $D_k(\mathbf{h}) \in \mathbb{C}^N$. The vector $\mathbf{h} \in \mathbb{C}^N$ corresponds to N values of the function h evaluated at the points $\mathbf{u} = (u_j)_{j=0}^{N-1}$.

A result of the FFT procedure will be a new vector $\mathbf{f} = (f_k)_{k=0}^{N-1}$, where each of the elements f_k correspond to a specified value of $x = x_k$. For example, for the

purpose of density evaluations x_k will typically be chosen in a way that the values are located around the mode. In the context of option pricing, Carr and Madan (1999) demonstrate that the vector \mathbf{f} will contain option values corresponding to carefully chosen $\mathbf{x} = (x_k)_{k=0}^{N-1}$ in a sense that the resulting values are around the at-the-money level, i.e. the values of x are typically kept close to zero.

Following Carr and Madan (1999) we denote the grid size of the vector \mathbf{u} with η and λ is the spacing of \mathbf{x} . In the case of conventional FFT procedures η and λ are restricted by imposing an inverse relation

$$\eta\lambda = \frac{2\pi}{N}. \quad (5.6)$$

The finer the summation grid spacing η , the coarser the output spacing returned from the FFT procedure will be and *vice versa*.

The fundamentally inflexible nature imposed by the restriction (5.6) was addressed by Bailey and Swarztrauber (1991, 1994) who overcome this constraint by developing a generalization of the conventional DFT, the Fractional Fourier Transform (FRFT).

It is defined as

$$G_k(\mathbf{h}, \alpha) = \sum_{j=0}^{N-1} e^{-i2\pi jk\alpha} h_j, k = 0, \dots, N-1 \quad (5.7)$$

The *fractional* parameter α may be any arbitrary real or complex valued number. In this framework both η and λ may now be chosen freely which will together determine the FRFT parameter $\alpha = \eta\lambda$. The ordinary FFT and its inverses are special cases of the FRFT for $\alpha = \frac{1}{N}$. A N -point FRFT can be implemented by invoking two forward and one inverse $2N$ -point FFT calculations. The algorithms works as follows, define two $2N$ -point sequences \mathbf{y} and \mathbf{z} as

$$\begin{aligned} y_j &= h_j e^{-i\pi j^2 \alpha} & 0 \leq j < n \\ y_j &= 0 & m \leq j < 2n \\ z_j &= e^{i\pi j^2 \alpha} & 0 \leq j < m \\ z_j &= e^{i\pi (j-2n)^2 \alpha} & m \leq j < 2n \end{aligned} \quad (5.8)$$

The FRFT is then given by

$$G_k(\mathbf{h}, \alpha) = e^{-i\pi k^2 \alpha} D_k^{-1} \odot [D_j(\mathbf{y}) \odot D_j(\mathbf{z})], 0 \leq k < n \quad (5.9)$$

where D_k^{-1} denotes an inverse FFT calculation and \odot denotes element-by-element vector multiplication. The exponential factors do not depend on the function to be integrated and may be precomputed. The computational cost of a N -point FRFT procedure is about a $4N$ -point FFT in terms of the number of elementary operations. The additional benefit by employing a FRFT instead of running a single FFT is due to

the fact that a FRFT with smaller N may achieve the same accuracy as using a FFT with much larger N .

5.2 Examples of Characteristic Functions for Particular Price Dynamics

In order to illustrate the basic concepts and investigate the standard numerical procedures we will briefly introduce three candidates of exponential Lévy processes and exponential affine models. We just state the corresponding characteristic functions and refer to the respective references for detailed discussion and derivations. Comprehensive treatments on Lévy processes and affine models with Fourier pricing applications can be found in [Cont and Tankov \(2004\)](#), [Boyarchenko and Levendorskiĭ \(2002\)](#) and [Schoutens \(2003\)](#).

Black–Scholes Our benchmark model and one of the simplest examples of Lévy processes and affine (jump) diffusion is standard Brownian motion. This is the only continuous process from the wide class of Lévy processes. In this sense the classical Black–Scholes model can be categorized as a continuous exponential Lévy model. The characteristic function for an exponential Brownian motion with instantaneous variance σ^2 is given by

$$\phi_T(u) = \mathbb{E}[e^{iuX_T}] = \exp\left[i\omega uT - \frac{\sigma^2 u^2}{2}T\right]. \quad (5.10)$$

To prevent arbitrage the drift correction parameter ω must be chosen in a way that the discounted price process remains a martingale. By imposing $\phi_T(-i) = \mathbb{E}[e^{X_T}] = 1$ we find that $\omega = -\frac{1}{2}\sigma^2$. The analytic continuation of the characteristic function is defined by the whole complex plane.

Finite Moment Log Stable This Lévy process with infinite activity was proposed by [Carr and Wu \(2003\)](#) to address the observation for S&P 500 index options that the volatility skew does not flatten as time to maturity increases. The characteristic function is described by

$$\phi_T(u) = \mathbb{E}[e^{iuX_T}] = \exp\left[iu\omega T - (iu\sigma)^\alpha T \sec \frac{\pi\alpha}{2}\right], \quad (5.11)$$

where $\omega = \sigma^\alpha \sec \frac{\pi\alpha}{2}$ is the convexity adjustment term to sustain the martingale property. The tail index $\alpha \in (1, 2]$ controls the tail behavior and σ describes the width of the risk neutral density. For $\alpha = 2$ the Finite Moment Log Stable model (FMLS) coincides with the Black–Scholes model, where the Black–Scholes volatility σ_{BS} is related to the dispersion measure for the FMLS model σ_{LS} via $\sigma_{BS} = \sigma_{LS}\sqrt{2}$. The domain for the strip of regularity \mathcal{S}_X is restricted to $\Im[z] < 0$.

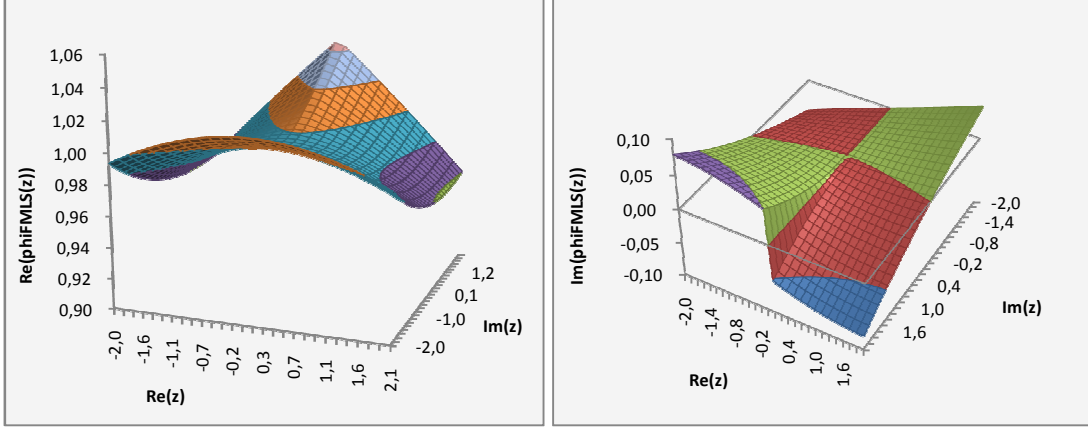


Figure 6: Finite Moment Log Stable model in the complex plane. Left: Real part. Right: Imaginary part. Model parameters: $\alpha = 1.6$ and $\sigma = 0.1$.

An intuitive way to illustrate the strip of regularity \mathcal{S}_X for a given model is to plot the characteristic function by the movements of its real and imaginary parts on the plane of complex numbers. By varying the state variables and model parameters it is then possible to gain some insights on the model inherent dynamics and properties. In [Figure 6](#) and [Figure 7](#) this is shown for the FMLS and [Heston \(1993\)](#) model respectively for some arbitrarily chosen parameters.

Heston (1993) The Heston dynamics are one of the most prominent stochastic volatility specifications where the instantaneous variance follows a mean reverting square root process. More precisely the instantaneous variance $v_t = \sigma^2$ is allowed to be stochastic and time dependent and as such relaxing the assumption of stationary increments. The characteristic function for the [Heston \(1993\)](#) is

$$\phi_T(u) = \mathbb{E}[e^{iuX_T}] = \exp[A(u) + B(u)v_0], \quad (5.12)$$

where $A(u)$ and $B(u)$

$$A(u) = \frac{\kappa\theta}{\sigma_v^2} \left\{ (\beta - d)T - 2 \ln \left(\frac{ge^{-dT} - 1}{g - 1} \right) \right\}, \quad (5.13)$$

$$B(u) = \frac{\beta - d}{\sigma_v^2} \left(\frac{1 - e^{-dT}}{1 - ge^{-dT}} \right), \quad (5.14)$$

with

$$d = \sqrt{\beta^2 - 4\hat{\alpha}\gamma}, \quad (5.15)$$

$$g = \frac{\beta - d}{\beta + d}, \quad (5.16)$$

and auxiliary variables

$$\hat{\alpha} = -\frac{1}{2}u(u + i), \beta = \kappa - iu\sigma_v\rho, \gamma = \frac{1}{2}\sigma_v^2. \quad (5.17)$$

There is no explicit convexity correction for the diffusion process in this specification, instead it is contained in the definition of $\hat{\alpha}$. The Heston model belongs to the class of affine diffusions. These are defined in a way that the logarithm of the conditional characteristic function for $x = \ln S$ and v , conditional upon the instantaneous value of the stochastic volatility state variable, is a linear function of these state variables.

The domain for the extended characteristic function is the strip \mathcal{S}_X given by the interval (a_-, a_+) , where $a_- < 0$ and $a_+ > 1$ solve [see [Lee \(2004\)](#)]

$$g(-ia)e^{d(-ia)T} = 1. \quad (5.18)$$

For the FMLS model the price process follows a Lévy process which is by definition a time-homogenous process and hence the analytical strip \mathcal{S}_X does not depend on the number of finite moments. For the Heston model, however, without stationary increments the number of moments is not invariant to the time horizon. The time evolution of the characteristic function is plotted in [Figure 7](#) with two different time horizons on the Gauss plane. As the time increases the number of moments decrease. In other words the singularities move along the imaginary axis toward the real axis which in turn narrow increasingly the strip of regularity. This issue is known as the moment stability of affine stochastic volatility models and is especially important for long dated options. For certain circumstances under which the moments of the price process can explode (become infinite) in finite time, compare e.g. [Lord and Kahl \(2007\)](#), [Andersen and Piterbarg \(2007\)](#), [Keller-Ressel \(2008\)](#).

Although known for some time now, there are still substantial research efforts made to gain a better understanding of this model. For a recent review and some lesser known features of the [Heston \(1993\)](#) model see [Zeliade Systems \(2009\)](#).

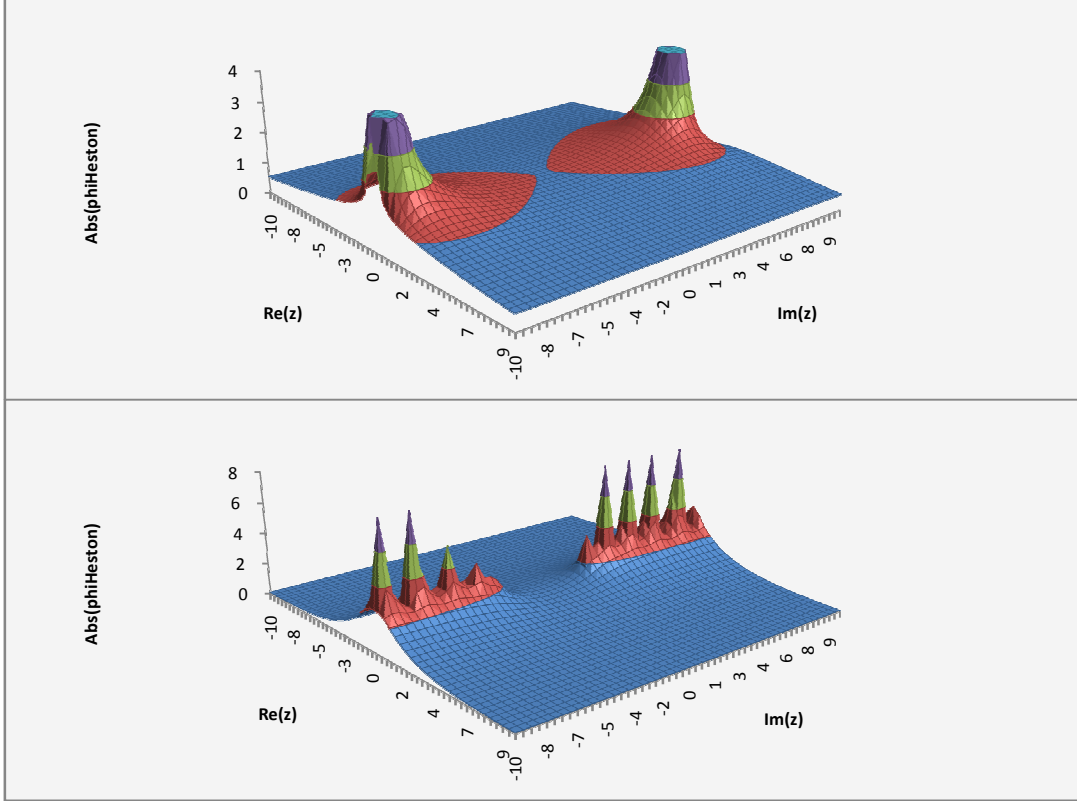


Figure 7: Heston (1993) model in the complex plane. Top: One year to maturity. Bottom: Eight years to maturity. Model parameters: $\kappa = 1$, $\theta = 0.02$, $\rho = 0$, $\sigma_v = 0.4$ and $v_0 = 0.02$.

Depending on the valuation formula [e.g. the [Carr and Madan \(1999\)](#) formulation] the above specified characteristic functions might have to be rewritten into the form of

$$\exp[\ln S_0 + rT]\phi_T(u). \quad (5.19)$$

Having specified three different model specifications we are now ready to explore the pricing formulae and density functions using Fourier inversion methods.

5.3 Distribution Functions

Before considering option pricing applications we will investigate how to recover distribution functions from tractable characteristic functions. On one hand this is *per se* an interesting and important topic for applications to statistical inference and on the other hand option prices are obtained by integrating a payoff function according to a particular probability density.

Direct Integration

In this part we will first have a glance of some qualitative properties of the different quadrature schemes and chosen models. Then the different integration algorithms are compared with respect to accuracy and computational efficiency.

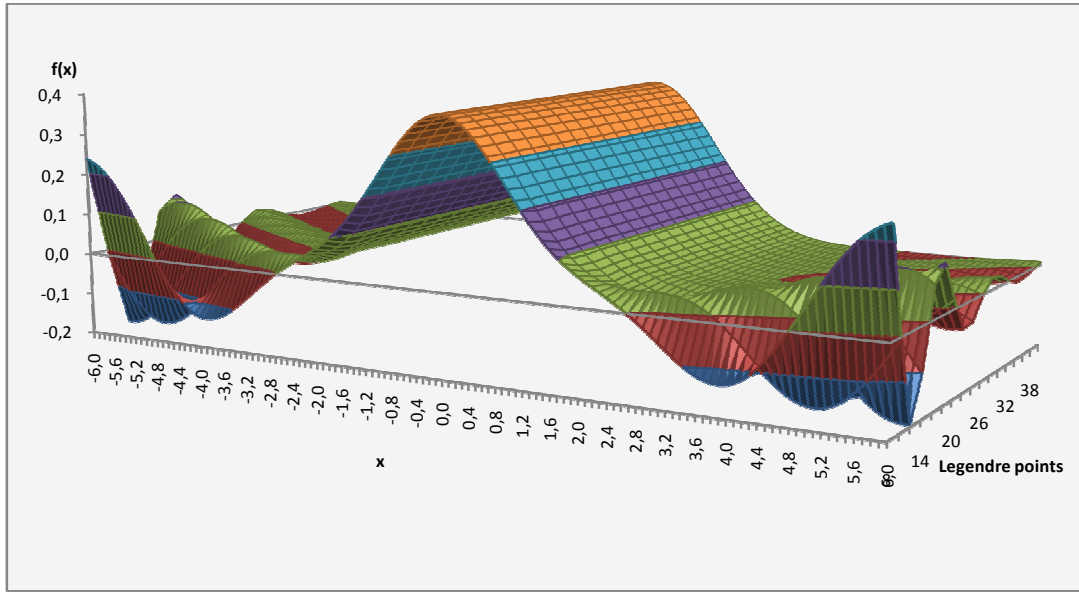


Figure 8: Standard Normal Density function as a function of Legendre points.

In Figure 8 the density of a Standard Normal random variable is plotted as a function of Gauss–Legendre integration points. It can be seen that the center of the density is captured quite well by only a few points, however, by simple observation we can see that for the tails of the probability function a lot more points are necessary to achieve a minimum degree of accuracy. The oscillatory behavior is typical for Gaussian quadratures where each quadrature has its own characteristics and purposes, a Gauss–Laguerre integration mimics qualitatively the same picture only distinguished by a slightly different curvature.

In order to assess the accuracy of the above mentioned numerical integration schemes we begin with the ubiquitous Black–Scholes model as a benchmark to test against. Before being interested in high precision results we show some qualitative properties of two basic Gaussian quadratures, namely the Legendre and Laguerre integration.

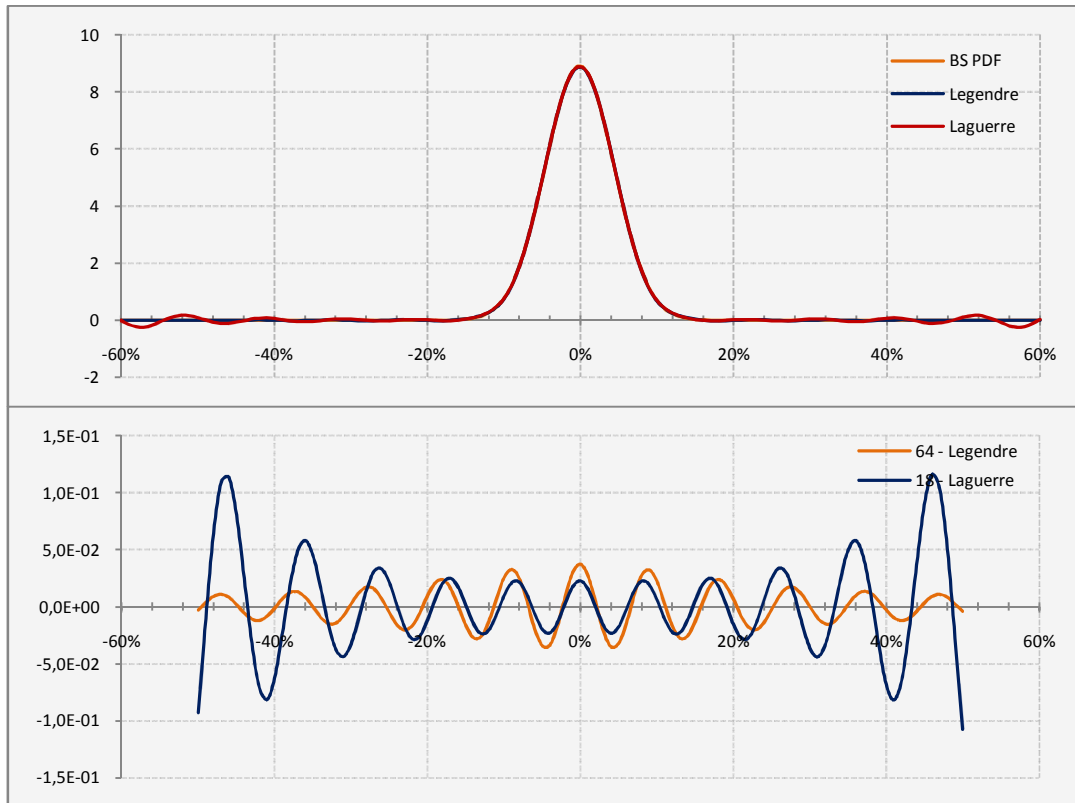


Figure 9: Black-Scholes density function. Top: Density with time to maturity 0.05 and volatility of 20%. Bottom: Absolute error of 64 point Gauss-Legendre and 18 point Gauss-Laguerre integration.

In the exhibit above the density function for the Black-Scholes model is shown. As one can see, the Legendre quadrature has increasingly 'good' fit in the tails whereas the Laguerre integration shows a better fit in the center of the density. Note the difference in this example, the Laguerre quadrature with only 18 points shows similar quantitative properties in magnitude as the Legendre quadrature with 64 points. This indicates that the Gauss-Laguerre scheme seems to cope quite well with this kind of problems. Choosing 64 points for the Laguerre nodes result in an absolute error well below $1e-12$ in the range of $[-0.5, 0.5]$. To receive the same precision for a simple Legendre quadrature more than 170 nodes are required.

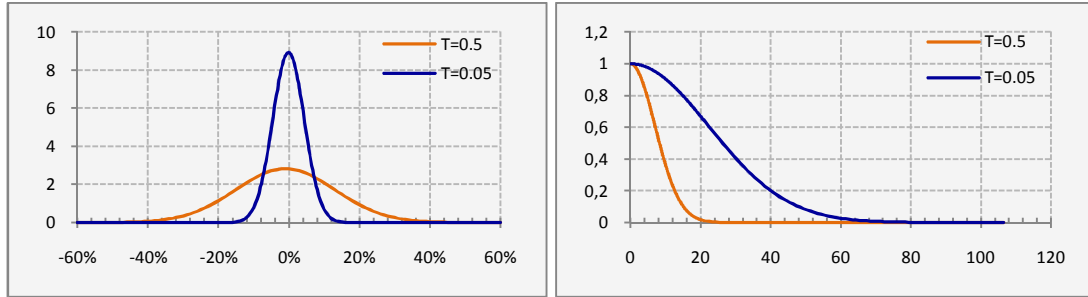


Figure 10: Black-Scholes probability density function for two different times to maturity and volatility of 20%. Left: Probability density functions. Right: Fourier integrands.

As previously noted, there is an inverse functional relation between space domain and image domain. A steep function in space usually becomes wide in the characteristic function, a behavior which becomes apparent by the inspection of typical Fourier integrands. For increasing T the return densities become smoother and have fatter tails, which lead to thinner tails of the characteristic function making it less well behaved. This effect will differ for various price processes depending on their decaying behavior towards infinity. This can lead to serious consequences for numerical procedures, which will be discussed in detail later.

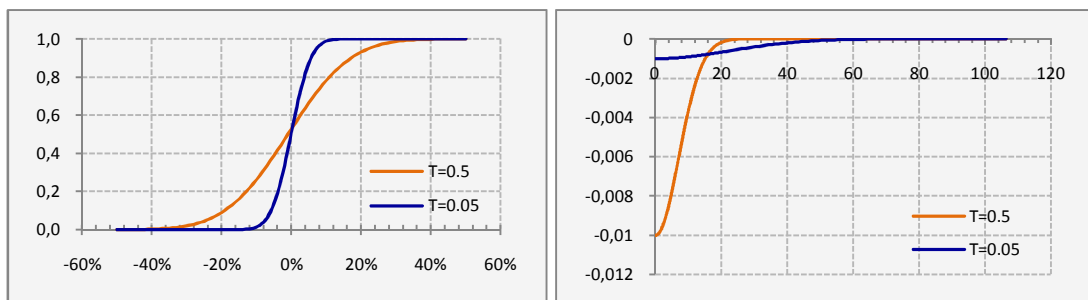


Figure 11: Black-Scholes cumulative density function for two different times to maturity and volatility of 20%. Left: Cumulative density functions. Right: Fourier integrands.

In [Figure 12](#) the density function for the FMLS model is illustrated together with the corresponding Black-Scholes density and Fourier integrands. For choosing $\alpha < 2$ the model inherent skewness to the left property is clearly visible and as one can see the tail on the left of the density decays slower than the log normal commonly referred to as a fat tail.

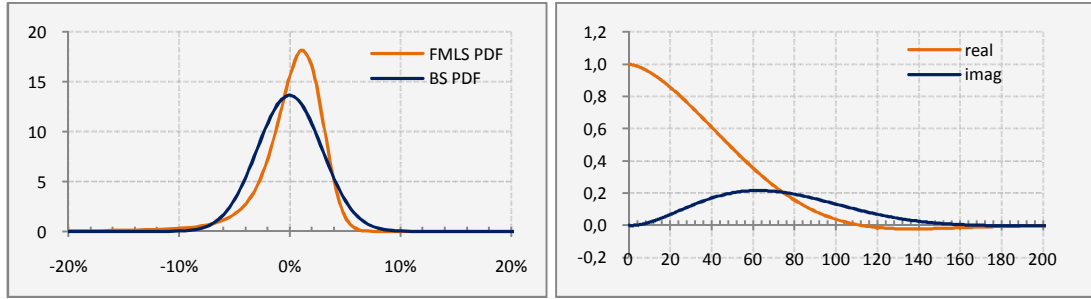


Figure 12: FMLS density and integrand. Left: Density with $T = 0.05$, $\alpha = 1.6$ and $\sigma = 0.1$ together with the corresponding Black-Scholes density. Right: Real and imaginary parts of the FMLS integrand for the density approximation.

In Section 3.2 four different formulae are presented which allow to approximate the cumulative density function. These are now compared with respect to convergence properties and efficiency with the help of the [Heston \(1993\)](#) model specification.

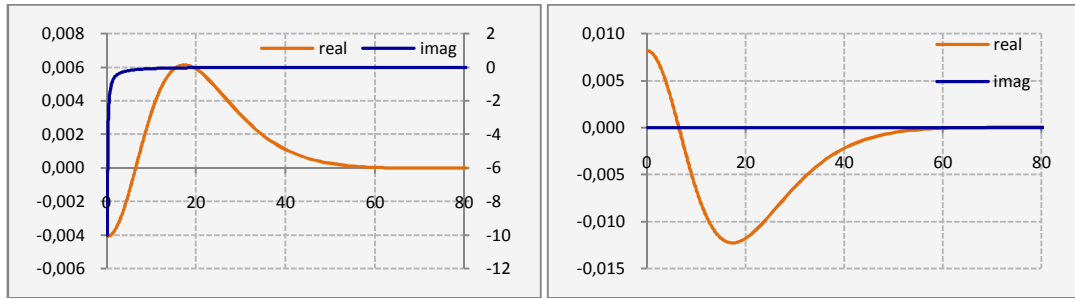


Figure 13: Integrands in the Heston model with different inversion formulae. Left: Inversion formula using the real part [Eq. (3.15)]. Right: Inversion formula using Eq. (3.14).

From [Figure 13](#) we see the different curves of the integrands employing different Inversion formulae. The exhibit on the left shows the integrand using the real part of the function evaluation [Eq. (3.15)], using the imaginary part shows exactly the same picture [Eq. (3.16)] with the exception that the real and imaginary parts are simply interchanged. Using (3.14) the resulting integrands for the real parts pretty much resemble the same behavior, only mirrored and slightly different in magnitude. Using the composite Gauss-Legendre integration the CPU times with respect to equations (3.15) and (3.16) are virtually identical (averaging over 100 density evaluations from -0.5 up to 0.5 needs 0.035 seconds in CPU time), for (3.14), however, the running time nearly doubles which seems logical since with this representation the quadrature has to evaluate the characteristic functions two times (0.067 seconds on average). The representation as in (3.21) behaves similar to (3.14), but needs only the timings like equations (3.15) and (3.16) since the integrand needs to be evaluated only once.

The number of evaluations of the characteristic function is clearly the determining factor and is especially pronounced in the case of the [Heston \(1993\)](#) model involving two complex exponentiations (without counting repeating terms), one complex logarithm and one complex square root.

Now we turn to the issue of getting precise values for the desired Fourier integrals. The analytic Black–Scholes model serves as a benchmark for the different integration methods. As is well known, even for the Black–Scholes model which is generally considered analytic or closed form, we need a numerical approximation for the required Cumulative Standard Normal Distribution. Following the exposition in West (2005) we rely on the therein proposed Hart (1968) algorithm which is accurate to double precision throughout the real line. In Figure 14 we summarize the main results in terms of the achieved accuracy versus CPU time in seconds. The most efficient algorithms will be located in the left down corner. As a measure for the error we take the root mean squared errors (RMSE) resulting from averaging the PDF calculations from -0.6 up to 0.6 involving 121 values. For the generation of the Gauss nodes and the adaptive Gauss–Kronrod quadrature we use the routines implemented in the ALGLIB library³. The adaptive Simpson and Gauss–Lobatto procedures are direct implementations of the algorithms described in Gander and Gautschi (2000).

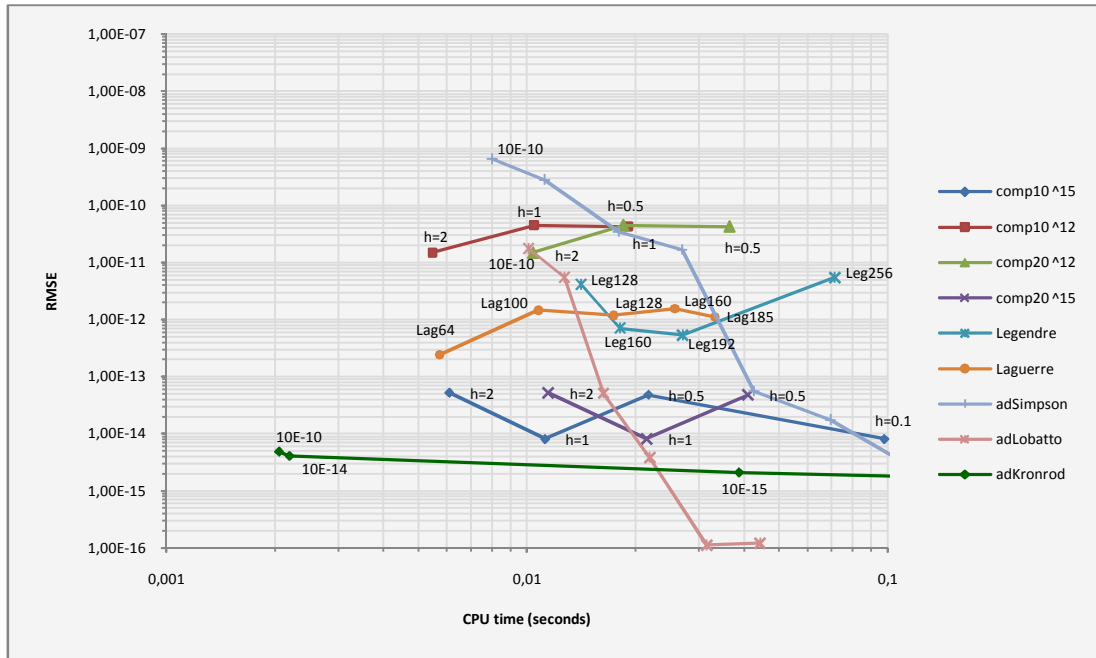


Figure 14: Accuracy vs. CPU time. Accuracy measured as root mean squared error (RMSE) in relation to the computation time in seconds (CPU time) on a double log-scale.

For the Gauss–Laguerre and Gauss–Legendre quadratures the number of integration points is included, for the composite Gauss–Legendre the number of points per subinterval is indicated in conjunction with the corresponding local stopping criteria. The adaptive schemes are indicated with the desired tolerance level for the routines beginning with $10\text{e-}10$ upwards.

Having expected a more regular pattern with downward sloping curves from the upper left to the right down corner we see that this behavior is not given in all cases.

³ Available at <http://www.alglib.net/>

For instance the error arising from the composite schemes should theoretically approach zero as the step size h tends to zero. One potential reason for this contrary and seemingly irregular behavior may be traced back to the increasing number of numerical operations which can accumulate to a substantial amount of rounding errors working within a finite precision computation environment. The number of significant digits for the nodes and weights for the Gauss quadratures in double precision floating point arithmetic are restricted to 16 digits. Decreasing the step size any further will increase the rounding errors dramatically leading to completely meaningless results. Using composite Newton–Côtes procedures this effect is less pronounced (not shown here), since the subintervals are approximated by analytic functions.

Simply increasing the number of integration nodes for the plain Gauss quadratures also does not lead automatically to more precise values. This will depend heavily on the properties of the used polynomials, i.e. whether the orthogonal polynomials are capable to approximate the evaluated function well enough [compare [Figure 9](#)] and as we can see choosing higher order schemes need not necessarily imply higher accuracy. In addition, there are numerical impediments as well, e.g. for double precision the highest number of nodes for the Gauss–Laguerre scheme that can be generated is 365, otherwise the algorithm will produce an overflow [see e.g. [Dobránszky \(2008\)](#)].

All considered adaptive procedures perform quite well, as expected the Gaussian schemes are far superior to the Simpson rule albeit this routine works remarkably well. In terms of computational efficiency the best overall performance is achieved by the adaptive Gauss–Kronrod algorithm, whereas the most precise values are obtained with the adaptive Gauss–Lobatto routine.

FFT and FRFT

The FFT and FRFT are computationally efficient algorithms for the calculation of density functions. In this section we address some implementational issues and assess the accuracy with respect to analytical solutions.

For the PDF inversion we need to discretize the Fourier integral

$$\begin{aligned} f_X(x) &= \frac{1}{\pi} \int_0^\infty \Re[e^{-iux} \phi_X(u)] du, \\ &\approx \frac{1}{\pi} \sum_{j=0}^{N-1} \Re[e^{-iu_j x} \phi_X(u_j)] \eta. \end{aligned} \quad (5.20)$$

where η denotes the step size for the summation grid.

In order to calculate the integral in (5.20) we need to specify the number of summands for the integral approximation N which should be a power of 2 to use the computational efficiency of the FFT and the size of η determining the grid spacing in Fourier domain. Both values will determine the effective upper bound for the

integration $a = N\eta$. The FFT returns N values of x , where $x_k = -b + \lambda k$ with grid spacing of $\lambda = 2\pi/(\eta N)$ yields the return grid. This implies that the returned values are within the range $(-b, b)$ centered around zero with $b = N\lambda/2$. Further setting $u_j = \eta j$ the PDF finally becomes

$$f_X(x_k) \approx \frac{1}{\pi} \sum_{j=0}^{N-1} \Re[e^{-i\lambda\eta jk} e^{iu_j b} \phi_X(u_j) \eta w_j], \quad (5.21)$$

where w_j are some weightings implementing the chosen integration rule. Common choices are the Trapezoidal rule with integration weights $w_j = \frac{1}{2}$ for $j = 0$ or $j = N - 1$ and 1 otherwise, and the Simpson's rule weightings $w_j = \frac{1}{3} [3 + -1j+1-\delta j]$ where δn is the Kronecker delta function which is 1 for $n=0$ and zero otherwise. Running a FFT then delivers an approximation of the discretized Fourier integral.

As we know from Section 3.2, the probability density function is an absolutely integrable function and does not impose any major impediments in conjunction with FFT methods. For the cumulative density functions, however, this is not the case. The FFT cannot directly be applied to recover the CDF, since the integrand is singular at the required evaluation point $u = 0$. In order to circumvent this problem it is possible to proceed in exactly the same way as shown in Section 4.4 by damping the function by some carefully chosen parameter α in a way that the integrand is well behaved and directly applicable for the FFT [see e.g. Kim & al. (2009)].

If there is a damping constant $\alpha > 0$ such that the characteristic function under consideration is absolutely integrable for all complex z with $\Im[z] = \alpha$, then we are able to define a *modified* CDF

$$F_\alpha(x) = e^{-\alpha x} \mathbb{P}(X \leq x). \quad (5.22)$$

Just like the modified option price we can define a modified characteristic function

$$\phi_\alpha(u) = \frac{1}{\alpha - iu} \phi_X(iu + \alpha). \quad (5.23)$$

The cumulative density is then given by applying the Fourier inversion to the dampened transform and finally undamping the inverted function

$$\begin{aligned} F(x) &= \frac{e^{\alpha x}}{2\pi} \int_{-\infty}^{\infty} e^{-iux} \phi_\alpha(u) du, \\ &= \frac{e^{\alpha x}}{\pi} \int_0^{\infty} \Re[e^{-iux} \phi_\alpha(u)] du. \end{aligned} \quad (5.24)$$

Using this representation in conjunction with a discretization scheme as in (5.20) and (5.21) we are now able to use the FFT to evaluate the cumulative density function for a whole range of values in one single stroke.

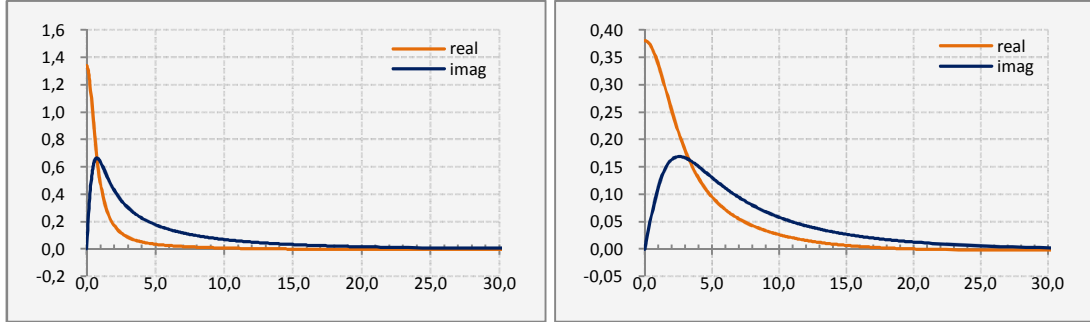


Figure 15: Damping of the Fourier transform for the cumulative density function. Heston model. Left: Damping factor $\alpha = 0.75$. Right: Damping factor $\alpha = 2.75$.

Without the damping constant the integrand exhibit divergent behavior around zero and is therefore not suited for the FFT. With increasing α the integrand becomes less steep and smoother, aiding the numerical quadrature to evaluate the integral precisely [see Figure 15]. However, choosing α too big will render the numerical integration unstable as well. This relationship is illustrated in Figure 16 by contrasting the FFT calculations with the analytical solutions in the Black–Scholes model. As we can see, there is a range of values for α delivering quite accurate results and will then slowly worsen for α getting bigger. The minimum error in this example is around $\alpha = 1.5$.

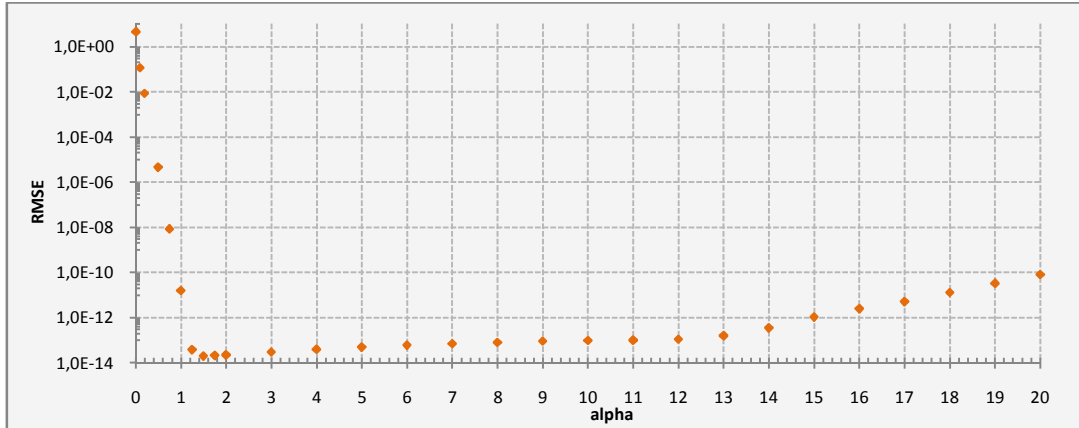


Figure 16: Root mean squared error (RMSE) of FFT cumulative density approximations as a function of damping factor α in the Black–Scholes model $N = 4096$ and $\eta = 0.25$.

Having specified how to distretize the Fourier integrals and how to overcome the impediments for the FFT with respect to the cumulative densities, we will now give some practical examples. In the following we adapt the example in Chourdakis (2005) for densities in the Black–Scholes model with time to maturity 0.25 and 30% volatility. For instance using $N = 4096$ and $\eta = 0.25$ for the FFT we get an output spacing of $\lambda = 0.00614$ and an upper integration bound of 1023.75. For the FRFT we set the desired output range for the density values to $[-0.6, 0.6]$, for example using $N = 128$ and $\eta = 0.25$ implies an output grid with $\lambda = 2 \times \frac{0.6}{128} = 0.009375$ and an upper bound of 31.75 (with the restriction imposed by the FFT the output spacing in

this case would be $\lambda = 0.19635$). The fractional parameter is determined by $\alpha = \frac{\eta\lambda}{2\pi}$ and results in 0.0078125 for aforementioned parameters. In Table 2 we list the resulting errors and corresponding running times for the above mentioned example parameters and other combinations of N and η .

The error measure is calculated only at grid points belonging to the FFT and FRFT sampling grid. Preceding in this way we can avoid interpolation and hence no interpolation error will affect the results. The results show that the two methods are capable of returning very accurate values for the density function compared to analytical values. Further, as expected, the runtimes of the FRFT are usually a lot faster than the corresponding FFT (using the FFT implementation in the ALGLIB library).

Table 2: Approximation error and timing of FFT vs. FRFT.

	N	η	RMSE	CPU time (sec)
FFT	2048	0.25	1.667E-14	0.057
	2048	0.50	1.166E-14	0.055
	4096	0.25	1.667E-14	0.108
	4096	0.50	1.167E-14	0.108
	8192	0.25	1.821E-14	0.260
	8192	0.50	1.276E-14	0.255
FRFT	64	0.50	4.070E-06	0.014
	64	1.00	9.208E-16	0.014
	128	0.25	3.359E-06	0.029
	128	0.50	9.813E-16	0.029
	128	1.00	1.579E-15	0.029
	256	0.25	9.122E-16	0.074
	256	0.50	1.551E-15	0.074
	256	1.00	2.765E-15	0.073

As we have seen it is impossible with the conventional FFT to evaluate the integral in (5.24) on a fine grid and get a fine resolution for the density values at the same time. For example, the FFT for the Black-Scholes density with $N = 4096$ and $\eta = 0.25$ returns only 107 out of the 4096 values within $[-0.6, 0.6]$. With respect to the range of interest for our illustration, more than 97% are outside the region of interest.

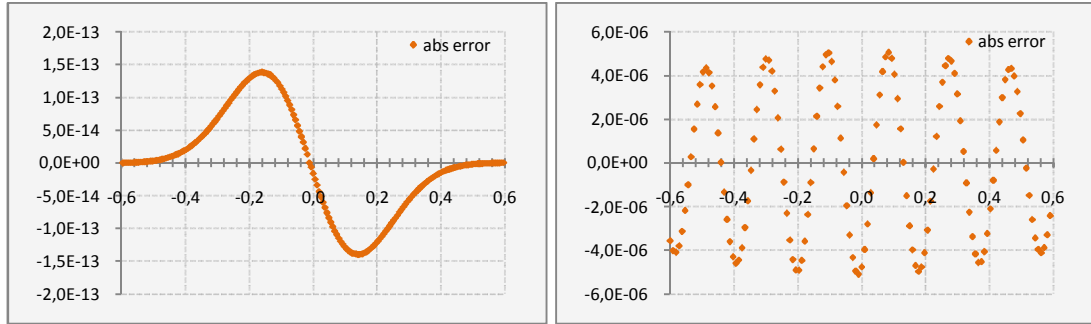


Figure 17: Pattern of absolute error of FFT and FRFT probability density approximations versus analytical solution in the Black–Scholes case. Left: FFT $N = 4096$ and $\eta = 0.25$. Right: FRFT $N = 128$, $\eta = 0.25$.

With the FRFT we have an appealing possibility of breaking the relation between η and λ and explicitly specifying both the summation grid of the Fourier integral and the desired output range. However, both the FFT and FRFT have the limitation that the grid points must be chosen equidistantly thus precluding the use of more sophisticated integration algorithms like Gaussian quadrature.

Conducting the same experiments for the cumulative density reveal quite similar implications with respect to the choice of FFT or FRFT, though the choice of the damping parameter α is critical for either of the two algorithms.

Findings for the [Heston \(1993\)](#) and FMLS model against direct integration methods reveal similar qualitative characteristics, nevertheless an exact quantification of the errors is not an easy task since in this case approximations in one form are just compared to approximations in another form.

5.4 Option pricing

In the previous section we implemented a number of numerical integration schemes for probability function calculations. Now we proceed and apply the same techniques to the described Fourier pricing algorithms. Again we illustrate typical shapes of the Fourier integrands, compare their convergence properties, and investigate the impact of changing the numerical quadratures with respect to accuracy and running times.

Black–Scholes Style Formula

[Heston \(1993\)](#) pioneers the use of Fourier inversion methods in option pricing by assuming a Black–Scholes like functional form as solution to the valuation problem. The difference of two probabilities under appropriate changes of measure then yield to the theoretical value. In the sequel, we compare this concept with the analytical solution of the Black–Scholes formula. In [Figure 18](#) we exemplify some typical shapes for the two integrands involved. In the left exhibit, an at-the-money option with zero interest rates is shown. We can see a perfect symmetry of the two integrands. The two resulting integral values employing inversion formula (3.17) correspond perfectly to the $\Phi(d_1)$ and $\Phi(d_2)$ values in the analytic case with $d_1 = 0.075$ and $d_2 = -0.075$

yielding $\Phi(0.075) = 0.529893$ and $\Phi(-0.075) = 0.470107$ finally giving 5.978528811 for both the call and put.

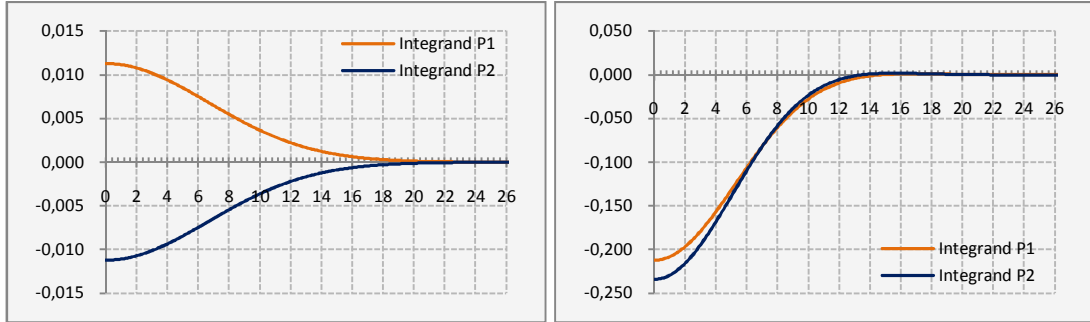


Figure 18: Integrands of the Black-Scholes model in the Black-Scholes style formula. Left: $S = 100$, $K = 100$, $T = 0.25$, $r = 0$, $\sigma = 0.3$. Right: $K = 80$.

On the right the integrands are displayed with strike 80 corresponding to the risk neutral probabilities of finishing in-the-money with $\Phi(d_1) = 0.940929$ and $\Phi(d_2) = 0.921117$ resulting in 20.403599348 for the call and 0.403599348 for the put respectively.

The functional form expresses the option value as the difference of two binaries, also referred to as digital options. To be more precise the call value resembles the result of subtracting a Cash-or-Nothing call from an Asset-or-Nothing call. We exemplify this relation for the FMLS model using the entries in Table 1. The results are summarized in Table 3, note that the Cash-or-Nothing call has to be scaled by the current strike value.

Table 3: Call price as the difference of an Asset-or-Nothing call and a Cash-or-Nothing call in the FMLS model. Model parameters are $S = K = 100$, $T = 1$, $r = 0.05$, $\alpha = 1.6$ and $\sigma = 0.1$ where the contour of integration is chosen along 1.75.

Asset-or-Nothing	73.085400047
Cash-or-Nothing \times Strike	63.443665532
Call	9.641734515

While having the same appealing intuitive properties like in the Black-Scholes case, this approach has several deficiencies with respect to the numerical evaluations of the Fourier integrals. The numerical approximation of a Fourier integral will introduce a discretization error and a truncation error [compare Section 6] which will double by evaluating two integrals. This might be alleviated by considering equation (4.14), however, it remains to evaluate the characteristic function for the price dynamics twice which is a time critical factor. Another crucial factor are the convergence properties of the integrands. From (4.14) and (4.15) likewise it becomes apparent that the integrands decay approximately in a linear fashion, whereas all other approaches under consideration have a quadratic rate of decay, usually leading to substantial savings in computation time.

Attari (2004) and Bates (2006) Formulae

As we know from the approaches developed by [Attari \(2004\)](#) and [Bates \(2006\)](#) it is possible to obtain single integration solutions and sharing the cumulative density function analogy of the Black–Scholes style formula for finding option prices. In this framework we do not have to specify a specific damping factor or contour of integration in the complex plane to make the Fourier integrals well behaved which is definitely simplifying implementational matters. Further, another similarity between both formulae is that they share a quadratic term in the denominator exhibiting exactly the same advantageous convergence properties compared to the Black–Scholes like solution.

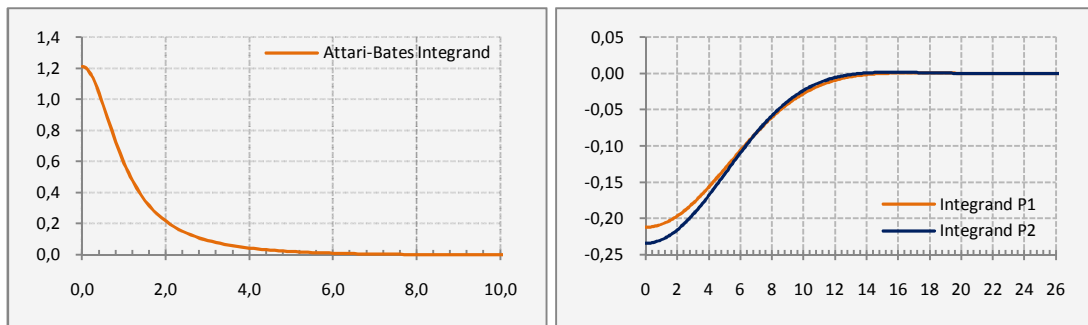


Figure 19: Rate of decay in the [Attari \(2004\)](#) and [Bates \(2006\)](#) valuation formulae in comparison to the Black–Scholes like solution. Left: Attari-Bates Integrand. Right: Black–Scholes style integrands. Model parameters are chosen as in the right panel of [Figure 18](#).

The curvatures of the integrands in [Figure 19](#) demonstrate the much faster rate of decay of the models with quadratic decay as the frequency variable approaches infinity.

Carr and Madan (1999) and Time Value Formulae

The Fourier inversion method developed by [Carr and Madan \(1999\)](#) attracted a lot of attention mainly due to two reasons. First, it allows to price options for a whole range of strikes in one go and secondly it introduces an additional degree of freedom which has a deep impact on the curvature of the involved Fourier integrands. This additional parameter is not only crucial for the application of the FFT to option pricing but as well serves as a scaling factor affecting the smoothness of the integrands. A well behaved integrand helps the numerical integration schemes significantly and hence is indispensable for highly accurate results in this framework. [Figure 20](#) gives an example that is based on the [Heston \(1993\)](#) model. As one can see, the choice of the damping factor α is an important one. In the left panel the divergent behavior around zero is clearly visible and in contrast, the right panel shows a smooth behavior of the integrands with reasonable choices for α that allow for a precise evaluation of the pricing formula. Many authors have discussed this pricing approach in rigorous detail, most notably the works by [Lee \(2004\)](#) extending the approach

significantly and providing an error analysis and Lord and Kahl (2007) who give detailed instructions on how to chose α to receive ‘very’ high precision values.

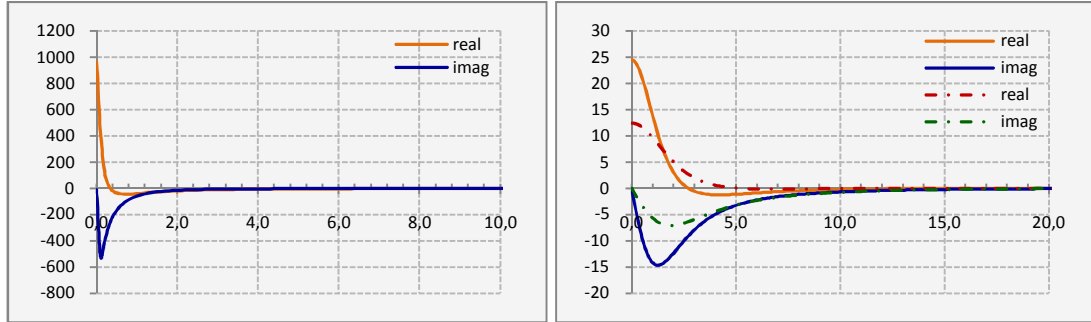


Figure 20: Damping factor α as scaling parameter. Left: Real and imaginary parts of the Heston call value integrand with $\alpha = 0.1$. Right: Real and imaginary parts of the Heston call value integrand with $\alpha = 1.75$ (solid lines) and $\alpha = 2.75$ (dashed lines). Model parameters: $S = K = 100$, $T = 1$, $r = 0.05$, $\kappa = 2$, $\theta = 0.01$, $\rho = -0.5$, $\sigma_v = 0.25$ and $v_0 = 0.02$.

In the sequel we focus on some typical observations made within this framework, for a deep analysis we refer to the mentioned literature. The interplay between α and the resulting function values is visualized in Figure 21. An α near the origin of the call formula and an α around one for the put formula show complete meaningless results, with increasing α the prices approach the true values (obtained with the adaptive Gauss–Kronrod quadrature). As was mentioned in Section 4.4, there is an upper bound on α as well which depends on the number of moments of the particular price process.

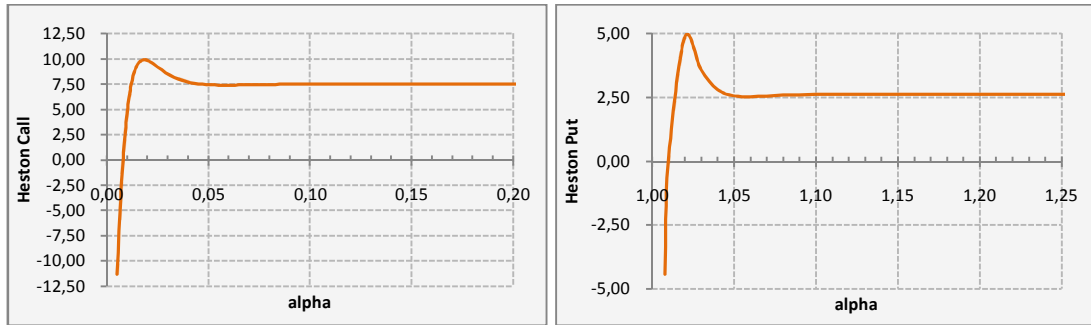


Figure 21: Heston values as a function of damping factor α . Left: Call options formula, true price: 7.504536548. Right: Put options formula, true price: 2.627478999. Model parameters: $S = K = 100$, $T = 1$, $r = 0.05$, $\kappa = 2$, $\theta = 0.01$, $\rho = -0.5$, $\sigma_v = 0.25$ and $v_0 = 0.02$.

The examples illustrated in Figure 22 based on FFT and the fractional Fourier transform show typical error patterns emerging from the use of these methods. They are only for illustration purposes, a detailed overview comparing these methods and assessing their accuracy is given in Chourdakis (2005).

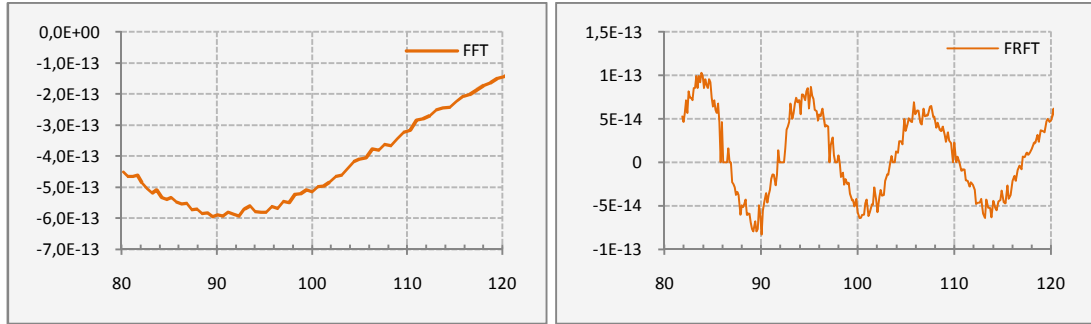


Figure 22: Comparison of Black-Scholes call option prices. Left: FFT with $N = 4096$ and $\eta = 0.25$. Right: FRFT with $N = 128$ and $\eta = 0.2$ for the strike range 80 – 120. Model parameters: $S = K = 100$, $T = 0.5$, $r = 0.04$, $\sigma = 0.2$ and damping factor $\alpha = 1.75$.

The second approach considered by Carr and Madan (1999) subtracts the intrinsic value from the option and thus deals with time values of the option only. This simple procedure ensures the square integrability of the valuation function and does not require choosing a damping factor. Unfortunately, the function has a sharp peak at $k = 0$, in the neighborhood of this peak the FFT has serious problems due to the fact that in this area very high frequencies are required to accurately evaluate the integrand which are omitted by a Fourier inversion over a finite range of integration. The source of divergence results from the non differentiability of the intrinsic value around the at-the-money level. Additionally, the original formulation in Carr and Madan (1999) creates a discontinuity at $k = 0$ which troubles the numerical inversion even more. These findings can be seen in Figure 23 where the time value function is plotted and contrasted to the analytical solution of the Black-Scholes model. A simple solution to the discontinuity problem is proposed in McCulloch (2003) [as described in Section 4.4].

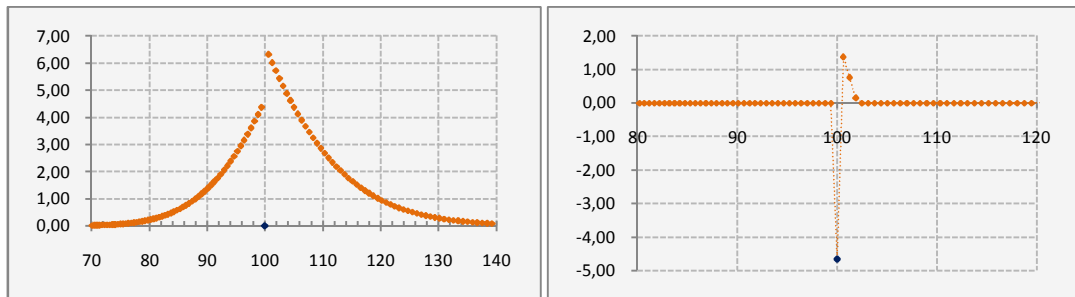


Figure 23: Out-of-the-Money Time Value function and absolute error in the Black-Scholes model. FFT with $N = 4096$ and $\eta = 0.25$. Model parameters: $S = K = 100$, $T = 0.5$, $r = 0.04$, $\sigma = 0.2$ and damping factor $\alpha = 1.75$. The blue points indicate where exactly $S = K$ or $k = 0$, at this point our FFT algorithm did not return a value.

The divergent behavior of the Time Value method can be alleviated by damping the very high frequencies by a hyperbolic sine function. An example is given in Figure 24. Without damping the extreme frequencies one can observe the highly oscillatory curvature of the integrand in the left exhibit.

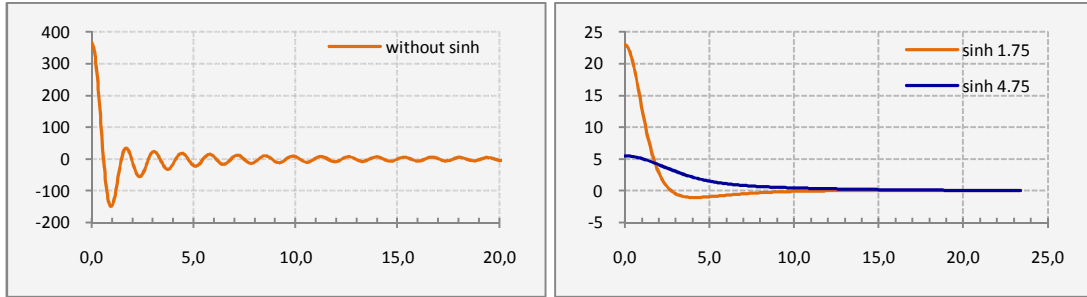


Figure 24: Integrand for the Time Value method. FMLS model with $S = K = 100$, $T = 0.5$, $r = 0.05$, $\alpha = 1.6$ and $\sigma = 0.14$.

By introducing a `sinh` damping function the integrand becomes progressively better behaved and hence more suitable for numerical integration schemes. However, for choosing the damping factor too big the integrand will get too close to zero and inhibits precise evaluation.

The Time Value method is usually considered as a robust and stable method, but, as [Borak & al. \(2005\)](#) note, due to the sharp cusp around the at-the-money level it may lead to some undesired numerical artefacts for the resulting volatility smiles.

Lipton (2002) and Lewis (2001) Formulae

With the introduction of a damping factor [Carr and Madan \(1999\)](#) make a big step to numerically highly efficient pricing algorithms. By multiplying the option price function by an exponential function to ensure the integrability of the Fourier transform the pricing problem is effectively shifted into the complex plane which requires the characteristic function to be evaluated in a specific domain of the complex plane depending on the payoff function and the particular stochastic process.

From [Lewis \(2001\)](#) we have a clear exposition of the interplay between the conditions on the payoff functions and the price processes made explicit by directly applying the Plancherel–Parseval identity to the convolution representation of the pricing kernel with the payoff in Fourier space. By carefully choosing the contour of integration along the complex plane and checking for singularities a flexible pricing framework for arbitrary payoff functions and price processes is established. Throughout the paper we illustrate several applications of this framework, for instance the binary options in the Black–Scholes section above or the calculations of Greeks and the state price density in the following section. Here we examine the algorithms for plain European call and put options.

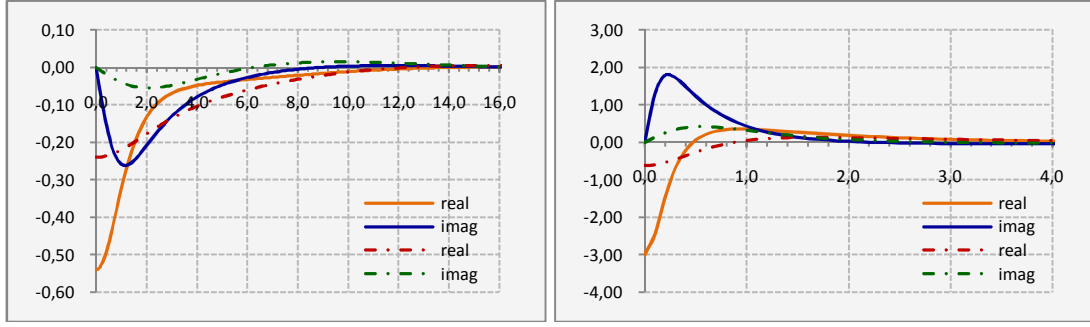


Figure 25: Effect of choosing a contour of integration. Left: Real and imaginary parts of the Heston call value integrand with $z_i = 2.5$ (solid lines) and $z_i = 4.5$ (dashed lines). Right: Real and imaginary parts of the Heston put value integrand with $z_i = -0.25$ (solid lines) and $z_i = -0.75$ (dashed lines). Model parameters: $S = 100$, $K = 80$, $T = 1$, $r = 0.05$, $\kappa = 2$, $\theta = 0.01$, $\rho = -0.5$, $\sigma_v = 0.25$ and $v_0 = 0.02$.

The graphics shown in Figure 25 depict the valuation formula in Eq. (4.54). In the left panel two examples of possible lines of integration along $z_i > 1$ are shown, for this region the call price function is well defined [Call = 24.119720814]. For the right panel two arbitrary values $z_i < 0$ are chosen which define the put value function [Put = 0.218074775]. The effect of a particular contour of integration with respect to the curvature of the integrands is considerable.

By moving the contour and applying Residual Calculus two alternative formulations for the call and put formulae are obtainable. As illustrated in the entry of the covered call and cash-secured put in Table 1 the strip of regularity is defined for $0 < \Im[z] < 1$. This is true for both the call and put formula only distinguished by a different resulting residue. The effect of specifying a particular line of integration in this narrow strip seems to be more sensible than in the previous case. In Figure 26 the resulting option values as a function of the contour parameter z_i are contrasted to the ‘true’ value calculated by the aid of the adaptive Gauss–Kronrod quadrature.

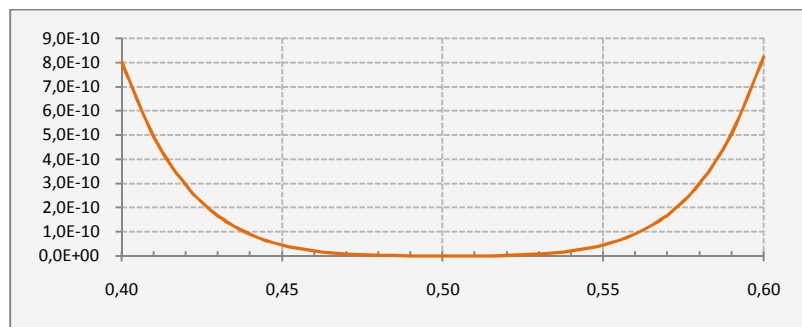


Figure 26: Absolute error of the Heston call value as a function of the contour parameter z_i .

As was pointed out in Section 4.5 the choice of $z_i = \frac{1}{2}$ is not only facilitating implementations but ensures accurate results for this particular valuation formula. The same observations hold for put value formulation and the Lipton (2002) formulae as well as they are equivalent formulations.

5.5 Greeks and State Price Densities

The accurate valuation of financial claims is not only the key in financial modeling, the hedging of these derivative instruments is at least as important. In order to do so we need the various sensitivities of the specific models with respect to the state variables and model parameters commonly referred to as Greeks. Expositions of common Greeks in the Black–Scholes style Fourier valuation framework can be found e.g. in [Schöbel and Zhu \(1999\)](#), [Minenna and Verzella \(2008\)](#) and including some higher order Greeks like Vomma and Charm, Dual Delta or Dual Gamma we refer to [Reiß and Wystup \(2001\)](#). A detailed description, possible uses and pitfalls of these higher order Greeks in a Black–Scholes world may be found in a series of papers from [Haug \(2003a,b\)](#). All these Greeks may be obtained by using simple and straightforward finite differences schemes, however, in case that the characteristic function is known these are directly available in an analytical form just like the derivatives prices or density functions. An exposition of the derivation of Greeks in the single integral solutions is relatively rare yet, therefore we present some arbitrarily chosen hedge parameters in these frameworks.

In the [Carr and Madan \(1999\)](#) approach the hedge ratio Delta Δ is given as follows

$$\begin{aligned}\Delta &= \frac{\partial C}{\partial S}, \\ &= \frac{\partial}{\partial S} \left\{ \frac{e^{-\alpha k}}{\pi} \int_0^\infty \Re \left[e^{-iuk} \frac{e^{-rT} \phi_T(u - (\alpha + 1)i)}{\alpha^2 + \alpha - u^2 + i(2\alpha + 1)u} \right] du \right\}, \\ &= \frac{e^{-\alpha k}}{\pi} \int_0^\infty \Re \left[e^{-iuk} \frac{e^{-rT} \frac{\partial \phi_T(u - (\alpha + 1)i)}{\partial S}}{\alpha^2 + \alpha - u^2 + i(2\alpha + 1)u} \right] du.\end{aligned}\tag{5.25}$$

Calculating the partial derivative we get

$$\frac{\partial \phi_T(u - (\alpha + 1)i)}{\partial S} = \frac{\phi_T(u - (\alpha + 1)i)(\alpha + 1 + iu)}{S}.\tag{5.26}$$

Hence yielding

$$\Delta = \frac{e^{-\alpha k}}{S\pi} \int_0^\infty \Re \left[e^{-iuk} \frac{e^{-rT} \phi_T(u - (\alpha + 1)i)(\alpha + 1 + iu)}{\alpha^2 + \alpha - u^2 + i(2\alpha + 1)u} \right] du,\tag{5.27}$$

which may be further simplified to [compare Eq. (4.36)]

$$\Delta = \frac{e^{-\alpha k}}{S\pi} \int_0^\infty \Re \left[e^{-iuk} \frac{e^{-rT} \phi_T(u - (\alpha + 1)i)}{\alpha + iu} \right] du.\tag{5.28}$$

The Gamma Γ of an option is given by the second derivative of the option with respect to the underlying

$$\Gamma = \frac{\partial \Delta}{\partial S} = \frac{\partial \Delta}{\partial x} \frac{\partial x}{\partial S}, \quad (5.29)$$

$$= \frac{e^{-\alpha k}}{S^2 \pi} \int_0^\infty \Re[e^{-iuk} e^{-rT} \phi_T(u - (\alpha + 1)i)] du. \quad (5.30)$$

The Delta and Gamma Greeks shown above in addition to the sensitivity Rho are model free in the sense that they do not rely on the particular characteristic function. If we are interested in calculating the Vega v for example, we have to differentiate the characteristic function with respect to the model parameter describing the volatility or variance which will be evidently model dependent. Even more involved is the situation for Theta, i.e. the sensitivity with respect to the time to maturity, the time is a relevant factor for both the general valuation formula and the particular characteristic functions conditional upon the current time state. For the [Heston \(1993\)](#) model Greeks are illustrated in detail e.g. in [Nagel \(2001\)](#) and [Reiß and Wystup \(2001\)](#) and will not be repeated here.

In the following we will illustrate the concepts within the Lipton–Lewis valuation framework and work out a number of Greeks for the FMLS model. Recalling (4.61) and differentiating yields for the Delta

$$\Delta = 1 - \frac{K e^{-rT}}{S \pi} \int_0^\infty \Re \left[\left(iu + \frac{1}{2} \right) e^{(iu + \frac{1}{2})k} \phi_T \left(u - \frac{i}{2} \right) \right] \frac{du}{u^2 + \frac{1}{4}}, \quad (5.31)$$

and

$$\Gamma = \frac{K e^{-rT}}{S^2 \pi} \int_0^\infty \Re \left[e^{(iu + \frac{1}{2})k} \phi_T \left(u - \frac{i}{2} \right) \right] du, \quad (5.32)$$

for the Gamma. The general form for Vega is given by

$$v = \frac{\partial C}{\partial v_0} = -\frac{K e^{-rT}}{\pi} \int_0^\infty \Re \left[e^{(iu + \frac{1}{2})k} \frac{\partial \phi_T \left(u - \frac{i}{2} \right)}{\partial v_0} \right] \frac{du}{u^2 + \frac{1}{4}}, \quad (5.33)$$

where v_0 denotes the variance or volatility depending on the particular model. Considering the FMLS model we do not have either of the two for $\alpha < 2$, but we have the scale parameter σ governing the width of the distribution. Differentiating the characteristic function of the FMLS process with respect to σ results in

$$\begin{aligned} & \frac{\partial \exp \left[T \left(iu \sigma^\alpha \sec \frac{\pi \alpha}{2} - (iu \sigma)^\alpha \sec \frac{\pi \alpha}{2} \right) \right]}{\partial \sigma} \\ &= T \left(\frac{i u \sigma^\alpha \alpha \sec \frac{\pi \alpha}{2}}{\sigma} - \frac{(i u \sigma)^\alpha \alpha \sec \frac{\pi \alpha}{2}}{\sigma} \right) \end{aligned} \quad (5.34)$$

$$\times \exp \left[T \left(iu\sigma^\alpha \sec \frac{\pi\alpha}{2} - (iu\sigma)^\alpha \sec \frac{\pi\alpha}{2} \right) \right].$$

For Rho the calculation yields

$$\begin{aligned} \frac{\partial C}{\partial r} = & -\frac{Ke^{-rT}}{\pi} \left\{ \int_0^\infty \Re \left[\left(iu + \frac{1}{2} \right) T e^{(iu+\frac{1}{2})k} \phi_T \left(u - \frac{i}{2} \right) \right] \frac{du}{u^2 + \frac{1}{4}} \right. \\ & \left. - T \int_0^\infty \Re \left[e^{(iu+\frac{1}{2})k} \phi_T \left(u - \frac{i}{2} \right) \right] \frac{du}{u^2 + \frac{1}{4}} \right\}. \end{aligned} \quad (5.35)$$

To complete the first order Greeks Theta reads

$$\begin{aligned} \frac{\partial C}{\partial T} = & \frac{Ke^{-rT}}{\pi} \left\{ \int_0^\infty \Re \left[\left(iu + \frac{1}{2} \right) r + \frac{\phi_T \left(u - \frac{i}{2} \right)}{T} \right] \right. \\ & \times e^{(iu+\frac{1}{2})k} \phi_T \left(u - \frac{i}{2} \right) \left. \frac{du}{u^2 + \frac{1}{4}} \right. \\ & \left. - r \int_0^\infty \Re \left[e^{(iu+\frac{1}{2})k} \phi_T \left(u - \frac{i}{2} \right) \right] \frac{du}{u^2 + \frac{1}{4}} \right\}. \end{aligned} \quad (5.36)$$

Higher order Greeks can be derived in exactly the same manner by further differentiating the first order Greeks. For illustration purposes we arbitrarily pick up three higher order Greeks.

Firstly we consider the DdeltaDtime, Charm or Delta Bleed which is the Delta's sensitivity to changes in time. The DdeltaDtime Greek indicates of what happens with the option's Delta when maturity comes closer. It is defined as

$$\begin{aligned} -\frac{\partial \Delta_c}{\partial T} = & -\frac{Ke^{-rT}}{S\pi} \left\{ \int_0^\infty \Re \left[\left(iu + \frac{1}{2} \right) \left(\left(iu + \frac{1}{2} \right) r + \frac{\phi_T \left(u - \frac{i}{2} \right)}{T} \right) \right] \right. \\ & \times e^{(iu+\frac{1}{2})k} \phi_T \left(u - \frac{i}{2} \right) \left. \frac{du}{u^2 + \frac{1}{4}} \right. \\ & \left. - r \int_0^\infty \Re \left[e^{(iu+\frac{1}{2})k} \phi_T \left(u - \frac{i}{2} \right) \right] \frac{du}{u^2 + \frac{1}{4}} \right\}. \end{aligned} \quad (5.37)$$

Secondly, the DgammaDvol, also known as Zomma, is the sensitivity of Gamma with respect to changes in volatility or variance

$$\frac{\partial \Gamma}{\partial v_0} = \frac{K e^{-rT}}{S^2 \pi} \int_0^\infty \Re \left[e^{(iu + \frac{1}{2})k} \frac{\partial \phi_T(u - \frac{i}{2})}{\partial v_0} \right] du. \quad (5.38)$$

Thirdly, the DvegaDvol, Vomma or also known as Vega convexity or Volga, is the sensitivity of the Vega to changes in volatility or variance

$$\frac{\partial^2 C}{\partial v_0^2} = \frac{\partial v}{\partial v_0}. \quad (5.39)$$

For the FMLS model taking the second derivative of the option gives

$$\begin{aligned} \frac{\partial v}{\partial v_0} = & -\frac{K e^{-rT}}{\pi} \int_0^\infty \Re \left[T \frac{i u \sigma^\alpha \alpha^2 \sec \frac{\pi \alpha}{2}}{\sigma^2} - \frac{i u \sigma^\alpha \alpha \sec \frac{\pi \alpha}{2}}{\sigma^2} \right. \\ & - \frac{(i u \sigma)^\alpha \alpha^2 \sec \frac{\pi \alpha}{2}}{\sigma^2} + \frac{(i u \sigma)^\alpha \alpha \sec \frac{\pi \alpha}{2}}{\sigma^2} \\ & \times e^{(iu + \frac{1}{2})k + T(i u \sigma^\alpha \sec \frac{\pi \alpha}{2} - (i u \sigma)^\alpha \sec \frac{\pi \alpha}{2})} \\ & + T^2 \left(\frac{i u \sigma^\alpha \alpha \sec \frac{\pi \alpha}{2}}{\sigma} - \frac{(i u \sigma)^\alpha \alpha \sec \frac{\pi \alpha}{2}}{\sigma} \right)^2 \\ & \left. \times e^{(iu + \frac{1}{2})k + T(i u \sigma^\alpha \sec \frac{\pi \alpha}{2} - (i u \sigma)^\alpha \sec \frac{\pi \alpha}{2})} \right] \frac{du}{u^2 + \frac{1}{4}}. \end{aligned} \quad (5.40)$$

For expository purposes, we give a numerical example for the FMLS model and summarize the resulting Greeks in [Table 4](#).

Other Greeks can be derived in a similar way, however, depending on the particular characteristic function these may result in quite lengthy expressions. We can see that many terms appear repeatedly, so we can temporarily store intermediate results which will simplify the implementation and can reduce computation time significantly. The implications in terms of computational efficiency and accuracy are practically identical to the observations made throughout the paper.

Table 4: Greeks for the Finite Moment Log Stable model. FMLS model with $S = K = 100$, $T = 0.5$, $r = 0.05$, $\alpha = 1.8$ and $\sigma = 0.11$. The first entry for each item is for the call while the second is for the put respectively.

Call	5.952366338		
Put	3.483357541		
Delta	0.653499430	Rho	29.698788334
	-0.346500570		-19.066707268
Gamma	0.033587476	Charm	0.092109339
	0.033587476	DdeltaDtime	-0.092109339
Vega	38.456732518	Zomma	-0.265054082
	38.456732518	DgammaDvol	-0.265054082
Theta	-7.670146141	Vomma / Volga	-0.715079076
	-2.793596581	DvegaDvol	-0.715079076

On several occasions we already pointed out the great importance of the concept and usefulness of Arrow–Debreu prices, or state price densities respectively, with respect to the fundamental risk neutral valuation principle and Fourier pricing alike. At this point we present a graphical illustration to emphasize these important theoretical underpinnings.

For this purpose we employ the Fourier transform of an Arrow–Debreu security as is shown in Table 1. The state price density or discounted risk neutral density [compare Eq. (2.3)] then results from an infinite collection of those Arrow–Debreu securities as in Figure 27.

Formally this reads

$$\delta(e^x - K) = \frac{e^{-rT}}{\pi} \int_{0-\infty}^{iz_i+\infty} e^{-iz(\ln S_0 + rT)} \phi_T(-z) K^{iz} dz, \quad (5.41)$$

$$= \frac{e^{-rT}}{\pi} \int_{iz_i-0}^{iz_i+\infty} e^{-iz(\ln \frac{S_0}{K} + rT)} \phi_T(-z) dz. \quad (5.42)$$

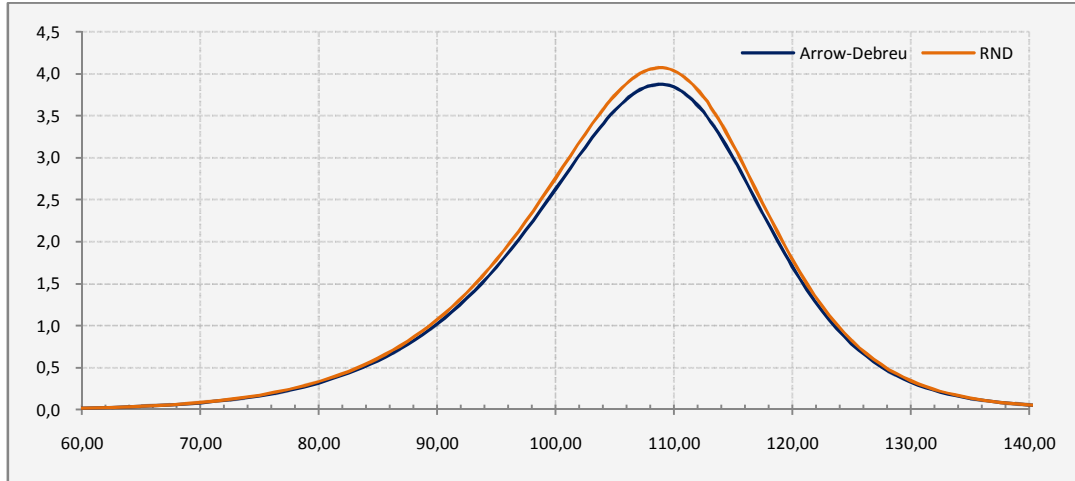


Figure 27: Continuum of Arrow–Debreu securities and risk neutral density (RND) in the Heston model. Model parameters: $S = 100$, $T = 1$, $r = 0.05$, $\kappa = 2$, $\theta = 0.01$, $\rho = -0.5$, $\sigma_v = 0.25$ and $v_0 = 0.02$.

As we can see summing up these ‘Dirac spikes’ representing the prices of a claim with a delta function payoff at infinitely small increments depict a well formed density.

5.6 Concluding Remarks and Further Results from the Literature

The major computational workload for all discussed methods is determined by the number of evaluations of the characteristic function. Driving factor for the number of evaluations needed to obtain a given level of accuracy are the convergence properties of the particular methodology. For option pricing applications the Black–Scholes like valuation formula and variants hereof fail the requirement of sufficiently fast decaying integrands in comparison to the other methods which all decay much faster due to a quadratic term in the denominator. The models evaluating the Fourier integrals on a particular contour of integration in the complex plane additionally offer a fine tuning parameter affecting convergence rates which, if chosen carefully, is able to provide a good compromise between speed and accuracy.

All conducted numerical experiments are based on straightforward implementations of the algorithms without any (intended) optimizations. The CPU-time requirements for the calculations depend on many factors like CPU clock or used programming language and thus the displayed times should be viewed more in a relative sense. In order to increase the computational efficiency of the Gauss quadratures the nodes and weights can be pre-calculated and stored for later use (which is done for the composite Gauss quadratures). Furthermore, we strongly recommend to always use the highest precision available for the particular quadrature nodes, in the literature abscissas and weights are often tabulated for less than double precision which can deteriorate numerical results significantly⁴.

⁴ High-precision abscissas and weights tabulated up to 100 nodes and C/C++ source code for the Gauss–Legendre quadrature are available at http://www.holoborodko.com/pavel/?page_id=679

An important topic to pay attention to is that the implementation of characteristic functions might require the evaluation of complex logarithms as is the case in Heston's formula [see e.g. [Mikhailov and Nögel \(2003\)](#)]. These are multivalued functions which can introduce discontinuities while evaluating the specific integrands and lead to meaningless option prices. This phenomena was first pointed out by [Schöbel and Zhu \(1999\)](#) and was tackled since then by several authors, amongst others, [Kahl and Jäckel \(2006\)](#), [Lord and Kahl \(2008\)](#), [Fahrner \(2007\)](#) or [Guo and Hung \(2007\)](#). For our studies we used the '*formulation 2*' of the characteristic function described in e.g. [Albrecher & al. \(2006\)](#) or [Gatheral \(2006\)](#).

The calculation of option prices and density approximations by the various numerical algorithms lead to different types of errors. By imposing an upper integration limit with a finite number may result in a truncation error [see Section 6.4]. Evaluating the integrand only at a limited number of points introduces sampling errors and for FFT based methods interpolation errors arise from the fact that these algorithms return values only on an equidistant grid [compare Section 6.2]. Another source of error are roundoff errors introduced by inexact computer arithmetic.

In the literature on characteristic function calculus a number of possibilities are developed to control these errors. Providing error bounds for the numerical inversion of characteristic functions is a crucial ingredient for this task [see e.g. [Hughett \(1998\)](#)]. The results from Probability Theory have been amended to option pricing purposes by considering option prices as normalized probability functions. For example, [Pan \(2002\)](#) builds upon the results from [Davies \(1973\)](#) to provide an error analysis to target pricing errors. Another thorough error analysis framework and error minimizing algorithms are presented in [Lee \(2004\)](#).

Numerical integration schemes and FFT algorithms are subject to ongoing active research efforts. These improvements will surely affect applications in financial modeling as well. One example is the work from [Minenna and Verzella \(2007\)](#) who apply non uniform FFT algorithms which allow for non uniform sampling of the characteristic function and employ Gaussian quadratures by interpolating an oversampled FFT to the pricing of options.

6 Numerical Issues and Possible Refinements to the Inverse Fourier Methods

The focus of this section lies on implementational issues and practical details. Computational performance and complexity are extremely important in density calculations and pricing. We investigate different approaches that have positive effects on computational speed and can help to stabilize Fourier inversion methods.

6.1 Inversion of the Option minus the Black–Scholes Approximation

In order to compute option prices [Tankov \(2009\)](#) presents a slightly different formulation of the Time Value method proposed in [Carr and Madan \(1999\)](#) and [Cont and Tankov \(2004\)](#). The pricing problem is defined by the Fourier transform of the time value of the option

$$z_T(k) = \mathbb{E}[(e^x - e^k)^+] - (e^x - e^k)^+. \quad (6.1)$$

Then the Fourier transform of the time value of a call option, assuming an adjusted log strike $k = \ln \frac{Ke^{-rT}}{S_0}$, is given by

$$\zeta_T(u) = \int_{-\infty}^{\infty} e^{iuk} z_T(k) dk = \frac{\phi_T(u - i) - 1}{iu(iu + 1)}. \quad (6.2)$$

Finally, the option prices result by inverting the Fourier transform

$$C(S_0, K, T) = (S_0 - Ke^{-rT})^+ + \frac{S_0}{\pi} \int_0^{\infty} e^{-iuk} \zeta_T(u) du. \quad (6.3)$$

As was already noted by [Carr and Madan \(1999\)](#) the time value method may result in a very wide and potential oscillatory Fourier transform with a poor convergence rate. [Cont and Tankov \(2004\)](#) argue this is due to the non smooth behavior of the time value, which is a non differentiable function, causing the Fourier transform to decay too slowly at infinity. This numerically challenging problem can be reduced severely by subtracting an analytically integrable complementary function from the original integrand. Proceeding this way, a methodology described in e.g. [Manno \(1988\)](#), will reduce the underlying curvature of the function to be integrated. The integration of the now better behaved composite function can then be evaluated with standard numerical quadratures and will most likely improve resulting accuracy.

In the context of option pricing this simple method was first considered by [Andersen and Andreasen \(2000\)](#), who use the Black–Scholes model as a control variate to stabilize the numerical Fourier inversion. The Black–Scholes model is a smooth function of the strike and makes the modified option prices differentiable. The characteristic function from the Gaussian will be subtracted from the original integrand and the Black–Scholes prices will be added afterwards [see [Tankov \(2009\)](#)]

$$\tilde{z}_T(k) = \mathbb{E}[(e^x - e^k)^+] - \frac{1}{S} c_{BS}^\sigma(k), \quad (6.4)$$

leading to

$$\tilde{\zeta}_T(u) = \int_{-\infty}^{\infty} e^{iuk} \tilde{z}_T(k) dk = \frac{\phi_T(u - i) - \phi_T^\sigma(u - i)}{iu(iu + 1)}, \quad (6.5)$$

where $\phi_T^\sigma(u) = \exp \left[-\frac{\sigma_{BS}^2}{2} T(u^2 + iu) \right]$ and eventually inverting yields to

$$C(S_0, K, T) = C_{BS}^\sigma(S_0, K, T) + \frac{S_0}{\pi} \int_0^\infty e^{-iuk} \tilde{\zeta}_T(u) du. \quad (6.6)$$

For this approach to work well we need to know an appropriate volatility level of the Black–Scholes model. One way to approximate the standard deviation of the particular price process in question is proposed in [O’Sullivan \(2005\)](#)

$$\sigma_{BS} = \sqrt{-\left. \frac{\partial^2 \phi_X(u)}{\partial u^2} \right|_{u=0} + \left(\left. \frac{\partial \phi_X(u)}{\partial u} \right|_{u=0} \right)^2}, \quad (6.7)$$

which can be simplified to

$$\sigma_{BS} = \sqrt{(-\Re[\phi_T''(0)]) - (\Im[\phi_T'(0)])^2}. \quad (6.8)$$

The standard deviation can now be calculated either analytically or by a simple finite difference scheme, for example [Dobránszky \(2009\)](#) opts to numerically approximate the derivatives with $\text{eps}=1\text{e-}5$.

Another possibility to approximate the wanted σ_{BS} is to determine the corresponding cumulants c_k of the distribution as is shown in [Fang and Oosterlee \(2008\)](#). While c_2 corresponds to the second moment [Fang and Oosterlee \(2008\)](#) recommend to include the fourth cumulant c_4 (or even c_6) as well since especially for short time to maturities the Levy processes might exhibit sharp peaks and fat tails, which may be accounted for by inclusion of higher order cumulants

$$\sigma_{BS} = \sqrt{c_2 + \sqrt{c_4}}. \quad (6.9)$$

Cumulants for the Heston model and some popular Lévy processes can be found in the appendix, Table 11 from [Fang and Oosterlee \(2008\)](#). For the FMLS model there does not exist a second moment for $\alpha < 2$, hence the second (real valued) cumulant does not exist either. In this case the numerical approximation seems to be the only reasonable choice (twice differentiation results in a complex valued cumulant as a function of the frequency variable).

All methods work well and do not impose any numerical impediments, however, depending on the characteristic function, the analytical expressions may become quite large, which in turn would favor the numerical approximation. While accurate approximations of the standard deviations lead to optimized Fourier inversion, even an *ad hoc* choice for σ_{BS} like 0.1 or 0.2 will improve convergence significantly. On a side note we emphasize the fact that the obtained values for σ_{BS} describe the standard deviation of the stochastic process and do not necessarily have to coincide with concepts like implied volatility.

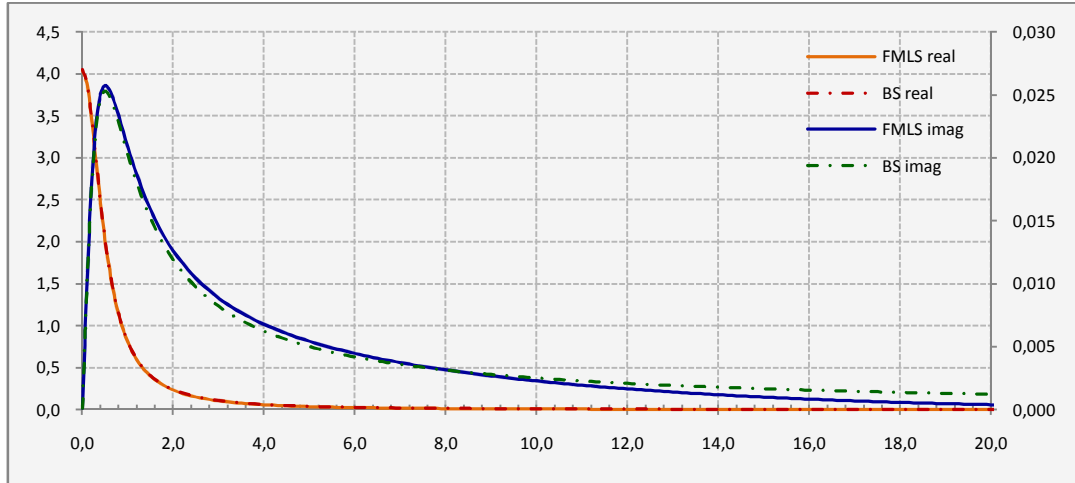


Figure 28: Control variate for the FMLS model in the Lipton–Lewis framework. FMLS model parameter: $S = K = 100$, $T = 0.5$, $r = 0.05$, $\alpha = 1.8$ and $\sigma = 0.1$. The solid lines depict the FMLS integrand and the dashed lines result for the Black–Scholes integrand based on the standard deviation given by 31.62% for the FMLS process (imaginary parts are denoted on the right scale). The implied volatility for the model parameter with call price 5.567831374 is given by 15.15%.

The use of Black–Scholes control variates is applicable to all the mentioned valuation formulae presented in this text [see e.g. [Dobránszky \(2009\)](#) for the Lipton–Lewis formula and [Figure 28](#)]. The use of the Black–Scholes model not only improves numerical evaluations of the Fourier integrals, it further allows a thorough error control in a valuation framework [see [Tankov \(2004\)](#)]. Other control variates are conceivable if the characteristic functions of both models were close, which, however, will unlikely be the case since ‘analytical’ solutions to other sophisticated price dynamics typically involve infinite summation or special functions.

Without going into detail the same method works for density approximations as well. An example is given in [Jaschke and Jiang \(2002\)](#) for the approximation for the cumulative density function

$$F(x) - \Phi(x; \mu, \sigma) = \frac{1}{2} - \frac{1}{2\pi} \int_{-\infty}^{\infty} \frac{e^{-iux}}{iu} \left(\phi_X(u) - e^{-iu\mu - \frac{\sigma^2 u^2}{2}} \right) du. \quad (6.10)$$

Applying the inverse Fourier transform to $F(x) - \Phi(x; \mu, \sigma)$ mitigates the problem that the integrand has a pole at zero. Alternatives to the normal distribution may be more appropriate to the problem at hand provided they have analytical densities and corresponding Fourier transforms.

6.2 Interpolation Issues

One fundamental property of conventional FFT and FRFT methods is that the resulting values are located on an equally spaced output grid. Quite probably not all desired values will exactly agree on this equidistant grid, calling for some interpolation methods to find the intermediate values. This is vitally important for density calculations where the desired x -values are irregularly spaced and for option

prices which will be equally spaced on a log strike grid whereas options listed on the markets are usually denoted on a strike level, not the log strike level.

In the literature the authors often regard simple linear interpolation as an adequate algorithm yielding sufficiently accurate results. The main reasons are the additional computational workload or the argument that choosing the discretization sufficiently small, the interpolation error will be negligible. Exceptions are e.g. McCulloch (2003) or Chourdakis (2005) in the context of option pricing and Menn and Rachev (2006) for density approximations. McCulloch (2003) argues that simple linear interpolation may give an interpolation error in excess of the Fourier inversion computational error due to the convexity of the pricing function. Instead the use of cubic spline interpolation is favored for the call and put formulae which are capable to capture the curvature of the functions. These implications are exhibited in Figure 29 where the respective pricing errors of the two methods are displayed for a range of option values.

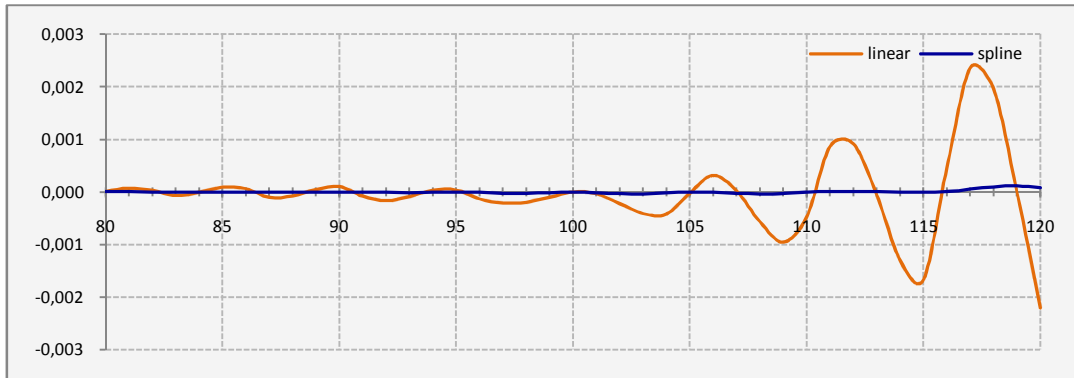


Figure 29: Linear vs. cubic spline interpolation for option pricing. Relative errors for FFT call option pricing in the Black–Scholes model with $N = 256$, $\eta = 0.5$, $\alpha = 1.75$. Model parameters: $S = K = 100$, $T = 0.25$, $r = 0.04$, $\sigma = 0.3$.

In comparison to the linear interpolation the cubic spline method is much more accurate in error terms. If computation time is critical one might use this result to reduce the number of summation points N and instead optimize the number of discretization points in Fourier space to obtain a characteristic function evaluated on a fine grid.

In numerical experiments Menn and Rachev (2006) confirm that cubic splines offer much better overall performance than linear interpolation with respect to density calculations. Whereas linear interpolation error is negligible in the tails where the curvature almost vanishes it will have a significant impact in the center of the distribution around the mode [see Figure 30]. Further Menn and Rachev (2006) are able to approximate an error estimate of the cubic spline interpolation quantitatively for α -stable distributions.

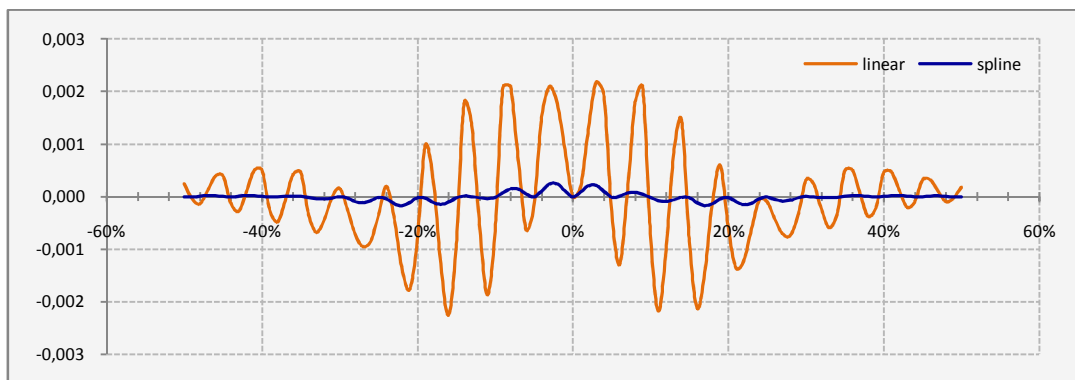


Figure 30: Linear vs. cubic spline interpolation for density approximations. Absolute error for FFT density approximations with in the Black–Scholes model with $N = 256$, $\eta = 0.5$.

Without saying other interpolation schemes will work perfectly well depending on the particular problem. One choice would be e.g. to consider a convex interpolation for option prices since this is a convex function of the strike [compare e.g. [Hagan and West \(2006\)](#)].

To summarize we can state that the potential increase in runtime using more sophisticated interpolation algorithms is in many cases justified by a potentially substantial improvement in accuracy.

6.3 Caching Technique

The FFT valuation framework along the lines of [Carr and Madan \(1999\)](#) is usually considered as the *de facto* standard for the fast pricing for a series of option prices. This is because the FFT, like the FRFT, is able to deliver outputs for a whole range of different strike levels in one go. Though, the simultaneous calculation for a given set of strikes is not restricted to the FFT or FRFT methods. For instance, in [Bates \(1996\)](#) the simple observation was made, that the values of the characteristic function for given model parameters do not depend on a particular strike level. Thus, it is possible to compute these values once, store them in a cache and reuse as desired for any strike. For a detailed discussion of this *caching technique* we refer to [Kilin \(2007\)](#) where this algorithm is contrasted to the FFT and FRFT methods using a number of affine (jump) diffusions and time changed Lévy processes. Using the [Attari \(2004\)](#) pricing algorithm [compare Section 4.2] for the direct integration method and conducting some calibration exercises with all three methods the author is able to show that the caching technique is orders of magnitude faster than FFT and FRFT.

An important aspect to note is that the caching technique can be used in conjunction with a whole range of sophisticated integration schemes like Gaussian quadratures. Therefore, the integration algorithm is not restricted to equally spaced grid points as is the case for the FFT and FRFT.

The same technique works for density approximations as well. The values for arbitrary x -values are not related to the evaluations of the characteristic function for specific model parameters. This makes the method a viable tool for computationally

intensive density calculations without the need for FFT methods and regularly spaced grid points.

In conclusion, the caching technique is a perfect candidate for tasks where the computational workload is high like calibration to market prices, calculations of corresponding hedge parameters or volatility surface and portfolio simulations.

6.4 Transforming the Domain of Integration

In theory all the considered Fourier integrals so far are continuous Fourier integrals, i.e. are defined continuously from minus infinity or zero to plus infinity. In practice though, we usually have to evaluate these integrals numerically. This implies that we have to discretize the integral in some form for summation and, further, have to truncate the infinite or semi infinite integral to a finite one (apart from the Gauss–Laguerre quadrature). For the discretization we have discussed a number of possibilities, now we consider potential ways of how to truncate the integration domain.

A very elegant way is to determine the asymptotics for the characteristic functions letting the frequency variable approach infinity. This is done for some popular price dynamics like [Heston \(1993\)](#), [Schöbel and Zhu \(1999\)](#) and the [Black and Scholes \(1973\)](#) model in [Lord and Kahl \(2007\)](#). They then evaluate the transformed integration domain by applying an adaptive Gauss–Lobatto quadrature. This way highly accurate derivative prices are achievable, but not in all cases it is possible to transform the domain of integration analytically.

Alternatively [Chourdakis \(2005\)](#) outlines a numerical method based on the fact that the absolute real and imaginary parts of the characteristic function $\phi_X(u)$ are less or equal than its modulus

$$\begin{aligned} |\Re[\phi_X(u)]| &\leq |\phi_X(u)|, \\ |\Im[\phi_X(u)]| &\leq |\phi_X(u)|. \end{aligned} \tag{6.11}$$

As we know from [Section 3.1](#) the characteristic function equals zero at infinity, that is we may regard the characteristic function as zero in a numerical sense for large u . Using these facts we may then use the modulus of the characteristic function to find a critical u_{max} such that

$$|\phi_X(u_{max})| \leq 10^{-m}, \tag{6.12}$$

where m denotes the desired precision level. Usually simple integer search methods will suffice for practical tasks avoiding the need for computationally intensive solver methods. Due to the oscillatory nature of Fourier integrals it may be theoretically possible that there is a contribution of the characteristic function beyond the determined truncation point, which nevertheless imposed no problems during made numerical experiments.

Instead of determining an upper integration limit *a priori* an alternative is to let the numerical quadrature choose an upper truncation point adaptively. For instance, the composite Gauss–Legendre quadrature [Eq. (5.3)] is predestined for this procedure which is proposed in e.g. Sepp (2003) or Yan and Hanson (2006) and which we use intensively throughout the paper. The number of summations N of the sub-intervals each evaluated by a Gauss–Legendre quadrature is determined by a local stopping criterion. Sepp (2003) recommends to stop the integration if the contribution of the last strip becomes less than $10e-12$ with a step size $h = 1$ for the single integral solutions and $h = 10$ for the Black–Scholes style valuation formula, whereas Yan and Hanson (2006) stop the integration if the ratio of the contribution of the last strip to the total integration becomes smaller than $0.5e-7$ and consider $h = 5$ as a good compromise between speed and accuracy for the Black–Scholes like formula.

In Lewis (2000) an approximation for an upper truncation level u_{max} is provided in the example code on p 68 for the Heston (1993) model

$$u_{max} = \max \left[1000, \frac{Q}{\sqrt{v_0 T}} \right], \quad (6.13)$$

where Q is set to 10 in this particular case. This ‘dimensionless’ relation reflects the inverse dependency of the integrand on the time to maturity, a property we have seen in the manifold graphical illustrations of various integrands [compare also to Section 6.5]. For other models and pricing algorithms other choices for Q and 1000 may be more appropriate and should be tested thoroughly. Q can be roughly interpreted as the number of standard deviations for the particular price process in view, which means, the heavier the tails of a distribution the bigger Q should be. Whereas for a thin tailed Black–Scholes model a value of say 5 is usually more than sufficient, 10 or even more seems appropriate for stochastic volatility and jump processes.

A similar procedure again for the Heston (1993) model together with the Attari (2004) algorithm is presented in Staunton (2006)

$$u_{max} = -Q \frac{\ln 0.0001}{\sqrt{T}}, \quad (6.14)$$

where Q is set to 10 as well. This formulation also respects the fact that the integrand depends inversely on the time to maturity, but does the scaling without a specific volatility or variance amendment.

There are a number of possibilities to find an upper integration point, which is definitely an important implementational issue to ensure accurate results. Simply making some *ad hoc* choices about the truncation levels should be avoided at all costs. This might work just fine for some circumstances, but inherits the risk that a significant part of the integrand is missed leading to meaningless results or that there is virtually no contribution to the final result rendering the procedure quite inefficient and random.

Since we deal with integrals on a semi-infinite domain, another possibility would be the use of Gauss–Laguerre quadratures not caring about truncation altogether. A reasonable procedure would be to choose a Laguerre quadrature with a high degree, say like $N = 128$, store the nodes and weights and stop integration when the contribution of the last strip becomes smaller than a predefined tolerance level. This would reduce the numerical complexity for relatively well behaved functions, but inherits the risk of not being sufficiently determined especially for short expiration dates and is not appropriate for highly oscillatory integrands and thus should be employed only with precaution.

6.5 Transforming the Fourier Integrands

The relevant domain of integration may vary quite significantly depending on the model parameters and more importantly the remaining time to maturity. In [Nagel \(2001\)](#) the author is outlining a standardizing procedure to transform the Fourier integrals which will narrow the differences with respect to the meaningful integration regions. The integrands are normalized by the standard deviation of the return process on maturity. The author illustrates the procedure for the Black–Scholes like valuation formula; here we will adapt this method to the single integral solutions. Considering for instance the [Lewis \(2001\)](#) approach we substitute the Fourier variable u with the scaled version $u \rightarrow u_{mod} = \frac{u}{\sqrt{v_0 T}}$, where v_0 denotes the instantaneous variance of the price dynamics. Applying the transformation to (4.57) the modified version with u_{mod} then reads

$$C(S_0, K, T) = S_0 - \frac{4\sqrt{SK}e^{-rT/2}}{\pi} \times \frac{\int_0^\infty \Re \left[e^{iu_{mod}k} \phi_T \left(u_{mod} - \frac{i}{2} \right) \right] \frac{du}{1 + u_{mod}^2}}{\sqrt{v_0 T}}, \quad (6.15)$$

where we finally have to rescale the resulting integral to obtain the desired option prices. The concept works equally fine for the other presented pricing algorithms as well. The standard deviation of the distribution function can be computed via explicit calculation of the second moment or corresponding cumulant respectively or by approximating the standard deviation with finite differences as in Section 6.1.

The impact from this moment scaling procedure results in a drastically reduced length of the needed integration range and a much less pronounced sensitivity to the maturity. These implications are illustrated below for the [Heston \(1993\)](#) model.

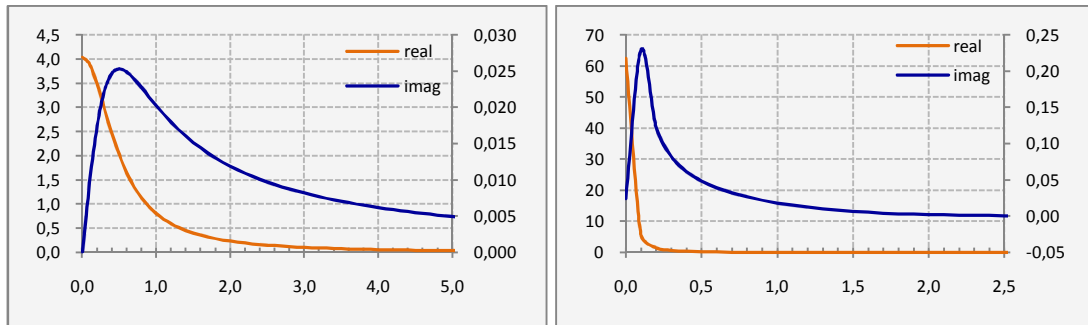


Figure 31: Impact of transforming the Fourier integrands. Left: Integrand with a standard numerical integration. Right: Slope with normalized integrands.

Using the transformation procedure allows applying the numerical quadrature on a predefined integration interval and therefore is potentially able to ease the numerical implementation. However, in this case a much finer resolution of the quadrature is needed to obtain sufficiently accurate results in comparison to the standard algorithm without the modification.

6.6 Log Spacing

To minimize computation one would like to have the lowest number of sampling points possible. In the context of Fourier inversion from image domain to space domain we can exploit the knowledge that the function to be integrated usually will exhibit a general decline in amplitude with increasing transform variable. Instead of sampling as often at low frequencies as at high frequencies, it seems reasonable to evaluate the integrand less frequently at higher frequencies.

In the following we adopt an idea from Meisel (1968) and implement an integration scheme in which the sampling intervals increase on a logarithmic scale. The characteristic function is then evaluated using unequally sampled intervals, where the intervals are equally spaced on a logarithmic scale. For this purpose we apply a simple procedure similar to the `logspace` function found in many standard numerical packages⁵ and amend it to ensure it starts at zero. At least we have to specify a starting and final value of the sequence and the number of samples to generate. Further possibilities are to decide whether or not to include the last sample or to define the base of the log space (which usually is base 10 by default).

⁵ See e.g. <http://docs.scipy.org/doc/numpy/reference/generated/numpy.logspace.html>

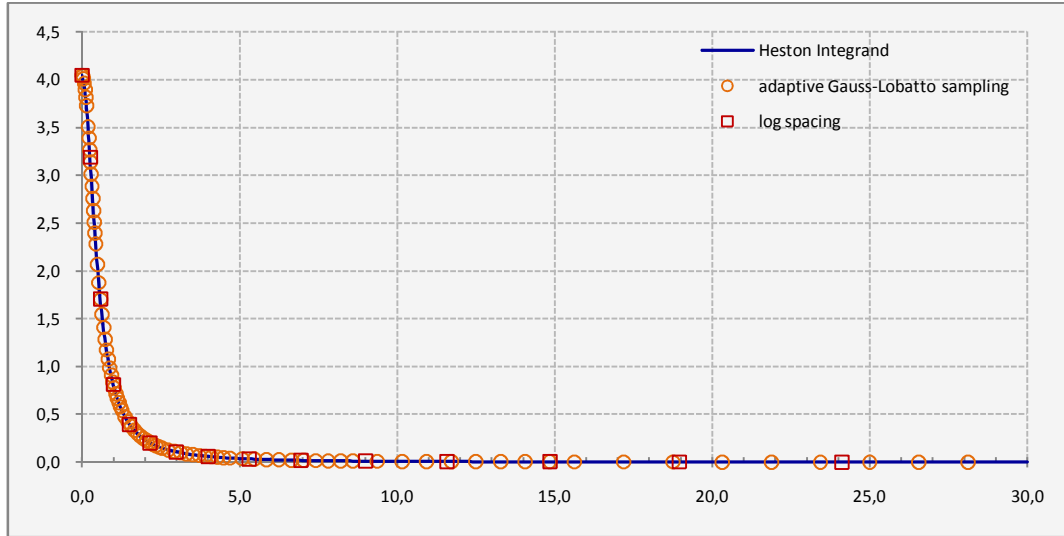


Figure 32: Sampling intervals on a log scale in comparison to adaptively sampled intervals. Log spacing parameter with starting value $a = 0$, final value $b = 10$ and number of steps = 100. Heston model parameter: $S = K = 100$, $T = 0.5$, $r = 0.05$, $\kappa = 2$, $\theta = 0.01$, $\rho = -0.5$, $\sigma_v = 0.1$ and $v_0 = 0.02$.

In conjunction with the composite Gauss–Legendre quadrature using an adaptive upper integration limit we are able to compute the Heston call price accurate up to at least 13 digits over the full strike range from 50 to 150 in comparison to the adaptive Gauss–Kronrod quadrature with a chosen tolerance level of $1e-15$ for the given example in Figure 32.

Table 5: Timings for different quadrature schemes. CPU time in seconds averaging over 100 call price calculations with strikes ranging from 51 to 150 (Heston calls with parameters as in Figure 32). For all routines the tolerance level is set to $1e-15$.

Quadrature	CPU time (sec)
adaptive Simpson	0.09266
adaptive Gauss–Lobatto	0.08451
adaptive Gauss–Kronrod	0.01797
composite Gauss–Legendre	0.04123
log spacing	0.00849

The time needed for this operation is only a negligible fraction of the time the adaptive procedure takes. In Table 5 the log spacing procedure is compared to other numerical quadratures as well. The time differences are quite remarkable and suggest that this approach is a very powerful method to help improve the numerical evaluation of Fourier integrals in terms of accuracy and in minimizing computation time.

Combining the log spacing technique with the caching technique gave the fastest density approximations and pricing for a set of options along the strike and time

dimension in comparison to all the other mentioned methods during numerical experiments.

7 Conclusion

Financial modeling in the area of option pricing involves detailed knowledge about stochastic processes describing the asset payoffs. For sophisticated price dynamics these are most conveniently characterized through functions in Image space. By a mapping of the probability function from spatial domain to the unit circle in the complex plane, expected values of a future payoff are then available in the form of an integral representation. With Fourier inversion methods these integral transforms allow the pricing for a whole range of possible payoff structures.

In this work we outline general features of Fourier transform techniques applicable to both the modeling of density functions and option pricing. Further we describe a number of modeling alternatives and accentuate on the similarities and subtleties of the different frameworks. Then we present several commonly used numerical quadratures to evaluate the integral representations and exemplify their use to density approximations and derivatives pricing. Finally, we present ‘*best practices*’ on how the quantitative modeling of the Fourier techniques may be improved by considering implementational issues, methodological aspects and computational performance.

The Fourier pricing techniques and Fourier inversion methods for density calculations add a versatile tool to the set of advanced techniques for pricing and management of financial derivatives.

References

- Abate, S. and W. Whitt (1992) The Fourier-series method for inverting transforms of probability distributions, *Queueing Systems: Theory and Applications* **10**(1–2), 5–88.
- Agliardi, R. (2009) The quintessential option pricing formula under Lévy processes, *Applied Mathematics Letters* **22**(10), 1626–1631.
- Albrecher, H., P. Mayer, W. Schoutens and J. Tistaert (2006) The Little Heston Trap, Working Paper, Linz and Graz University of Technology, K.U. Leuven, ING Financial Markets.
- Allen, R. L. and D. W. Mills (2004) *Signal Analysis: Time, Frequency, Scale, and Structure*, IEEE Press (Wiley–Interscience), New York.

- Andersen, L. and J. Andreasen (2000) Jump-diffusion Processes: Volatility Smile Fitting and Numerical Methods for Pricing, *Review of Derivatives Research* **4**, 231–262.
- Andersen, L. and J. Andreasen (2002) Volatile Volatilities, *Risk*, December, 163–168.
- Andersen, L. and V. Piterbarg (2007) Moment explosions in stochastic volatility models, *Finance and Stochastics* **11**, 29–50.
- Andreasen, J. (2006) Stochastic Volatility for Real, Working Paper, Bank of America.
- Andricopoulos, A., M. Widdicks, P. Duck and D. Newton (2003) Universal Option Valuation using Quadrature Methods, *Journal of Financial Economics* **67**, 447–471.
- Attari, M. (2004) Option Pricing using Fourier Transforms: A Numerically Efficient Simplification, Working Paper, Charles River Associates. Available at SSRN: <http://ssrn.com/abstract=520042>
- Bailey, D. and P. Swarztrauber (1991) The fractional Fourier transform and applications, *SIAM Review* **33**, 389–404.
- Bailey, D. and P. Swarztrauber (1994) A fast method for the numerical evaluation of continuous Fourier and Laplace transforms, *SIAM Journal on Scientific Computing* **15**, 1105–1110.
- Bakshi, G. and D. Madan (2000) Spanning and derivative-security valuation, *Journal of Financial Economics* **55**, 205–238.
- Barone-Adesi, G. and R. E. Whaley (1987) Efficient analytic approximation of american option values, *Journal of Finance* **42**, 301–320.
- Bates, D. S. (1996) Jumps and Stochastic Volatility: Exchange Rate Processes Implicit in Deutsche Mark Options, *Review of Financial Studies* **9**(1), 69–107.
- Bates, D. S. (2006) Maximum Likelihood Estimation of Latent Affine Processes, *Review of Financial Studies* **19**, 909–965.
- Benhamou, E. (2000) Fast Fourier Transform for Discrete Asian Options, EFMA 2001 Lugano Meetings. Available at SSRN: <http://ssrn.com/abstract=269491>

- Binkowski, K. (2007) Pricing of European Options using Empirical Characteristic Functions, Macquarie University, Sydney.
- Black, F. and M.S. Scholes (1973) The Pricing of Options and Corporate Liabilities, *Journal of Political Economy* **81**, 637–654.
- Borak, S., K. Detlefsen and W. Härdle (2005) FFT Based Option Pricing, Discussion Paper, Sonderforschungsbereich (SFB) 649, Humboldt Universität Berlin.
- Borovkov, K. and A. Novikov (2002) On a new approach to calculating expectations for option pricing, *Journal of Applied Probability* **39**, 889–895.
- Bouziane, M. (2008) *Pricing Interest-Rate Derivatives – A Fourier-Transform Based Approach*, Lecture Notes in Economics and Mathematical Systems 607, Springer, Berlin.
- Boyarchenko, S.I. and S.Z. Levendorskii (2002) *Non-Gaussian Merton-Black-Scholes Theory*, World Scientific.
- Breeden, D. and R. Litzenberger (1978) Prices of state-contingent claims implicit in option prices, *Journal of Business* **51**, 621–651.
- Cardi, G. (2005) Exotic Options under Lévy Processes, Ph.D. Dissertation, University of Bergamo.
- Carr, P. P. (2003) Option Pricing using Integral Transforms, Presentation. Available at <http://www.math.nyu.edu/research/carrp/papers/pdf/integtransform.pdf>
- Carr, P. P. and D. B. Madan (1999) Option valuation using the fast Fourier transform, *Journal of Computational Finance* **2**(4), 61–73.
- Carr, P. P. and L. Wu (2003) The Finite Moment Log Stable Process and Option Pricing, *Journal of Finance* **58**, 753–777.
- Carr, P. P. and L. Wu (2004) Time-changed Lévy processes and option pricing, *Journal of Financial Economics* **71**, 113–141.
- Chourdakis, K. (2005) Option pricing using fractional FFT, *Journal of Computational Finance* **8**(2), 1–18.
- Cont, R. (2001) Empirical properties of asset returns: stylized facts and statistical issues, *Quantitative Finance* **1**, 223–236.

- Cont, R., J. da Fonseca and V. Durrleman (2002) Stochastic Models of Implied Volatility Surfaces, *Economic Notes* **31**(2), 361–377.
- Cont, R. and P. Tankov (2004) *Financial Modelling with Jump Processes* (Financial Mathematics Series), Chapman & Hall/CRC, New York.
- Cooley, J. and J. Tukey (1965) An algorithm for the Machine Calculation of Complex Fourier Series, *Mathematics of Computation* **19**, 297–301.
- Cox, J. C. and S. A. Ross (1976) The valuation of options for alternative stochastic processes. *Journal of Financial Economics* **3**, 145–166.
- Davies, R. B. (1973) Numerical inversion of a characteristic function, *Biometrika* **60**(2), 415–417.
- Davis, P. J. and P. Rabinowitz (1984) *Methods of Numerical Integration* (Computer Science and Applied Mathematics), 2nd ed., Academic Press, New York.
- Delbaen, F. and W. Schachermayer (2006) *The Mathematics of Arbitrage*, Springer, Berlin.
- Dempster, M. A. and S. S. Hong (2002) Spread Option Valuation and the Fast Fourier Transform, Technical Report WP26/2000, University of Cambridge.
- Dobránszky, P. (2008) Numerical Quadratures to Calculate Lévy Base Correlation, Technical Report, Finalyse SA, FORTIS Merchant Banking and KU Leuven.
- Dobránszky, P. (2009) Option Pricing Using Numerically Evaluated Characteristic Functions, Presentation on the 3rd Conference on Numerical Methods in Finance, Paris. Available at <http://peter.dobranszky.com/files/NumericallyEvaluatedCFs.pdf>
- Duffie, D., J. Pan and K. Singleton (2000) Transform analysis and asset pricing for affine jump–diffusions, *Econometrica* **68**, 1343–1376.
- Duffy, D. G. (2004) *Transform Methods for Solving Partial Differential Equations*, 2nd ed., Chapman & Hall/CRC, New York.
- Dufresne, D., J. Garrido and M. Morales (2009) Fourier Inversion Formulas in Option Pricing and Insurance, *Methodology and Computing in Applied Probability* **11**, 359–383.

- Eberlein, E., K. Glau and A. Papapontoleon (2009) Analysis of Fourier Transform Valuation Formulas and Applications, to appear in *Applied Mathematical Finance*, [arXiv:0809.3405v4](https://arxiv.org/abs/0809.3405v4)
- Eberlein, E. and U. Keller (1995) Hyperbolic Distributions in Finance, *Bernoulli* **1**(3), 281–299.
- Epps, T. W. (1993) Characteristic Functions and Their Empirical Counterparts: Geometrical Interpretations and Applications to Statistical Inference, *American Statistician* **47**, 33–38.
- Fahrner, I. (2007) Modern Logarithms for the Heston Model, *International Journal of Theoretical and Applied Finance* **10**, 23–30.
- Fang, F. and C. Oosterlee (2008) A novel pricing method for European options based on Fourier-cosine series expansions, *SIAM Journal on Scientific Computing* **31**(2), 826–84.
- Fang, F., R. Lord and C. W. Oosterlee (2006) Fast and accurate Methods in Pricing Early Exercise Options under Lévy Processes, Working Paper, Rabobank International, Delft University of Technology and Center for Mathematics and Computer Science (CWI), Amsterdam. Available at <http://mpira.ub.uni-muenchen.de/1952/>
- Filipović, D. (2001) A General Characterization of one Factor Affine Term Structure Models, *Finance and Stochastics* **5**(3), 389–412.
- Fusai, G. and A. Roncoroni (2008) *Implementing Models in Quantitative Finance: Methods and Cases* (Springer Finance), Springer, Berlin.
- Gander, W. and W. Gautschi (2000) Adaptive Quadrature—Revisited, *BIT* **40**(1), March, 84–101.
- Gatheral, J. (2006) *The Volatility Surface: A Practitioner's Guide* (Wiley Finance Series), John Wiley & Sons, New York.
- Geman, H., N. El Karoui and J.-C. Rochet (1995) Changes of Numéraire, Changes of Probability Measure and Option Pricing, *Journal of Applied Probability* **32**(2), 443–458.
- Gil-Pelaez, J. (1951) Note on the inversion theorem, *Biometrika* **38**(3–4), 481–482.

- Guo, J. and M. Hung (2007) A Note on the Discontinuity Problem in Heston's Stochastic Volatility Model, *Applied Mathematical Finance* **14**, 339–345.
- Grundke, P. (2007) Computational aspects of integrated market and credit portfolio models, *OR Spectrum* **29**, 259–294.
- Gurland, J. (1948) Inversion formulae for the distribution of ratios, *Annals of Mathematical Statistics* **19**, 228–237.
- Hagan, P. S. and G. West (2006) Interpolation methods for curve construction, *Applied Mathematical Finance* **13**(2), 89–129.
- Hart, J. F. & al. (1968) *Computer Approximations* (SIAM Series In Applied Mathematics), John Wiley & Sons, New York. Algorithm 5666 for the error function.
- Haug, E. (2003a) Know Your Weapon Part 1, *Wilmott Magazine*, May, 49–57.
- Haug, E. (2003b) Know Your Weapon Part 2, *Wilmott Magazine*, July, 50–56.
- Harrison, J. and D. Kreps (1979) Martingales and arbitrage in multiperiod securities markets, *Journal of Economic Theory* **20**(3), 381–408.
- Harrison, M. and S. Pliska (1981) Martingales and stochastic integrals in the theory of continuous trading, *Stochastic Processes Applications* **11**(3), 215–260.
- Heston, S. L. (1993) A Closed-form Solution for Options with Stochastic Volatility with Application to Bond and Currency Options, *Review of Financial Studies* **6**(2), 327–343.
- Heston, S. L. and S. Nandi (2000) A Closed-Form GARCH Option Pricing Model, *Review of Financial Studies* **13**(3), 585–625.
- Huang, J. and L. Wu (2004) Specification Analysis of Option Pricing Models Based on Time-Changed Lévy Processes, *Journal of Finance* **59**, 1405–1440.
- Hughett, P. (1998) Error Bounds for Numerical Inversion of a Probability Characteristic Function, *SIAM Journal on Numerical Analysis* **35**(4), 1368–1392.
- Hurd, T. R. and Z. Zhou (2009) A Fourier transform method for spread option pricing, Preprint, [arXiv:0902.3643v1](https://arxiv.org/abs/0902.3643v1)

- Itkin, A. (2005) Pricing options with VG model using FFT, [arXiv:physics/0503137v1](https://arxiv.org/abs/physics/0503137v1)
- Jaschke, S. R. and Y. Jiang (2002) Approximating Value at Risk in Conditional Gaussian Models, In: *Applied Quantitative Finance*, Eds. W. Härdle, T. Kleinow and G. Stahl, Springer, Berlin.
- Ji, M. and F. Zapatero (2008) Empirical Performance of Lévy Option Pricing Models. Available at SSRN: <http://ssrn.com/abstract=1266380>
- Judd, K. L. (1998) *Numerical Methods in Economics*, The MIT Press, Cambridge.
- Kahl, C. and P. Jäckel (2006) Not-so-complex logarithms in the Heston model, Working Paper, University of Wuppertal and ABN AMRO.
- Keller-Ressel, M. (2008) Affine Processes – Theory and Applications to Finance, Ph.D. Dissertation, Vienna University of Technology.
- Kilin, F. (2007) Accelerating the Calibration of Stochastic Volatility Models, Working Paper, Frankfurt School of Finance & Management and Quanteam AG.
- Kim, Y., S. Rachev, M. Bianchi and F. Fabozzi (2009) Computing VaR and AVaR in infinitely divisible distributions, Technical Report, University of Karlsruhe.
- Kou, S. G. (2002) A jump-diffusion model for option pricing, *Management Science* **48**, 1086–1101.
- Kruse, S. and U. Nögel (2005) On the pricing of forward starting options in Heston's model on stochastic volatility, *Finance and Stochastics* **9**, 223–250.
- Lee, R. W. (2004) Option Pricing by Transform Methods: Extensions, Unification, and Error Control, *Journal of Computational Finance* **7**(3), 51–86.
- Leippold, M. and L. Wu (2002) Asset pricing under the Quadratic Class, *Journal of Financial and Quantitative Analysis* **37**(2), 271–295.
- Lévy, P. (1925) *Calcul des Probabilités*, Gauthier-Villars et Cie, Paris.
- Lewis, A. (2000) *Option Valuation under Stochastic Volatility: With Mathematica Code*, Finance Press, Newport Beach.

- Lewis, A. (2001) A Simple Option Formula for General Jump-Diffusion and other Exponential Lévy Processes, Envision Financial Systems and OptionCity.net, California. Available at <http://optioncity.net/pubs/ExpLevy.pdf>
- Lipton, A. (2001) *Mathematical methods for foreign exchange*, World Scientific.
- Lipton, A. (2002) The vol smile problem, *Risk*, February, 61–65.
- Lord, R. and C. Kahl (2007) Optimal Fourier Inversion in Semi-Analytical Option Pricing, Discussion Paper TI No.2006–066/2, Tinbergen Institute. Available at SSRN: <http://ssrn.com/abstract=921336>
- Lord, R. and C. Kahl (2008) Complex logarithms in Heston-like models. Rabobank International and ABN AMRO, Available at SSRN: <http://ssrn.com/abstract=1105998>
- Lord, R., F. Fang, F. Bervoets and C. Oosterlee (2007) A Fast Method for Pricing Early-Exercise Options with the FFT, *Lecture Notes In Computer Science* 4488, 415–422.
- Lukacs, E. (1970) *Characteristic Functions*, 2ed ed., Charles Griffin & Co, London.
- Manno, V. P. (1988) A simple procedure for reducing numerical integration errors near singularities, *Communications In Applied Numerical Methods* 4, 713–716.
- Madan, D. B., P. P. Carr and E. C. Chang (1998) The Variance Gamma Process and Option Pricing, *European Finance Review* 2, 79–105.
- McCulloch, J. H. (2003) The Risk-Neutral Measure and Option Pricing under Log-Stable Uncertainty, Working Paper, Ohio State University.
- McKeeman, W. M. (1962) Algorithm 145: Adaptive numerical integration by Simpson's rule, *Communications of the ACM* 5(12), p 604.
- Meisel, W. (1968) A Numerical Integration Formula Useful in Fourier Analysis, *Communications of the ACM* 11, p 51.
- Menn, C. and S. T. Rachev (2006) Calibrated FFT-based density approximations for α -stable distributions, *Computational Statistics & Data Analysis* 50, 1891–1904.
- Merton, R. C. (1973) Theory of rational option pricing, *Bell Journal of Economics and Management Science* 4, 141–183.

- Merton, R. C. (1976) Option pricing when the underlying stock returns are discontinuous, *Journal of Financial Economics* **3**, 125–144.
- Mikhailov, S. and U. Nögel (2003) Heston's Stochastic Volatility Model – Implementation, Calibration and some Extensions, *Wilmott Magazine*, July, 74–79.
- Minenna, M. and P. Verzella (2007) Fast Option Pricing using Non Uniform Discrete Fourier Transform on Gaussian Discretization Grids, CONSOB, University of Milano Bicocca.
- Minenna, M. and P. Verzella (2008) A revisited and stable Fourier transform method for affine jump diffusion models, *Journal of Banking & Finance* **32**, 2064–2075.
- Nagel, H. (2001) *Optionsbewertung bei stochastischer Volatilität*, Deutscher Universitäts Verlag, Gabler, Wiesbaden.
- Nunes, J. P. and T. R. Alcaria (2009) Two Extensions to Forward Start Options Valuation, ISCTE Business School, Caixa Económica Montepio Geral. Available at SSRN: <http://ssrn.com/abstract=1329370>
- O'Sullivan, C. (2005) Path Dependent Option Pricing under Lévy Processes, EFA 2005 Moscow Meetings Paper. Available at SSRN: <http://ssrn.com/abstract=673424>
- Pan, J. (2002) The jump-risk premia implicit in options: Evidence from an integrated time-series study, *Journal of Financial Economics* **63**, 3–50.
- Raible, S. (2000) Lévy Processes in Finance: Theory, Numerics and Empirical Facts, Ph.D. Dissertation, University of Freiburg.
- Reiß, O. and U. Wystup (2001) Efficient Computation of Option Price Sensitivities using Homogeneity and other Tricks, *Journal of Derivatives* **9**, 41–53.
- Ross, S. A. (1976) Options and Efficiency, *The Quarterly Journal of Economics* **90**(1), 75–89.
- Rudin, W. (1987) *Real and Complex Analysis* (International Series in Pure and Applied Mathematics), 3rd ed., McGraw-Hill, New York.
- Schöbel, R. and J. Zhu (1999) Stochastic Volatility with an Ornstein Uhlenbeck Process: An Extension, *European Finance Review* **3**, 23–46.

- Schoutens, W. (2003) *Lévy Processes in Finance: Pricing Financial Derivatives* (Wiley Series in Probability and Statistics), John Wiley & Sons, Chichester.
- Sepp, A. (2003) Pricing European-Style Options under Jump Diffusion Processes with Stochastic Volatility: Applications of Fourier Transform, Working Paper, University of Tartu.
- Sepp, A. (2006) Extended CreditGrades Model with Stochastic Volatility and Jumps, *Wilmott Magazine*, September, 50–62.
- Staunton, M. (2006) Stochastic Volatility without Complex Numbers, *Wilmott Magazine*, May, 46–48.
- Stein, E. and J. Stein (1991) Stock Price Distributions with Stochastic Volatility: An Analytic Approach, *Review of Financial Studies* **4**, 727–752.
- Tahani, N. (2004) Valuing Credit Derivatives Using Gaussian Quadrature: A Stochastic Volatility Framework, *Journal of Futures Markets* **24**(1), 3–35.
- Tahani, N. and X. Li (2007) Pricing Interest Rate Derivatives under Stochastic Volatility, Working Paper, York University.
- Tankov, P. (2004) *Lévy Processes in Finance: Inverse Problems and Dependence Modelling*, Ph.D. Dissertation, École Polytechnique, Paris.
- Tankov, P. (2009) Calibration de Modèles et Couverture de Produits Dérivés, Lecture Notes, École Polytechnique et Université Paris VII, Edition 2009. Available at <http://people.math.jussieu.fr/~tankov/MA/>
- Titchmarsh, E. C. (1975) *Introduction to the Theory of Fourier Integrals*, Reprint of 2nd ed., Oxford University Press, London.
- Waller, L. A. (1995) Does the Characteristic Function Numerically Distinguish Distributions, *The American Statistician* **49**(2), 150–152.
- Waller, L. A., B. W. Turnbull and J. M. Hardin (1995) Obtaining Distribution Functions by Numerical Inversion of Characteristic Functions with Applications, *The American Statistician* **49**(4), 346–350.
- West, G. (2005) Better Approximations to Cumulative Normal Functions, *Wilmott Magazine*, May, 70–76.

- Wu, L. (2008) Modeling Financial Security Returns using Lévy Processes, In:
Handbooks in Operations Research and Management Science: Financial Engineering, Volume 15, Eds. J. Birge and V. Linetsky, Elsevier, North-Holland.
Available at <http://faculty.baruch.cuny.edu/lwu/papers/handbooklevy.pdf>
- Yan, G. and F. B. Hanson (2006) Option Pricing for a Stochastic-Volatility Jump-Diffusion Model with Log-Uniform Jump-Amplitudes, Proceedings of the 2006 American Control Conference, Minneapolis, Minnesota, June 14–16.
- Zeliade Systems (2009) Heston 2009, Zeliade Systems White Paper, September.
Available at <http://www.zeliade.com/whitepapers/zwp-0004.pdf>